UNIVERSITY OF TURKU

STUDIES ON THE PATHOGENESIS AND LABORATORY DIAGNOSIS OF LYME BORRELIOSIS

Annukka Pietikäinen

TURUN YLIOPISTON JULKAISUJA – ANNALES UNIVERSITATIS TURKUENSIS
SARJA - SER. D OSA - TOM. 1403 | MEDICA - ODONTOLOGICA | TURKU 2018

UNIVERSITY OF TURKU

STUDIES ON THE PATHOGENESIS AND LABORATORY DIAGNOSIS OF LYME BORRELIOSIS

Annukka Pietikäinen

TURUN YLIOPISTON JULKAISUJA – ANNALES UNIVERSITATIS TURKUENSIS
SARJA - SER. D OSA - TOM. 1403 | MEDICA - ODONTOLOGICA | TURKU 2018

University of Turku

Faculty of Medicine
Institute of Biomedicine
Medical Microbiology and Immunology
Turku Doctoral Programme of Molecular Medicine (TuDMM)

Supervised by

Associate professor Jukka Hytönen, MD, PhD
Institute of Biomedicine
University of Turku
Turku, Finland

Reviewed by

Docent Anne Jääskeläinen, PhD
Department of Virology
University of Helsinki
Helsinki, Finland

Docent Benita Westerlund-Wikström, PhD
Molecular and Integrative Biosciences Research Programme
Faculty of Biological and Environmental Sciences
University of Helsinki
Helsinki, Finland

Opponent

Docent Mirja Puolakkainen, MD, PhD
Department of Virology
University of Helsinki
Helsinki, Finland

ISBN 978-951-29-7500-6 (PRINT)
ISBN 978-951-29-7501-3 (PDF)
ISSN 0355-9483 (Print)
ISSN 2343-3213 (Online)
Grano Oy - Turku, Finland 2018

Messieurs, c'est les microbes qui auront le dernier mot.

– Louis Pasteur

ABSTRACT

Annukka Pietikäinen

Studies on the pathogenesis and laboratory diagnosis of Lyme borreliosis

University of Turku, Faculty of Medicine, Institute of Biomedicine, Medical Microbiology and Immunology, Turku Doctoral Programme of Molecular Medicine (TuDMM)

Annales Universitatis Turkuensis, Medica – Odontologica, Turku, Finland 2018

Lyme borreliosis, the most common tick-borne disease in the northern hemisphere, is caused by *Borrelia burgdorferi* sensu lato spirochetes (later *Borrelia*). They can infect humans through bites of infected *Ixodes* ticks. If the infection is not treated at the early local stage of the disease, spirochetes can disseminate via the blood vasculature into distant tissues of the human body and cause symptoms in the joints, the heart, and the nervous system. Infection of the central nervous system is called Lyme neuroborreliosis. Lyme neuroborreliosis is diagnosed based on neurological symptoms, pleocytosis, and intrathecal production of *Borrelia*-specific antibodies. Recently, chemokine CXCL13 has been introduced as a new biomarker for diagnostics of Lyme neuroborreliosis.

The first aim of this study was to characterize the dissemination of *Borrelia* by *in vitro* adhesion studies conducted under shear stress and by imaging the infection *in vivo* in mice. The second aim was to evaluate the use of cytokines as biomarkers for Lyme neuroborreliosis.

The studies revealed that decorin binding proteins of *Borrelia* act in a flow-tolerant manner mediating adherence into vascular endothelium under the mechanical force caused by the liquid flow. In addition to decorin, decorin binding proteins were shown to bind biglycan, a proteoglycan which is expressed on endothelium more abundantly than decorin. Moreover, dissemination of *Borrelia* can be imaged *in vivo* in mice using positron-emission tomography. The studies also showed that CXCL13 is the most specific cytokine biomarker for Lyme neuroborreliosis and the concentration of CXCL13 can reliably be measured of Lyme neuroborreliosis patients' cerebrospinal fluid samples with a point-of-care test. Overall, the studies gave new information on the pathogenesis of Lyme borreliosis and helped to improve the disease diagnostics.

Keywords: Lyme borreliosis, *Borrelia burgdorferi*, adhesion, dissemination, PET/CT, *in vivo* imaging, Lyme neuroborreliosis, cytokine, multiplex, CXCL13, point-of-care

TIIVISTELMÄ

Annukka Pietikäinen

Tutkimuksia Lymen borrelioosin patogeneesistä ja diagnostiikasta

Turun yliopisto, Lääketieteellinen tiedekunta, Biolääketieteen laitos, Lääketieteellinen mikrobiologia ja immunologia, Turun molekyylilääketieteen tohtoriohjelma (TuDMM)

Annales Universitatis Turkuensis, Medica – Odontologica, Turku, Suomi 2018

Pohjoisen pallonpuoliskon yleisimmän puutiaisvälitteisen infektion, Lymen borrelioosin, aiheuttajia ovat *Borrelia burgdorferi* sensu lato ryhmän spirokeettabakteerit (myöhemmin *Borrelia*). Ne voivat levitä ihmiseen infektoituneiden *Ixodes*-puutiaisten välityksellä. Jos tautia ei hoideta heti infektion aikaisessa paikallisessa vaiheessa, spirokeetat voivat levitä ihmiselimistössä verenkierron mukana useisiin kudoksiin aiheuttaen oireita muun muassa nivelissä, sydämessä ja hermostossa. Keskushermostoon levinnyttä infektiota kutsutaan Lymen neuroborrelioosiksi. Neuroborrelioosin diagnostiikka perustuu potilaan neurologisiin oireisiin sekä solumäärän ja *Borrelia*-spesifisten vasta-aineiden määritykseen aivoselkäydinnesteestä. Hiljattain myös kemokiini CXCL13 on otettu käyttöön Lymen neuroborrelioosin diagnostiikan biomarkkeriksi.

Tämän tutkimuksen tarkoituksena oli selvittää *Borrelia*-bakteerin virtauksen alla tapahtuvan endoteelisitoutumisen rooli infektion patogeneesissä, tutkia infektion leviämistä eri kudoksiin *in vivo* -kuvantamisen avulla hiirimallissa ja tutkia sytokiinien käyttöä Lymen neuroborrelioosin diagnostisina biomarkkereina.

Tutkimuksessa havaittiin, että *Borrelia*-bakteerin dekoriinia sitovat proteiinit sitoutuvat myös biglykaaniin, joka on dekoriinia yleisempi proteoglykaani verisuonten endoteelin pinnalla. Tämän biglykaani-interaktion avulla *Borrelia* kykenee sitoutumaan verisuonten endoteeliin nestevirtauksen aiheuttaman vastuksen alla. Lisäksi tutkimuksessa selvisi, että *Borrelia*-infektion kulkua voi kuvantaa elävässä eläimessä positroniemissiotomografian avulla. Tutkimuksessa havaittiin myös, että CXCL13 on soveltuvin sytokiini Lymen neuroborrelioosin diagnostiikan biomarkkeriksi ja että CXCL13:n pitoisuus voidaan määrittää potilaan aivoselkäydinnesteestä pikatestin avulla, mikä nopeuttaa huomattavasti tautidiagnostiikkaa. Kaiken kaikkiaan tutkimustulokset paljastivat tärkeää uutta tietoa *Borrelia*-infektion patogeneesistä ja auttavat Lymen borrelioosin diagnostiikan kehittämisessä.

Avainsanat: Lymen borrelioosi, *Borrelia burgdorferi*, sitoutuminen, leviämien, PET/TT, kuvantaminen, neuroborrelioosi, sytokiini, CXCL13, pikatesti

TABLE OF CONTENTS

ABBREVIATIONS

ACA	acrodermatitis chronica atropicans
AEC	3-amino-9-ethylcarbazole
ANOVA	analysis of variance
BBB	blood-brain-barrier
β-NGF	beta nerve growth factor
BSA	bovine serum albumin
BSK	Barbour-Stoenner-Kelly medium
cDNA	complementary deoxyribonucleic acid
CFSE	carboxyfluorescein diacetate succinimidyl ester
CNS	central nervous system
CSF	cerebrospinal fluid
CXCL13	chemokine (C-X-C motif) ligand 13
CXCR5	C-X-C motif chemokine receptor 5
DAPI	4',6-diamidino-2'-phenylindole dihydrochloride
Dbp	decorin binding protein
DC	dendritic cell
ECL	enhanced chemiluminescence
ECM	extracellular matrix
EDTA	ethylenediaminetetraacetic acid
EFNS	European federation of neurological societies
EM	erythema migrans
FDG	fluorodeoxyglucose
GAG	glycosaminoglycan
GAPDH	glyceraldehyde-3-phosphate dehydrogenase
G-CSF	granulocyte-colony stimulating factor
GFP	green fluorescent protein
HBMEC	human brain microvascular endothelial cell
HEPES	4-(2-hydroxyethyl)-1-piperazineethanesulfonic acid
HFF	human foreskin fibroblast
HRP	horseradish peroxidase
HUVEC	human umbilical vein endothelial cell
IFN-γ	interferon gamma
IL	interleukin
IPTG	isopropyl β-D-1-thiogalactopyranoside
LA	Lyme arthritis

LB	Lyme borreliosis
LNB	Lyme neuroborreliosis
LPS	lipopolysaccharide
LY	Lucifer yellow
MFI	mean fluorescence intensity
mRNA	messenger ribonucleic acid
MS	multiple sclerosis
PAMP	pathogen-associated molecular pattern
PBMC	peripheral blood mononuclear cell
PBS	phosphate buffered saline
PBS-T	phosphate buffered saline containing 0.05% Tween® 20
PET	positron emission tomography
PET/CT	positron emission tomography/computed tomography
PFA	paraformaldehyde
PMSF	phenylmethylsulfonyl fluoride
POC	point-of-care
PRR	pattern recognition receptor
qPCR	quantitative polymerase chain reaction
ra	receptor antagonist
RT	room temperature
RT-PCR	reverse transcription polymerase chain reaction
siRNA	small interfering ribonucleic acid
SUV_{gluc}	standardized uptake value with blood glucose correction
TBE	tick-borne encephalitis
TEER	transendothelial electrical resistance
TLR	toll-like receptor
TNF-α	tumor necrosis factor alpha
ZO-1	zonula occludens-1

LIST OF ORIGINAL PUBLICATIONS

This thesis is based on the following publications

I Salo Jemiina*, Pietikäinen Annukka*, Söderström Mirva, Auvinen Kaisa, Salmi Marko, Ebady Rhodaba, Moriarty Tara J., Viljanen Matti K., and Hytönen Jukka. Flow-tolerant adhesion of a bacterial pathogen to human endothelial cells through interaction with biglycan. *J. Infect. Dis.* 2016;213:1623-1631.

II Pietikäinen Annukka, Siitonen Riikka, Liljenbäck Heidi, Eskola Olli, Söderström Mirva, Roivainen Anne, and Hytönen Jukka. In vivo imaging of Lyme arthritis in mice by [^{18}F]fluorodeoxyglucose positron emission tomography/computed tomography. *Scand. J. Rheumatol*. 2018;47:37-47.

III Pietikäinen Annukka, Maksimow Mikael, Kauko Tommi, Hurme Saija, Salmi Marko, and Hytönen Jukka. Cerebrospinal fluid cytokines in Lyme neuroborreliosis. *J. Neuroinflammation*. 2016;13:273.

IV Pietikäinen Annukka, Oksi Jarmo, and Hytönen Jukka. Point-of-care testing for CXCL13 in Lyme neuroborreliosis. *Diagn Microbiol Infect Dis*. 2018;91:226-228.

* These authors contributed equally to this article.

1 INTRODUCTION

The causative agent of the tick-borne disease Lyme borreliosis (LB) is a group of spirochetes called *Borrelia burgdorferi* sensu lato (later *Borrelia*). *Borrelia* circulate mainly between *Ixodes* ticks and vertebrate animals, especially small rodents and birds, when ticks acquire their blood meal from the animals. Occasionally, ticks can feed also on humans. Upon the blood meal of an infected tick, *Borrelia* can escape the tick midgut and infect the human skin. If not treated at this stage of the disease, *Borrelia* can disseminate into distant tissues.

Borrelia can reach the distant tissues by exploiting the blood circulation. Dissemination via the vasculature is a multistep process. First, *Borrelia* enter the blood circulation after which they adhere to the vascular wall resisting the mechanical force of the flowing blood. So far, only one adhesin of *Borrelia* has been shown to mediate flow-tolerant interactions with the vasculature. After adhesion, spirochetes transmigrate across the endothelium to reach the tissues. Before this study, it has not been possible to image disseminated infection caused by genetically unmodified *Borrelia in vivo*.

When *Borrelia* disseminate into the central nervous system, patients develop Lyme neuroborreliosis (LNB). LNB is diagnosed based on neurological symptoms, cerebrospinal fluid (CSF) pleocytosis, and the detection of intrathecally produced *Borrelia*-specific antibodies. Recently, chemokine CXCL13, which is produced to the CSF of LNB patients in high concentrations, has been introduced as a new diagnostic tool for LNB. So far, multiplex analyses have not been performed to evaluate the use of other cytokines as biomarkers for LNB.

The aims of this study were to characterize the pathogenesis of *Borrelia* infection (vascular adhesion and dissemination; studies I-II), to develop *in vivo* imaging techniques for LB infection (study II), and to evaluate new methods for laboratory diagnosis of LNB (studies III-IV).

2 REVIEW OF LITERATURE

2.1 Lyme borreliosis

Lyme borreliosis (LB) is a multisystem infectious disease (Steere et al., 1984, Steere et al., 1977a). The first reports of erythema migrans (EM), an expanding skin rash characteristic for the disease, date back to the early 1900s (Sternbach and Dibble, 1996) and the first described human case of LB is the 5300 year old Tyrolean Iceman found from the Italian Alps (Keller et al., 2012). The disease, however, was thoroughly described only in the 1970s in Connecticut, USA (Stanek et al., 2011, Steere et al., 1977b). At that time, people from the small Old Lyme town informed local health department that many children living in the same area had developed a disease diagnosed as juvenile rheumatoid arthritis (Steere et al., 1977b). This oddity led to a deeper surveillance and research, the results of which showed that the diagnoses had not been correct mainly due to atypical clustering of the patients to certain areas. The clustered nature of the arthritis cases and other epidemiological data suggested that the disease could be an infectious disease spread by an arthropod vector. Consequently, the disease was named Lyme arthritis (LA). Later, ticks of the *Ixodes* genus were found to be the vectors (Steere et al., 1978) and the causative agent of the disease, a spirochete named *Borrelia burgdorferi* was isolated from the *I. dammini* ticks (currently known as *I. scapularis* (Oliver et al., 1993)) in the 1980s (Burgdorfer et al., 1982). As the multisystem nature of the disease unraveled, the disease was named Lyme disease (Stanek et al., 2011). Finally, when spirochete antibodies were detected in the blood of the patients, the *Ixodes* tick-borne spirochetes were confirmed to be the causative agents of Lyme disease (Barbour et al., 1983, Benach et al., 1983). In Europe, the disease is generally referred to as Lyme borreliosis (Stanek et al., 2011).

2.1.1 *Borrelia burgdorferi sensu lato*

B. burgdorferi sensu lato (later *Borrelia*) is defined as a group of spirochetes transmitted by tick vectors (Rudenko et al., 2011). The group consists of ca. 20 genospecies which can be divided into two clades; genospecies found in Europe and Asia and genospecies found in North America and Europe (Becker et al., 2016). Out of these, *B. burgdorferi* sensu stricto, *B. garinii*, and *B. afzelii* are clinically the most relevant pathogens but nine other genospecies (*B. bavariensis, B. bissettii, B. kurtenbachii, B. lusitaniae, B. spielmanii, B. valaisiana, B. andersonii*, *B. americana*, candidatus *B. mayonii*) are also regarded as potentially pathogenic (Brandt et al., 2014, Clark et al., 2014, Collares-Pereira et al., 2004, Fingerle et al., 2008,

Picken et al., 1996, Pritt and Petersen, 2016, Rijpkema et al., 1997, Rudenko et al., 2008, Rudenko et al., 2011, Ryffel et al., 1999, Wilhelmsson and Lindgren, 2016).

Borrelia are corkscrew-shaped 10-30 µm long and ca. 0.3 µm wide bacteria (Barbour, 1988, Goldstein et al., 1996, Steere et al., 2016). They are classified as Gram-negative although their cell wall is slightly different compared with other Gram-negative bacteria (Aberer and Duray, 1991, Hyde, 2017). *Borrelia* have a double membrane and a thin peptidoglycan layer situated between the two membranes (Radolf et al., 2012, Steere et al., 2016). However, while Gram-negative bacteria usually have an endotoxic lipopolysaccharide (LPS) structure in the outer membrane, LPS is absent from *Borrelia* (Takayama et al., 1987). Unlike many other Gram-negative bacteria, *Borrelia* have numerous outer membrane lipoproteins (Brandt et al., 1990). Many of these function as adhesins which mediate the binding of *Borrelia* to its vector and host structures (Brissette and Gaultney, 2014, Kung et al., 2013). *Borrelia* are motile with seven to ten periplasmic flagella between the outer membrane and the thin peptidoglycan layer (Barbour, 1988, Barbour and Hayes, 1986).

The highly fragmented genome of *Borrelia* is unique among bacteria (Figure 1.). The genome consists of a rather small (ca. 1 000 000 base pairs) linear chromosome which contains mainly housekeeping genes (Ferdows and Barbour, 1989, Fraser et al., 1997, Lin et al., 2012). Most of the genes encoding known virulence factors are located in several circular and linear plasmids (Barbour, 1989, Fraser et al., 1997, Kenedy et al., 2012). The plasmid content varies considerably among different *Borrelia* strains (Casjens et al., 2012, Casjens et al., 2017, Casjens et al., 2018, Margos et al., 2017a).

Phylogeny of *Borrelia* is rather complicated because evolutionary relations of *Spirochaetes* phylum remain poorly understood (Gupta et al., 2013). A unifying feature of the families in this phylum is that they are all motile with periplasmic flagella. Otherwise the members of the phylum are very diverse. Based on the 16S rRNA classification, *Borrelia* belong to the family of *Spirochaetaceae* along with relapsing fever *Borrelia*, *Treponema*, *Cristispira*, *Spirochaeta*, and *Sphaerochaeta*. However, a new classification system where *Borrelia* would be their own *Borreliaceae* family together with relapsing fever *Borrelia* and *Cristispira* has been proposed. Moreover, an active discussion about dividing the *Borrelia* genus into two distinct genera has been ongoing; relapsing fever *Borrelia* would form the *Borrelia* genus and the later characterized LB spirochetes would form a new *Borreliella* genus (Adeolu and Gupta, 2014). The debate about the division is still ongoing mainly due to 1) newly discovered spirochetes which resemble relapsing fever type bacteria but are still considered as LB spirochetes, 2) *B. miyamotoi,* which is transmitted by the same *Ixodes* vector as LB spirochetes but which causes

a relapsing fever type of disease, and 3) due to many public health and patient safety related concerns (Barbour et al., 2017, Margos et al., 2017b, Stevenson et al., 2018).

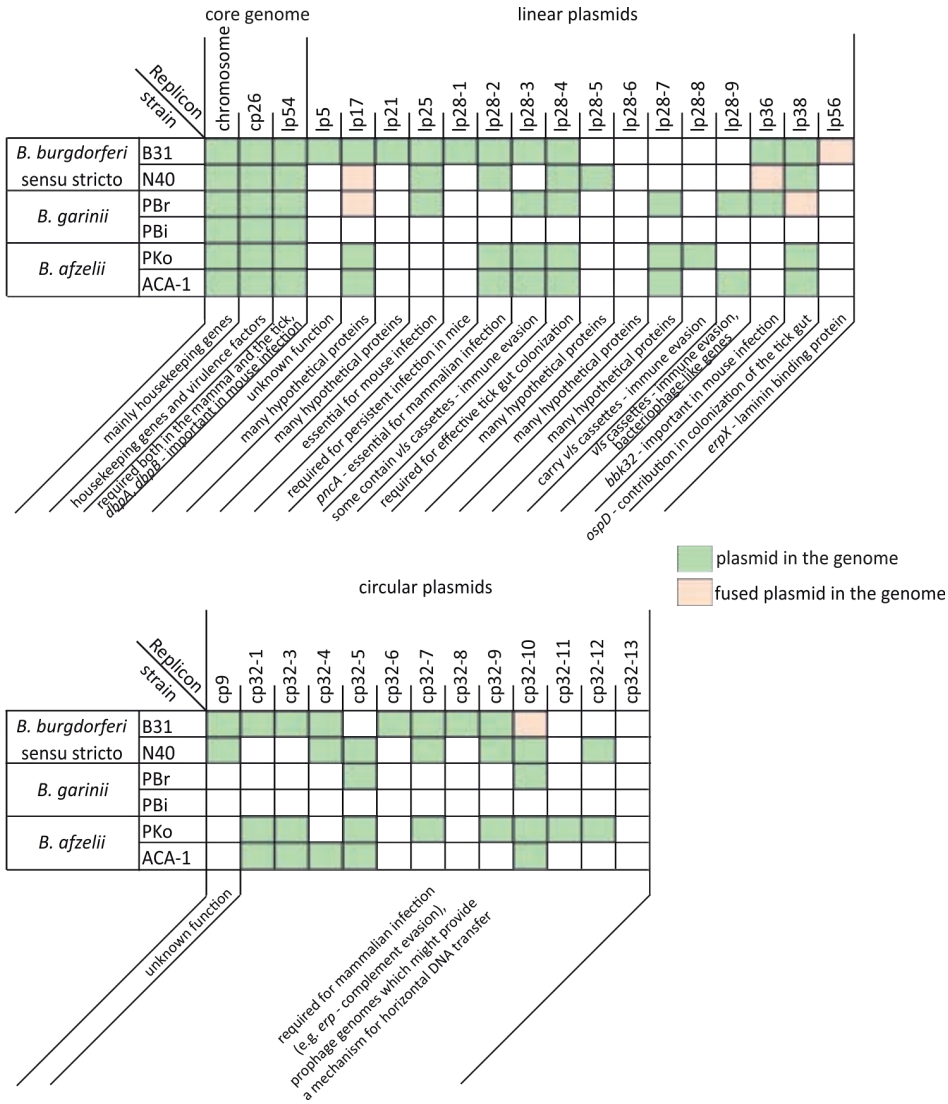

Figure 1. The genome structure of representative *Borrelia* genospecies/strains. The genome of *Borrelia* consists of a linear chromosome and multiple linear and circular plasmids. Chrmosome contains mainly housekeeping genes while the plasmids carry most of the virulence factor encoding genes (Casjens et al., 2000, Casjens et al., 2018, Rosa et al., 2005, Strother et al., 2005). The plasmid content varies between different *Borrelia* strains. Adapted from (BorreliaBase: www.borreliabase.org; accessed 9.10.2018).

2.1.2 *Clinical manifestations*

LB can be divided into three stages based on the clinical manifestations: 1) early localized, 2) early disseminated, and 3) the late disseminated disease (Sanchez, 2015). At the first stage of the disease, a characteristic sign of the infection is a localized skin rash called erythema migrans (EM). EM appears at the site of the tick bite and expands slowly as the bacteria migrate and multiply in the skin (Nadelman, 2015, Mason et al., 2016). However, not all patients develop EM. Several estimations of EM incidence in LB patients have been reported and the estimations vary considerably (50% - 90%) depending on when and where the study was conducted (Bacon et al., 2008, Hatchette et al., 2015, Huppertz et al., 1999, Singh and Girschick, 2004, Steere, 2001, Stinco et al., 2014). EM is a clear sign of the *Borrelia* infection if the lesion is over 5 cm in diameter (Nadelman, 2015). The shape of the rash is either round or oval. Sometimes the lesion starts to clear at the center causing a characteristic bulls-eye appearance. Other manifestations of the early localized disease are general flu like symptoms such as fever and malaise (Sanchez, 2015). Also, regional lymphadenopathy may occur.

If not treated at the early localized stage, the disease may progress into the early disseminated disease. *Borrelia* migrate from the skin into distant tissues hematogenously or via the lymphatic system. At this stage of the disease, symptoms may occur in multiple organs. Additional EM lesions may appear on the skin, the patient may develop lymphocytoma, and migratory pain in the joints may appear. If *Borrelia* invade the nervous system, the patient develops neurological symptoms (Lyme neuroborreliosis; LNB) such as facial palsy. The patient may suffer from severe headache and malaise. At this stage of the disease, also the heart may be affected. (Sanchez, 2015)

The late disseminated stage of LB is usually characterized by an often asymmetric oligoarticular arthritis that affects mainly large joints. This stage of the disease may also manifest itself in the skin as a chronic skin lesion called acrodermatitis chronica atropicans (ACA). This manifestation can eventually lead to skin atrophy. (Sanchez, 2015)

Generally speaking, different *Borrelia* genospecies are linked to different tissue manifestations. LA is mainly caused by *B. burgdorferi* sensu stricto, LNB is usually associated with *B. garinii,* and *B. afzelii* is the main genospecies associated with EM and ACA. (Coipan et al., 2016, van Dam et al., 1993, Ornstein et al., 2001, Rudenko et al., 2011)

2.1.2.1 ***Lyme neuroborreliosis***

In the disseminated stage of LB, patients may develop neurological symptoms affecting both peripheral and central nervous system (CNS) (Koedel et al., 2015, Sanchez, 2015, Steere et al., 2016). Overall, LNB affects ca. 10% of LB patients (Halperin, 2017, Stanek and Strle, 2018) but in children, the frequency of LNB is even higher (Kortela et al., 2017, Stanek and Strle, 2018).

LNB in the early disseminated phase of the disease is characterized by lymphocytic meningitis with headache and neck stiffness, cranial neuritis, facial palsy, painful meningoradiculitis, subtle encephalitis, mononeuritis multiplex, and pseudotumor cerebri (Koedel et al., 2015, Sanchez, 2015, Steere et al., 2016). In Europe, the most common symptom of early LNB is painful meningoradiculitis characterized by sharp pain which gets worse at night time, paresis of the extremities, and a facial palsy (Koedel et al., 2015). The development of these neurological symptoms correlates with the appearance of lymphocytic pleocytosis in the cerebrospinal fluid (CSF).

When a patient has had neurological symptoms continuously for over 6 months, the disease is referred to as late LNB (Koedel et al., 2015). In this stage of the disease, patients may have chronic encephalomyelitis, spastic paraparesis, ataxic gait, subtle mental disorders, and chronic axonal polyradiculopathy (Sanchez, 2015). Also, rare cerebrovascular manifestations have been described, and usually it takes about 3 - 4 months from the first sign of LB until the first cerebrovascular manifestations occur (Garkowski et al., 2017).

2.1.3 ***Epidemiology***

In nature, *Borrelia* circulate between hard tick vectors and reservoir hosts (Radolf et al., 2012). The life cycle of a tick vector consists of three phases; a larva, a nymph, and an adult. The transition from each stage to the next requires a blood meal. Also, adult female ticks lay eggs only after a blood meal. The current understanding is that the eggs are free from *Borrelia*, and thus, unfed larvae are uninfected (Rollend et al., 2013). However, some recent evidence point out the possibility of also larvae being infected with *Borrelia* (van Duijvendijk et al., 2016).

Different *Borrelia* genospecies infect different tick vectors, the main vector species being *I. ricinus*, *I. persulcatus*, *I. scapularis*, and *I. pacificus* (Becker et al., 2016, Steere et al., 2016). The main vectors in North America are *I. pacificus* and *I. scapularis* while in Europe and Asia the main vectors are *I. ricinus* and *I. persulcatus*. In Finland, both *I. ricinus* and *I. persulcatus* are discovered and they both

carry *Borrelia* (Laaksonen et al., 2017). Time required for the transmission of *Borrelia* from the vector to the host depends on both tick vector species and infecting *Borrelia* genospecies (Cook, 2015). The longer a tick feeds, the greater is the efficacy of *Borrelia* transmission from the tick to the host (Piesman et al., 1987). The transmission generally takes several hours, if not days (Cook, 2015). The transmission is slower if only one tick is attached when compared with a situation where multiple ticks are feeding on the same host at the same time (Eisen, 2018). It has been reported that 16.9% of the ticks are infected with *Borrelia* in Finland (Laaksonen et al., 2017). However, the infection rate can vary depending on the *Ixodes* species and on the geographic location (Laaksonen et al., 2018, Sormunen et al., 2016) albeit the distribution of *Borrelia* positive ticks has been shown to correspond to the distribution of *Ixodes* ticks in general (Laaksonen et al., 2017). An overall risk of a human infection after a tick bite, however, has been reported to be only 2.6% (Hofhuis et al., 2017).

Tick vectors exhibit a generalist feeding behavior meaning that they can feed on multiple different vertebrate species (Radolf et al., 2012). Larvae and nymphs usually feed on small vertebrates while adult ticks feed also on larger animals like deer. The main reservoir hosts of *Borrelia* include small rodents, birds, and lizards (Becker et al., 2016). Different *Borrelia* genospecies have been linked to different main host species. As an example, *B. garinii* is mainly infecting birds, while *B. burgdorferi* sensu stricto infects rodents and birds and *B. afzelii* rodents and lizards. Larger animals are incompetent hosts for *Borrelia* but they serve as important host species for the maintenance of the tick population (Radolf et al., 2012). Humans and pets, on the other hand, are incidental dead-end hosts for *Borrelia*.

LB is the most prevalent tick-borne disease in the northern hemisphere (Bacon et al., 2008, van den Wijngaard et al., 2017). *B. burgdorferi* sensu stricto is the main disease agent in North America while in Europe and Asia most LB patients are infected with *B. garinii* or *B. afzelii* (Stanek and Strle, 2018, Steere, 2001). As a consequence, due to organotrophic nature of the genospecies, clinical features of the disease are somewhat different in Eurasia and the USA; LA is the most common manifestation of a disseminated disease in North America while ACA and LNB are more common in Europe and Asia (Stanek et al., 2011, Steere, 2001).

The number of reported LB cases is constantly increasing all over the northern hemisphere (Bacon et al., 2008, Rizzoli et al., 2011, Sajanti et al., 2017). The reason for the increase is not completely understood but it is thought that the warming of the climate might enlarge the suitable habitat of the tick vectors by enabling the moving of the ticks more north (Rizzoli et al., 2011). In the USA, the annual incidence of LB varies greatly depending on the state. In tick endemic areas (such as Connecticut) the incidence can be on average as high as 73/100000 population

while in tick endemic areas in central Europe the incidence can be even 100-200/100000 population (Mead, 2015). A recent study indicates that the incidence of LB has increased also in Finland (Sajanti et al., 2017). The estimated overall incidence of LB in Finland in 2014 was 120/100000 population. The Åland Islands are hyperendemic for *Borrelia* since the incidence of LB in 2014 was ca. 1600/100000. The incidence of microbiologically confirmed (mainly disseminated) LB cases in Finland in 2016 by hospital district is presented in Figure 2. LB cases seem to follow a two-peaked age distribution where the first peak appears in the childhood (ca. 5 - 15 years) and the second peak either in the adulthood (ca. 45 - 55 years) or in the older age groups (> 60 years) (Bacon et al., 2008, Nelson et al., 2015, Sajanti et al., 2017, Steere et al., 2016).

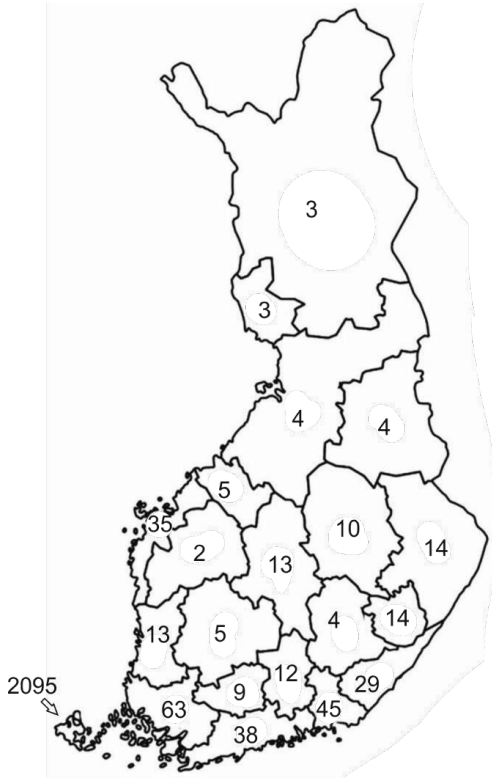

Figure 2. The incidence of microbiologically confirmed LB cases per 100 000 population by hospital district in 2016. The incidence of microbiologically confirmed (mainly disseminated) LB cases is the highest in the southern Finland, especially along the coast-line and in the archipelago. (The National Infectious Diseases Register: https://sampo.thl.fi/pivot/prod/fi/ttr/shp/fact_shp?row=area-12260&column=time-12059&filter=reportgroup-12465; accessed 15.10.2018; Kuntaliitto: population 31.12.2016: www.kuntaliitto.fi/asiantuntijapalvelut/sosiaali-ja-terveysasiat/erikoissairaanhoito; accessed 15.10.2018)

2.1.4 *Animal models and in vivo imaging*

Mice are widely used as animal models in infection research mainly because of the low cost of both the animals and their maintenance and because of their easy availability. There are a great number of different inbred mouse strains that have been developed for different purposes. C3H/He mice get a multisystem infection when infected with *Borrelia* (Barthold et al., 1990, Barthold et al., 1991) and they can be used as an animal model in LB research. C3H/He mice are particularly suitable animal models when studying LA since these mice develop significant joint swelling after infection (Miller et al., 2008, Salo et al., 2015, Yegutkin et al., 2010). Arthritis severity in mice is genetically determined and not all mouse strains develop severe LA (Wooten and Weis, 2001). The usefulness of C3H/He mice as an animal model for LA is further supported by the fact that the histopathological changes in the joints of *Borrelia* infected C3H/He mice resemble the changes seen in humans.

LA seen in mice does not require acquired immunity (B and T cells) but, instead, innate immunity mediated by e.g. toll-like receptors (TLRs) and subsequent cytokine secretion is involved (Glickstein and Coburn, 2006, Weis, 2002, Wooten and Weis, 2001). There are two isogenic C3H/He mouse strains (C3H/HeN and C3H/HeJ) which are both widely used for LB studies. C3H/HeN mice have a functional wild type TLR4 while C3H/HeJ mice have a mutated TLR4 (Tötemeyer et al., 2003). TLR4 recognizes LPS of Gram-negative bacteria and the mutated TLR4 reduces the ability to control bacterial growth in C3H/HeJ mice when compared with C3H/HeN mice. Although *Borrelia* do not have LPS, a few reports suggest that TLR4 might have a role also in LB (Bernardino et al., 2008, Glickstein and Coburn, 2006). Macrophages of C3H/HeJ mice lacking the functional TLR4 have been shown to produce less tumor necrosis factor alpha (TNF-α) when infected with *Borrelia* compared with macrophages with functional TLR.

Albeit mice can be used as animal models for LA, they are not suitable for LNB studies. Only a few studies demonstrating the signs of *Borrelia* infection in the brain of experimentally infected mice have been published (Divan et al., 2018, Javid et al., 2016, Kazragis et al., 1996, Kern et al., 2015, Pětrošová et al., 2017). Also, a rat model has been used to successfully isolate live spirochetes from the brain (Barthold et al., 1988) and the presence of *Borrelia* DNA in infected rat brains has been described (Pulzova et al., 2011). However, these rodent models do not develop human neuroborreliosis like symptoms most likely due to their inherent immune mechanisms (Garcia-Monco and Benach, 2013). Because these rodents are natural hosts for *Borrelia* in nature, their immune system has evolved to tolerate the spirochetes better than the immune system of humans, the accidental dead-end hosts for *Borrelia*. More appropriate animal model for LNB is nonhuman

primates. A few studies have been conducted with rhesus macaques which develop human LNB like symptoms such as meningitis and neuritis (Pachner et al., 2001b, Philipp et al., 1993, Ramesh et al., 2015, Roberts et al., 1998a).

There are a few studies describing different imaging techniques used to monitor *Borrelia* infection in the mouse model of LB. Studies using spinning disc intravital imaging of green fluorescent protein (GFP) expressing *Borrelia* in mouse vasculature and luciferase-expressing *Borrelia* imaged in mice with bioluminescence technology have revealed the importance of BBK32 and OspC adhesins of *Borrelia* in the infection process (Ebady et al., 2016, Hyde et al., 2011, Moriarty et al., 2008, Norman et al., 2008, Skare et al., 2016). In these studies, the role of BBK32 and OspC adhesins has been studied by comparing the infection caused by *Borrelia* strains expressing wild type BBK32 adhesin to infection caused by *bbk32* knock-out mutant strains, by comparing infection caused by *Borrelia* strains lacking the BBK32 adhesin to infection caused by *bbk32* complemented strains or by monitoring the expression of adhesins in different stages of infection in multiple tissues (OspC). Multiphoton laser scanning microscopy has been used to study GFP-expressing *Borrelia* in specific mouse tissues (Bockenstedt et al., 2012). This study identified *Borrelia* remnants in cartilaginous tissues after antibiotic treatment. However, there are no *in vivo* imaging techniques available which could be used to study infection and inflammation caused by genetically unmodified *Borrelia* strains.

2.2 Pathogen entry into the host

Human body contains multiple barriers that protect us from microbial and chemical threats. In addition to immunity, these barriers can be divided into physical, chemical, and anatomical barriers. For example, 1) lysozyme in tears and other secretions protect from pathogens by disrupting specific bonds of the peptidoglycan component in bacterial cell walls, 2) mucus and cilia in the respiratory tract move pathogens out of the body, 3) acidic stomach and rapid pH change in the gastrointestinal tract inhibit the growth of invading pathogens, 4) and normal microbiota competes for e.g. nutrients with pathogens. The most obvious tissue barrier is the skin. It forms a physical barrier that outlines human body and produces antimicrobial fatty acids. It is also covered by normal skin microbiota which is able to prevent pathogen growth. To be able to cause a disease, pathogens must over-come at least some of these tissue barriers. Examples of the protective physical, chemical, and anatomical barriers are presented in Figure 3. (Madigan et al., 2009)

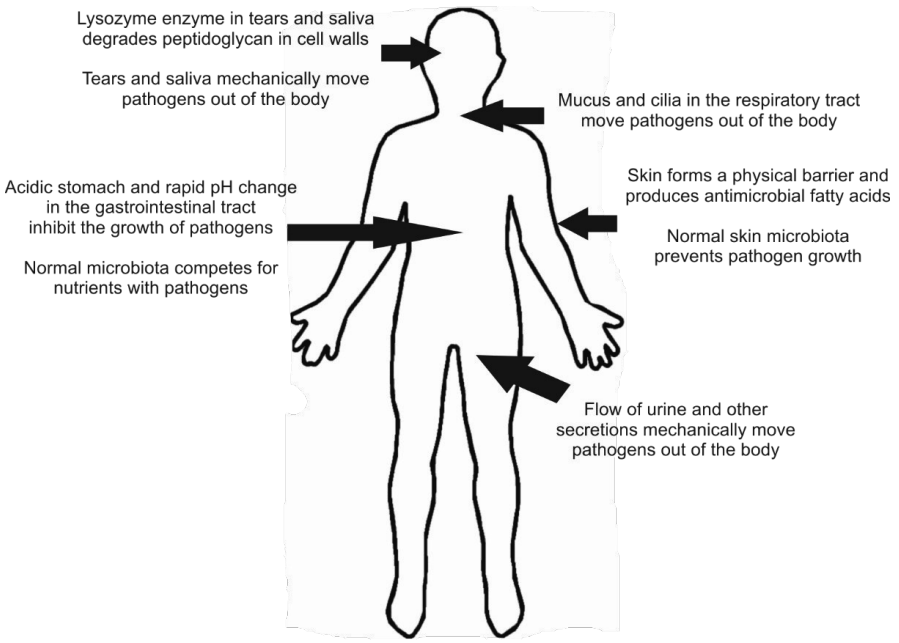

Figure 3. Examples of the barriers that protect humans from invading pathogens. Adapted from (Madigan et al., 2009).

2.2.1 *Entry of the host by vector-borne infectious agents*

Nearly 20% of human infectious diseases are spread by vectors (Rinker et al., 2016). The most common vectors are arthropods, the largest phylum in the animal kingdom (Baxter et al., 2017). Pathogens which are transmitted through the bites of blood-feeding arthropods (e.g. mosquitos and ticks) bypass the skin barrier and enter directly into the tissues and the bloodstream of the host. Arthropods serve as vectors for bacterial, viral, and eukaryotic pathogens (Kock, 2015) and they present great variation in susceptibility to infectious agents mainly due to their own immunological factors (Baxter et al., 2017). This phenomenon is known as a vectoral capacity. Many arthropod-borne diseases are serious illnesses. They include diseases such as malaria, Dengue fever, and Zika which are all transmitted by mosquitos. Examples of bacterial pathogens transmitted by arthropod vectors include *Yersinia pestis*, the causative agent of plague, and *Francisella tularensis*, the causative agent of tularemia (Kock, 2015).

Different species of ticks are able to transmit eukaryotic pathogens like *Babesia*, viral diseases such as tick-borne encephalitis (TBE), and bacterial agents such as *Borrelia* (Brites-Neto et al., 2015). In the tick, *Borrelia* reside in the midgut. Upon blood meal, *Borrelia* exit the gut, proceed to tick salivary glands and infect the

host along with the saliva of the tick (Piesman, 1995). This process requires the adaptation of *Borrelia* to rapidly changing conditions such as increase in temperature and decrease in pH (Caimano, 2018, Stevenson et al., 2006). These and other still unknown environmental signals result in an altered gene expression of *Borrelia*. For example, the spirochetes start to express surface proteins that are needed in mammalian infection, such as OspC, and downregulate the expression of genes that encode proteins required for survival in the tick, such as OspA. As a consequence, *Borrelia* are able to transmit from the tick into a mammalian host, bypass the skin barrier and, eventually, invade the host skin tissue and the bloodstream.

2.2.2 *Adhesion of Borrelia to vascular endothelium*

When the skin barrier has been bypassed, *Borrelia* begin to multiply and spread in the skin and after a short delay they start to spread into distant tissues (Radolf et al., 2012). This is thought to occur via the bloodstream (Berger et al., 1994, Moriarty et al., 2008, Norman et al., 2008, Wormser et al., 2005). However, in order to reach the distant tissues, *Borrelia* must first invade the blood circulation and then escape the bloodstream. Transmigration across the blood endothelium usually requires that the pathogen adheres to the vascular endothelium lining the blood vessels (Lemichez et al., 2010). Indeed, vascular endothelium forms yet another anatomical barrier that *Borrelia* must bypass in order to cause multisystem infection.

Endothelium of blood vessels is heterogeneous with many structural and functional differences depending on organ-specific requirements (Aird, 2007, Lemichez et al., 2010). Vascular endothelia from different anatomical sites express different sets of proteins (Aird, 2007, Page et al., 1992) which pathogens can exploit and use as binding ligands. Moreover, vascular endothelium is covered by a gel-like layer called glycocalyx (Gasic and Gasic, 1962, Ushiyama et al., 2016). It is composed of proteoglycans and glycosaminoglycans (GAG) (Ushiyama et al., 2016). The layer hinders the access of molecules and pathogens circulating in the blood to the endothelial surface. Thus, it is important for a pathogen to interact not only with the surface of endothelial cells but also with the extracellular glycocalyx matrix. Heparan sulphate is considered to be the main GAG expressed on endothelium and extracellular matrix (ECM) (Middleton et al., 2002). However, some inflammatory conditions have been shown to promote the alteration in the proportions of GAGs such as the increase in the amounts of dermatan and chondroitin sulphate.

Bacterial pathogens express various molecules on their surface which mediate adherence (Coburn et al., 2013). These adhesins use endothelial cell or glycocalyx molecules as binding ligands, thus, enabling the pathogen to contact the vascular

endothelium. *Borrelia* express numerous adhesins on their outer surface which mediate binding to many components of ECM and also to endothelial cells (Brissette and Gaultney, 2014, Coburn et al., 1998, Coburn et al., 2013, Leong et al., 1998, Parveen et al., 2003, Salo et al., 2011, Schmit et al., 2011, Szczepanski et al., 1990, Thomas and Comstock, 1989).

To be able to adhere to the vascular endothelium, pathogens must also resist the shear stress of the blood flow (Lemichez et al., 2010). However, if adhesion interactions to vascular wall were too strong, the pathogen might not be able to release itself from the endothelium to reach deeper tissues (Thomas et al., 2002). Moreover, the shear stress caused by the blood flow is not constant all over the vasculature but, instead, varies depending on e.g. vessel type and location (Ebady et al., 2016, Mairey et al., 2006, Papaioannou and Stefanadis, 2005, Pries et al., 1995, Soyer and Duménil, 2011). In low shear stress areas, the blood flow may even stop for a few seconds (Mairey et al., 2006). Due to these features of the vasculature, fine balanced interactions are required for a pathogen to adhere to the endothelium and to translocate across the endothelial barrier to other tissues.

Despite the crucial effect of flow on adhesion, only a few flow-tolerant adhesins have been described. These include the thoroughly characterized fibronectin and GAG binding BBK32 adhesin of *Borrelia* (Ebady et al., 2016, Moriarty et al., 2012, Niddam et al., 2017, Norman et al., 2008), monomannose-binding type I pili component FimH of *Escherichia coli* (Feenstra et al., 2017, Thomas et al., 2004), von Willebrand-factor binding protein of *Staphylococcus aureus* (Claes et al., 2014), CD147 binding type IV pili components PilE and PilV of *Neisseria meningitidis* (Bernard et al., 2014, Mikaty et al., 2009), and Tp0751 adhesin of *Treponema pallidum* (Kao et al., 2017).

The adherence of *Borrelia* into vascular endothelium is thought to resemble leukocyte trafficking (Moriarty et al., 2012, Norman et al., 2008). First, *Borrelia* form initial tethering contacts to the endothelium, after which more stable dragging connections can be formed finally allowing the transmigration of *Borrelia* from the bloodstream into distant tissues (Figure 4.).

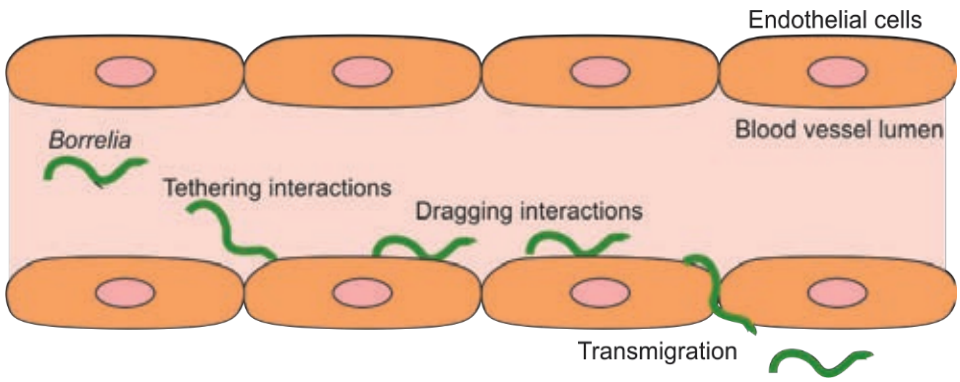

Figure 4. Interactions of *Borrelia* with the blood vessel endothelium. First, *Borrelia* form transient tethering interactions with the endothelial cells. Then, stronger dragging interactions occur, and finally, *Borrelia* transmigrate across the endothelium and penetrate deeper tissues. Adapted from (Moriarty et al., 2012).

2.2.2.1 ***Decorin and biglycan***

Decorin and biglycan are both small leucine-rich proteoglycans associated with ECM (Reitsma et al., 2007, Schaefer and Schaefer, 2010). Decorin has one GAG side chain attached to a ca. 40 kDa core protein (Reitsma et al., 2007). The GAG side chain is either dermatan sulphate or chondroitin-6-sulphate depending on the tissue (Heinegård and Oldberg, 1989, Hocking et al., 1996). As an example, in connective tissues, the GAG is usually dermatan sulphate (Roughley, 2006). The core protein of biglycan (ca. 45 kDa) is highly similar to the core protein of decorin (Fisher et al., 1989, Heinegård and Oldberg, 1989). However, unlike decorin, biglycan has two dermatan or chondroitin-6-sulphate side chains attached to the core (Fisher et al., 1989, Reitsma et al., 2007). Moreover, the GAGs of biglycan are smaller in size than the GAGs of decorin (Kinsella and Wight, 1988). Both of these proteoglycans can, however, exist also without any GAG side chains e.g. on endothelial cells (Valiyaveettil et al., 2004). The schematic structures of decorin, biglycan, chondroitin-6-sulphate, and dermatan sulphate are presented in Figure 5.

Despite the structural similarities, the expression pattern of biglycan differs from that of decorin. While decorin is expressed especially in connective tissue, biglycan is more abundantly expressed by endothelial cells (Bianco et al., 1990, Järveläinen et al., 1991, Kitaya and Yasuo, 2009, Nelimarkka et al., 1997, Snow et al., 1995). In addition, both decorin and biglycan can be expressed by various cell types in the brain tissue (Kikuchi et al., 2000, Mohan et al., 2010, Stichel et al., 1995).

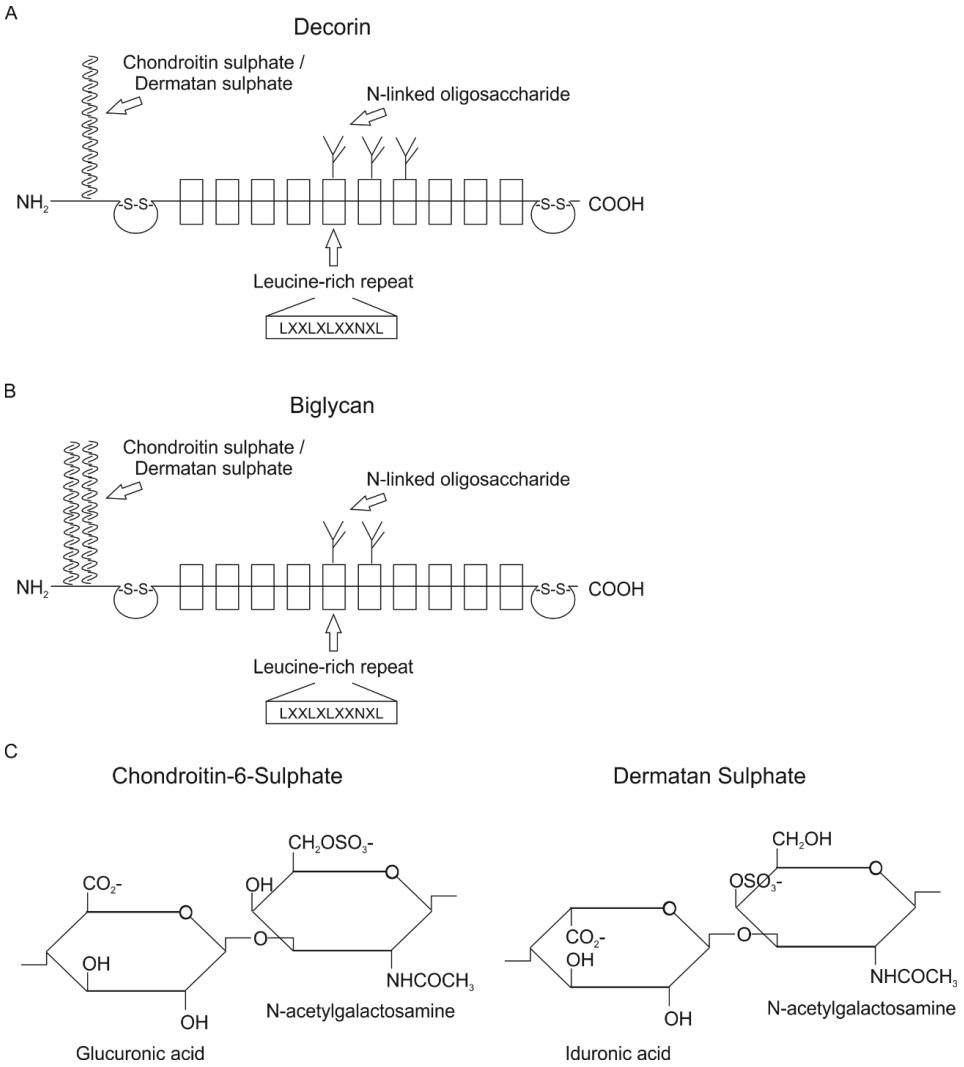

Figure 5. Schematic structures of decorin, biglycan, chondroitin-6-sulphate, and dermatan sulpahte. (A) Decorin core protein has ten leucine-rich repeat motifs with three attachment sites for N-linked oligosaccharides, and one GAG side chain. (B) Biglycan has only two attachment sites for N-linked oligosaccharides. Unlike decorin, it has two GAG side chains. (C) The GAGs of decorin and biglycan are composed of repeating units of chondroitin-6-sulphate or dermatan sulphate. Adapted from (Edwards, 2012, Järveläinen et al., 2015, Pichert et al., 2012, Roughley, 2006, Trowbridge and Gallo, 2002).

Biglycan and decorin are not present in the plasma of healthy individuals. However, in inflammatory conditions, these proteoglycans can be shed from the ECM and act as immunostimulatory danger-associated molecular patterns recognized by TLR 2 and 4 (Frevert et al., 2017, Schaefer et al., 2005). This interaction leads to the production of cytokines like chemokine (C-X-C motif) ligand 13 (CXCL13).

As an example, in lupus nephritis soluble biglycan stimulates TLRs to produce CXCL13 leading to the recruitment of autoantibody producing B1 cells and, eventually, increased damage in the kidneys (Frey et al., 2013, Moreth et al., 2010). In TLR2/4 dependent pathogen mediated inflammation, on the other hand, biglycan can strengthen the host inflammatory response.

2.2.2.2 ***Decorin binding proteins***

Decorin binding proteins A and B (DbpA/B; Dbps) are adhesins which are expressed on the surface of *Borrelia* during mammalian infection (Cassatt et al., 1998, Hodzic et al., 2003). They are encoded by *dbpBA* operon of a linear plasmid 54 (Hagman et al., 1998, Purser and Norris, 2000) which is present universally among *Borrelia* genospecies (Di et al., 2014). Dbps are anchored to the outer membrane of *Borrelia* via an N-terminal triacyl-modified cysteine (Schulze and Zückert, 2006).

Dbps have been shown to bind GAG side chains (dermatan and chondroitin sulphate) of decorin (Guo et al., 1998, Salo et al., 2011). Moreover, the decorin core protein potentially has a role in Dbp binding as well (Benoit et al., 2011, Guo et al., 1998). Decorin binding ability of Dbps is important for the development of joint manifestations of LB (Brown et al., 2001) and, moreover, both DbpA and DbpB are needed for the development of arthritis in mice (Salo et al., 2015, Xu et al., 2007). Mutant *Borrelia* strains expressing only DbpA or DbpB are not as efficient in colonizing the joints as the strains expressing both of these adhesins (Shi et al., 2008a). In addition, mutant *Borrelia* strains lacking both Dbps show an early dissemination defect in mice and, with low infectious doses, are not able to colonize mouse joints (Imai et al., 2013, Salo et al., 2015, Weening et al., 2008). Decorin binding ability of *Borrelia* is also important in colonization of the heart of experimentally infected mice and of human LB patients (Lin et al., 2014, Muehlenbachs et al., 2016, Shi et al., 2008b). Indeed, colocalization of *Borrelia* and decorin in the cardiac autopsy samples of LB patients can be observed (Muehlenbachs et al., 2016). Decorin-rich tissues form a protective niche for *Borrelia* against host immune defense (Liang et al., 2004a) and by quantifying DNA load in mouse tissues infected with *dbp* knock-out *Borrelia* strains and *dbp* complemented strains, it has been shown that Dbps have a role in the persistence of *Borrelia* DNA in the joints of mice after live *Borrelia* have been eradicated by antibiotic treatment (Salo et al., 2015). According to the Basic Local Alignment Serach Tool (BLAST; https://blast.ncbi.nlm.nih.gov/Blast.cgi; accessed 11.10.2018), Dbps are unique for *Borrelia* even though other bacteria can also bind the same ligands as Dbps (Laabei et al., 2018).

The amino acid sequences of Dbps are different among the *Borrelia* genospecies and even among different strains of the same genospecies (Heikkilä et al., 2002a, Heikkilä et al., 2002b, Roberts et al., 1998b, Schulte-Spechtel et al., 2006). Amino acid sequence identity of DbpA proteins varies between 40 - 100%. The sequences of DbpB, on the other hand, are more conserved. Amino acid sequence identity of DbpB varies between 60 - 100%. The structures of DbpA of *B. burgdorferi* sensu stricto B31 and N40, DbpA of *B. garinii* PBr and DbpB of *B. burgdorferi* sensu stricto B31 have been solved (Feng and Wang, 2015, Morgan and Wang, 2015, Wang, 2012). Dbps consist of five helices and a pocket-like structure composed of basic amino acids (Wang, 2012). This binding pocket contains the lysine amino acids which have been shown to be crucial in decorin binding and in mammalian infection (Brown et al., 1999, Fortune et al., 2014, Pikas et al., 2003, Wang, 2012). Overall, basic lysine residues in adhesins of different pathogens are important in ligand binding (Fechtner et al., 2013, Seymour et al., 2010).

Even though the basic structure of the Dbps is the same, some variation can nevertheless be observed (Morgan and Wang, 2015). Consequently, Dbps of different genospecies show great variability in their ligand binding ability (Benoit et al., 2011, Salo et al., 2011) which can then promote tissue tropism. DbpA of *B. garinii* PBr is linked to heart manifestations while DbpA of *B. burgdorferi* sensu stricto N40 promotes arthritis (Lin et al., 2014). Tissue tropism might also be affected by other binding motifs on Dbps. DbpA of *B. burgdorferi* sensu stricto B31 has also a heparin binding motif (Morgan and Wang, 2013). This motif, however, cannot be detected in all Dbps of different genospecies. Also liquid flow has an important role in the binding ability of Dbps (Salo et al., 2011). Recombinant DbpA of *B. garinii* SBK40 has been shown to be flow-dependent as it exhibits binding activity towards decorin only in flow conditions. In addition, it has been speculated that Dbps might also have affinity for biglycan (Brown et al., 2001).

2.3 Invasion of the central nervous system

Finally, pathogens need to escape the vasculature to invade the CNS. Vascular endothelium contains two different types of junctions between the cells; tight junctions and adherence junctions. Tight junctions are formed by molecules such as claudin, zonula occludens and occludin and adherence junctions are formed mainly by cadherins (Lemichez et al., 2010). Junctions prevent passive flow of molecules across the endothelium and they are tighter in arterioles than in capillaries or venules (Aird, 2007). Endothelium of arteries, capillaries, and veins of skin, brain, heart, and lung is nonfenestrated continuous endothelium. This means that water and small molecules can pass between the endothelial cells but larger compounds

(> 3 nm) have to pass through transendothelial channels or use transcytosis to cross the endothelium. In inflammatory conditions, however, the permeability of the vasculature increases.

The CNS is protected and passive influx of pathogens is prevented by different barriers depending on the anatomical location (Shechter et al., 2013, Spadoni et al., 2017). These barriers are the blood-leptomeningeal barrier, the blood-brain-barrier (BBB) and the blood-CSF-barrier.

2.3.1 *The blood-brain-barrier*

BBB is composed of specialized endothelial cells lining the lumen of capillaries and post-capillary venules (brain microvasculature) (Spadoni et al., 2017). In addition, BBB endothelial cell layer is surrounded by a basement membrane, astrocytes, and pericytes which are all essential components in maintaining an effective BBB function (Obermeier et al., 2013, Spadoni et al., 2017). A schematic structure of the BBB is presented in Figure 6.

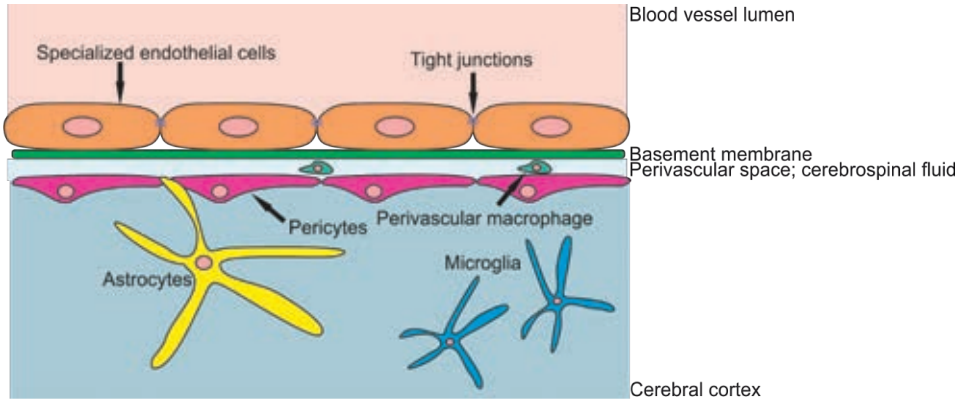

Figure 6. The components of the blood-brain-barrier (BBB). BBB is composed of specialized endothelial cells that are connected with tight junctions. Basement membrane is located beneath the endothelial cell layer. Cerebrospinal fluid circulates in the perivascular space. Cerebral cortex is further protected by pericytes and astrocytes which are also considered as essential components of the BBB. Microglia and macrophages patrol in the perivascular space and the cerebral cortex. Modified from (Coureuil et al., 2017, Ljubimova et al., 2017, Ransohoff and Engelhardt, 2012).

There is a high number of tight junctions between the endothelial cells of the BBB (Aird, 2007). As the number of tight junctions inversely correlates with the permeability of the endothelium, the endothelium of the BBB is extremely impermeable. Moreover, a relatively low number of leucocyte adhesion molecules are expressed

on the endothelium of the BBB which leads to the inhibition of leucocyte infiltration into the CNS (Spadoni et al., 2017). However, the perivascular space in the brain parenchyma contains a special population of antigen presenting cells (such as microglia) (Spadoni et al., 2017). When these cells encounter an antigen, they can present it to T cells, the cell population which has been reported to be able to cross the BBB and reach the CSF (Engelhardt et al., 2016, Ransohoff and Engelhardt, 2012, Spadoni et al., 2017). Activated T cells can then start producing pro-inflammatory cytokines, a phenomenon which eventually may lead to the leakage of the BBB and infiltration of other leucocytes into the CNS. Interestingly, shear stress has been shown to have a great impact on the endothelial physiology of the BBB models cultured *in vitro* (Cucullo et al., 2011). Liquid flow induces the expression of cell junction molecules, integrins, and vascular adhesion molecules.

2.3.2 ***Transmigration***

Pathogens gain access into the CNS either by transmigrating through the tissue barriers or by traversing via the olfactory, trigeminal or peripheral nerves. Out of these, the transmigration across the BBB is the most common and well-studied route of access. There are three possible mechanisms that pathogens can use for transmigration. Pathogens can cross the BBB or the blood-CSF-barrier transcellularly, paracellularly or by using host leucocytes as Trojan horses. Transcellular transmigration requires pinocytosis or a specific receptor-mediated mechanism. Trojan horse -mechanism requires that the pathogens can penetrate and survive inside host leucocytes. Paracellular transmigration, on the other hand, is enabled by the destruction of tight and adherence junctions between the endothelial cells. The destruction of the junctions leads to increased permeability of the BBB. (Dando et al., 2014)

The pathogen related virulence traits that destroy junctions are e.g. the exploitation of the host plasminogen system or the production of hemolysins which can be toxic to human brain microvascular endothelial cells (HBMECs) (Dando et al., 2014). These factors are used also by *Borrelia* (Grab et al., 2005, Shaw et al., 2012). Evidence suggests that *Borrelia* transmigrate across the vascular endothelium by using a paracellular route (Grab et al., 2005, Grab et al., 2009, Moriarty et al., 2008, Nyarko et al., 2006, Pulzova et al., 2011, Szczepanski et al., 1990) and OspA surface protein of *Borrelia* has been shown to be one of the adhesins mediating transmigration across the BBB (Pulzova et al., 2011). Although not studied using HBMECs, also integrin binding surface protein P66 of *Borrelia* has been shown to be essential in transmigration across vascular endothelium as evidenced by intravital imaging of mice infected with fluorescent *Borrelia* expressing wild type

P66, strains expressing mutated P66, or *p66* knock-out *Borrelia* strains (Kumar et al., 2015). In addition, motility of *Borrelia* is one of the key factors in vascular transmigration (Comstock and Thomas, 1991, Moriarty et al., 2008, Sadziene et al., 1991). Studies published on endothelial transmigration of *Borrelia* are presented in Table 1. Other factors that might have a role in transmigration of *Borrelia* are proteases. BbHtrA degrades various ECM components (e.g. decorin and biglycan) and cell junction protein E-cadherin, and this degradation likely facilitates the transmigration (Russell et al., 2013). Interestingly, GAG-binding ability of group B *Streptococcus* and *Haemophilus somnus* pathogens has been demonstrated to be important in the adherence and invasion of HBMECs (Chang et al., 2011) but the GAG-binding ability of *Borrelia* has not been studied in this context.

Although paracellular route of transmigration seems more likely, a few studies have shown that *Borrelia* could also invade and survive in endothelial cells (Comstock and Thomas, 1989, Ma et al., 1991, Wu et al., 2011). This suggests that *Borrelia* could also use the transcellular route to access the CNS. Moreover, intravital imaging of GFP-expressing *Borrelia* in mouse vasculature has suggested that while the majority of spirochetes use paracellular route in vascular transmigration, a part of the spirochetes is able to transmigrate through endothelial cells (Moriarty et al., 2008).

Table 1. Studies published on endothelial transmigration of *Borrelia*.

Reference	*Borrelia* strain	Cell line / Organsim	Factors mediating transmigration
Comstock and Thomas, 1989	*B. burgdorferi* HB19	HUVEC	Not determined
Szczepanski et al., 1990	*B. burgdorferi* B31 and HBD1	HUVEC	Damage of the cell monolayer
Comstock and Thomas, 1991	*B. burgdorferi* HB19, ECM-NY, SH-2-82, N40, CA-2-87	HUVEC	Viability/motility, surface-localized proteins of *Borrelia*
Sadziene et al., 1991	*B. burgdorferi* HB19	HUVEC	Motility
Coleman et al., 1995	*B. burgdorferi* BEP4	HUVEC	Plasmin of the host
Grab et al., 2005	*B. burgdorferi* N40 and 297	HBMEC and EAhy.926	Fibrinolytic system and matrix metallo-proteinases of the host
Nyarko et al., 2006	*B. burgdorferi* 297	HBMEC and EAhy.926	Coinfection with *Anaplasma phagocytophilum*
Moriarty et al., 2008; Norman et al., 2008	*B. burgdorferi* B31 derivatives	C57BL/6 mice	Motility
Grab et al., 2009	*B. burgdorferi* 297, B331, B356, and BL206	HBMEC	Calcium signaling of the host
Pulzova et al., 2011	*B. bavariensis* SKT-7.1 and *B. burgdorferi* SKT-2	Primary rat BMECs	OspA – CD40 interaction
Kumar et al., 2015	*B. burgdorferi* B31 derivatives	$CD1d^{-/-}$ mice (lack natural killer cells)	P66 and integrin binding

2.4 Immune response against *Borrelia burgdorferi*

2.4.1 *Innate immunity*

Human immune defense can be divided into two parts; innate and adaptive immune response. Innate immune mechanisms are the first line of defense against invading pathogens. These mechanisms include the physical barriers described in chapter 2.2, specialized leucocytes (macrophages, dendritic cells [DC], granulocytes, natural killer cells), antimicrobial peptides, and the complement system.

Unspecific innate immune system is activated immediately upon contact with an invading pathogen. When *Borrelia* migrate from the tick into the human skin, the microbes soon encounter the components of the innate immune system (Petzke and Schwartz, 2015) and EM at the tick bite site is caused by a local innate immune response (Petzke and Schwartz, 2015, Sigal, 1997). The innate immune cells that are present in EM lesions are macrophages, neutrophils, and DCs (Müllegger et al., 2000, Salazar et al., 2003).

Although the cell membrane of *Borrelia* lacks LPS, numerous surface lipoproteins serve as pathogen-associated molecular patterns (PAMPs) recognized by pattern recognition receptors (PRRs) of the host immune cells (Petzke and Schwartz, 2015). TLRs are PRRs that recognize mainly extracellular and endosomal signals (Petnicki-Ocwieja and Kern, 2014). The main TLR that interacts with *Borrelia* is TLR2/1 heterodimer which, among other antigens, has been shown to recognize lipoprotein OspA of *Borrelia* (Alexopoulou et al., 2002, Hirschfeld et al., 1999, Oosting et al., 2011a, Petnicki-Ocwieja and Kern, 2014).

However, upon the initial contact with the host, *Borrelia* can evade the immune system by exploiting the proteins of the tick vector (Ramamoorthi et al., 2005). The outer membrane protein OspC of *Borrelia* binds tick salivary protein Salp15. Salp15 protects *Borrelia* from the immune system e.g. by interacting with DCs and consequently dampening the immune response (Hovius et al., 2008). OspC can also prevent the phagocytosis of macrophages although the mechanism behind the phenomenon is not understood (Carrasco et al., 2015).

The complement system is composed of multiple proteins acting together as a cascade finally resulting in the destruction of the target (de Taeye et al., 2013). The complement system can be activated via three different pathways (classical, alternative, and lectin pathways). *Borrelia* can evade all these activation pathways either by exploiting the complement regulator proteins of the host, exploiting tick proteins or by using its own complement evasion mechanisms (Stone and Brissette,

2017, de Taeye et al., 2013). Overall, many pathogens have at least one complement evasion mechanism to help them tolerate the innate immunity (Ermert and Laabei, 2018, Fernández et al., 2017, Yang et al., 2016).

2.4.2 *Adaptive immunity*

Adaptive immunity is considered as the second line of defense against invading pathogens because it requires the recognition of the antigens and, thus, it is activated rather slowly. Adaptive immunity is composed of mainly T-cell mediated mechanisms and B-cell maturation and antibody secretion. However, in addition to innate immunity, *Borrelia* evade also antibody mediated immunity e.g. by antigenic variation and by up- or downregulating some of its surface proteins (Liang et al., 2004b, Rogovskyy and Bankhead, 2013, Zhang et al., 1997). These strategies help in preventing the antibody recognition. However, despite the ability of *Borrelia* to evade adaptive immunity, antibodies recognizing *Borrelia* structures and surface proteins are eventually formed as evidenced by the established serology based laboratory diagnosis of infected patients (Dessau et al., 2017, Stone and Brissette, 2017).

2.4.3 *Cytokines*

Cytokines are a defense mechanism which is shared by the innate and adaptive immune response. They are soluble proteins secreted by many different cell types and they mediate the communication between the cells of the immune system. Interestingly, in addition to classical immune cells, cytokines can also be produced by brain microvascular endothelial cells upon contact with microbes (McLoughlin et al., 2017).

Many studies have shown that different cell types start producing cytokines when stimulated with *Borrelia* (Berende et al., 2010). *Borrelia* trigger the secretion of both pro- and anti-inflammatory cytokines by interacting with PRRs (especially TLRs). The quantitative cytokine secretion upon contact with *Borrelia* is influenced by the age and genetic factors of the patient (Oosting et al., 2011b, Oosting et al., 2016). It has also been suggested that different *Borrelia* genospecies might trigger different immune pathways and secretion of different set of cytokines (Cerar et al., 2016, Oosting et al., 2016).

2.4.3.1 ***CXCL13***

Cytokines that can recruit immune cells to the inflammatory foci are called chemokines. CXCL13 (also known as BCA-1 or BLC) is a chemokine which has been shown to attract B cells and, in fact, all mature B cells express C-X-C motif chemokine receptor 5 (CXCR5) which interacts with CXCL13 (Cyster et al., 2000, Gunn et al., 1998). However, in addition to B cells, also some other cell types, like memory T cells, can have the CXCL13 receptor on their surface.

CXCL13 is mainly expressed in peripheral lymphoid organs, like the spleen and the lymph nodes, guiding B cells to these tissues (Cyster et al., 2000). Interestingly, also endothelial cells have been shown to express CXCL13 on their surface in some inflammatory conditions (Amft et al., 2001). However, it is not known whether CXCL13 is actually produced by endothelial cells. It may also be secreted by some other cell type and then transendothelially transported onto endothelial surface (Amft et al., 2001, Middleton et al., 1997, Middleton et al., 2002) where GAGs like heparin sulphate and dermatan sulphate bind these transcytosed cytokines and, as a consequence, promote leucocyte migration (Middleton et al., 2002).

Besides its role as a cell trafficking chemokine, CXCL13 has other functions as well. It has been linked to the persistence of chronic inflammation and the induction of pain receptors (Jiang et al., 2016, Wu et al., 2016). CXCL13 has also antimicrobial activity towards both Gram-negative and Gram-positive bacteria *in vitro* (Yang et al., 2003). This activity is shared also with some other chemokines and it is speculated that antimicrobial properties are due to the cationic nature of these molecules. It has not been reported whether CXCL13 has antimicrobial activity towards *Borrelia*.

2.4.4 ***Immunity of Lyme neuroborreliosis***

Immunity of LNB has mainly been studied in rhesus macaques (Pachner et al., 1995b, Pachner et al., 1995a, Pachner et al., 2001a, Pachner et al., 2001b, Pachner et al., 2002, Pachner and Steiner, 2007). T cells and plasma cells are the main immune cell types in these *Borrelia* infected animals and the inflamed spinal cords are characterized by the presence of increased amounts of IgG, IgM and complement component C1q (Pachner and Steiner, 2007). In human LNB patients, a strong *Borrelia*-specific IgM and IgG antibody response can usually be observed and the patients have increased amounts of leucocytes in their CSF.

Many different cytokines have been shown to be elevated in the CSF of LNB patients (Cepok et al., 2003, Cerar et al., 2013, Grusell et al., 2002, Grygorczuk et

al., 2004, Henningsson et al., 2011, Liba et al., 2013, Moniuszko et al., 2014, Nordberg et al., 2011, Rupprecht et al., 2009). The concentration of CXCL13 has been shown to be extremely high reaching concentrations of even thousands of picograms per ml (Henningsson et al., 2016, Hytönen et al., 2014, Remy et al., 2017, Rupprecht et al., 2009, Schmidt et al., 2011, Senel et al., 2010, Sillanpää et al., 2013, Wagner et al., 2017). High concentrations of CXCL13 can be detected in the CSF of LNB patients before any discernible *Borrelia* specific antibody production (Rupprecht et al., 2008). Indeed, it is considered that once *Borrelia* transmigrate the BBB, CXCL13 is secreted in the CSF by immune cells, after which CXCL13 recruits B cells to cross the BBB and enter the CSF. Only then B cell derived plasma cells start producing *Borrelia* specific antibodies to the CSF. A schematic figure of the process is presented in Figure 7.

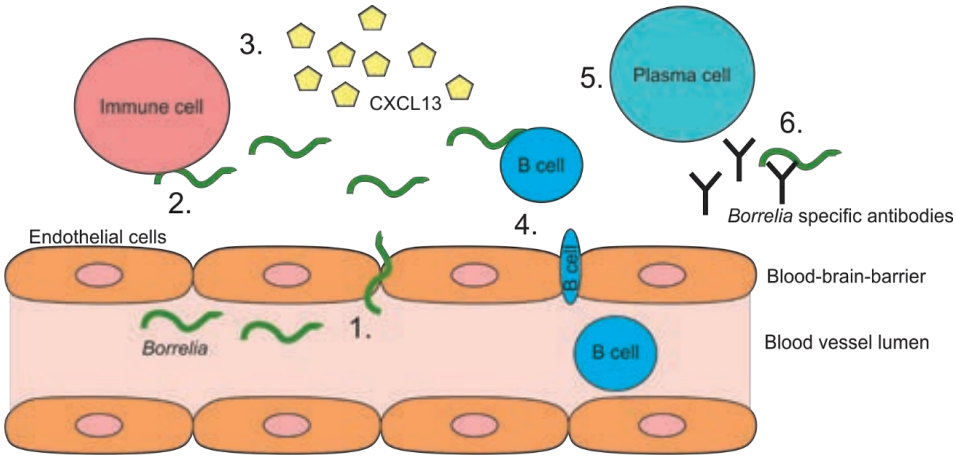

Figure 7. A schematic figure of the role of CXCL13 in immune reaction towards *Borrelia*. (1.) *Borrelia* transmigrate across the blood-brain barrier from the bloodstream into the central nervous system. (2.) Immune cells recognize *Borrelia* and (3.) start producing CXCL13. (4.) CXCL13 gradient recruits B cells into the CNS. (5.) B cells differentiate into plasma cells. (6.) Plasma cells secrete *Borrelia* specific antibodies. Adapted from (Rupprecht et al., 2008).

It is not clear which cell type or types are responsible for CXCL13 production in LNB. Studies have shown that it is produced by peripheral blood mononuclear cells (PBMCs) when the cells have been stimulated with *Borrelia in vitro* (Rupprecht et al., 2007). More precisely DCs of PBMC cell population seem to be the main cell type producing CXCL13 upon contact with *Borrelia* (Narayan et al., 2005). However, the role of PBMCs in CNS inflammation is unclear. Moreover, CXCL13 has been shown to be present also on endothelial cells of the periventricular areas of the brain in *Borrelia* infected rhesus macaques (Ramesh et al., 2009).

2.5 Laboratory diagnosis, treatment and prevention of Lyme borreliosis

2.5.1 *Laboratory diagnosis*

Although culturing of the infectious agents from a patient sample is the golden standard in the laboratory diagnosis of many pathogen mediated diseases, *Borrelia* culture and PCR based testing are both insensitive as diagnostic tools for LB. Instead, the laboratory diagnosis of LB rely on serology with the exception of EM (Dessau et al., 2017, Steere et al., 2016). Approximately half of the patients with EM have not yet developed *Borrelia* specific antibody response before they are diagnosed and treated and, thus, EM can be diagnosed clinically without the need of laboratory testing. All other disease manifestations are diagnosed and confirmed based on the clinical symptoms and serology based laboratory tests. However, serology based approach for laboratory diagnosis of LB has some drawbacks. In the first weeks of the infection, antibodies have not yet been formed and serological tests can give false negative results. It has been reported that in the USA, it takes over a month for all the patients to become *Borrelia* IgG positive (Steere et al., 2016). IgM response usually develops earlier, yet, in the early phase of LB, it is detectable only in less than 50% of the patients. Indeed, serological profiles of LB patients tend to be individual depending on e.g. the duration and dissemination of the disease, and on the treatment status (Aguero-Rosenfeld et al., 1996, Marques, 2015, Reed, 2002). Furthermore, both *Borrelia* specific IgM and IgG antibodies may persist for months after treated infection which hampers the use of serological testing in suspected reinfections. In the laboratory diagnosis of LB, also the seroprevalence of the population needs to be considered. In Finland, the overall seroprevalence of the population is 3.9% with some regional variation (van Beek et al., 2018). The highest prevalence can be found in the southern and eastern parts of Finland and the lowest prevalence in the North Finland.

Due to the above mentioned difficulties in serology based testing, novel methods to LB diagnostics are actively being developed. These methods include techniques such as transcriptomics, proteomics, and metabolomics (Badawi, 2017, Bouquet et al., 2016, Molins et al., 2015). Until any of these new methods are proven to work as diagnostic tests and have been verified with relevant patient material, serology is the best available laboratory method for diagnosis of LB. The patients are expected to have significant amount of *Borrelia* specific antibodies 6 – 8 weeks post infection and, moreover, patients whose disease has been ongoing for over 6 weeks, should have *Borrelia* specific IgG response (Dessau et al., 2017). A sole IgM response in these patients is not considered relevant without confirming IgM

specificity. The so-called two-tier laboratory testing approach in LB diagnostics combines multiple tests to achieve more accurate results (Dessau et al., 2017, Steere et al., 2016). The first step is an ELISA- or other solid-phase-based test which usually is quite sensitive but not necessarily specific. For this reason, positive samples in the first screen are confirmed with a second test which is a more specific immunoblot or a multiplex assay. The choice and the number of tests used, however, varies between laboratories.

Currently, there are no imaging methods available to be used as diagnostic tools for LB. However, some studies and case reports have been published on imaging of LB patients. Magnetic resonance imaging, single-photon emission computed tomography, and positron emission tomography (PET) imaging have revealed some differences in the metabolism of the brain, the lymph nodes, the spleen, and the joints of LB patients when compared with healthy controls (Aigelsreiter et al., 2005, Flemming et al., 2014, Kalina et al., 2005, Logigian et al., 1997, Newberg et al., 2002, Plotkin et al., 2005).

2.5.1.1 ***Laboratory diagnosis of Lyme neuroborreliosis***

According to the guidelines of the European federation of neurological societies (EFNS), the diagnosis of LNB in Europe should be based on relevant neurological symptoms, CSF pleocytosis, and the intrathecal production of *Borrelia* specific antibodies (Mygland et al., 2010). If all three criteria are fulfilled, LNB is considered as a definite diagnosis. In case only two of the above-mentioned criteria are fulfilled, a term "possible LNB" should be used. Although the guidelines state that there is not enough evidence for the use of CSF CXCL13 as a diagnostic marker for LNB and a clear cut-off value has not been defined, a growing body of evidence suggests that CSF CXCL13 is a sensitive and rather specific marker for LNB both in adults and children (Barstad et al., 2017, Bremell et al., 2013, Eckman et al., 2018, Hytönen et al., 2014, Markowicz et al., 2018, Pícha et al., 2016, Rupprecht et al., 2009, Schmidt et al., 2011, Senel et al., 2010, Sillanpää et al., 2013, Skogman et al., 2017, Tjernberg et al., 2011, Wutte et al., 2011, Yang et al., 2017). As explained in chapter 2.4.4, CXCL13 can be detected in the CSF before *Borrelia* specific antibodies are formed (Rupprecht et al., 2008). The use of CXCL13 in LNB diagnostics is further supported by the observation that the concentration of CXCL13 declines rapidly after antibiotic treatment (Bremell et al., 2013, Hytönen et al., 2014, Senel et al., 2010). Thus, it could be used as a biomarker for LNB in reinfections as well. However, increase in CSF CXCL13 concentration in some other diseases affecting the nervous system have also been reported (Dersch et al., 2015, Hytönen et al., 2014, Marra et al., 2010, Mothapo et al., 2015, Rubenstein

et al., 2013, Rupprecht et al., 2009, Schmidt et al., 2011). Interestingly, one of these conditions is neurosyphilis, a disease caused by *Treponema pallidum,* another spirochete. Also, patients with CNS lymphoma, cryptococcosis, HIV, African trypanosomiasis, and patients with some other inflammatory neurological diseases have been reported to have highly elevated CXCL13 concentartions in the CSF (Bremell et al., 2013, van Burgel et al., 2011, Courtioux et al., 2009, Kowarik et al., 2012, Schmidt et al., 2011). To overcome the lack of complete specificity of CXCL13 to LNB, combining the CSF leucocyte count to CXCL13 measurement has recently been suggested to further improve the specificity of CXCL13 (Markowicz et al., 2018). The laboratory tests used for detection of CXCL13 in the CSF are usually ELISA- or Luminex-based assays.

In addition to CXCL13, some studies have shown the elevation of other cytokines in the CSF of LNB patients but the diagnostic potential of these cytokines has not been further evaluated (Cepok et al., 2003, Cerar et al., 2013, Grusell et al., 2002, Grygorczuk et al., 2004, Gyllemark et al., 2017, Henningsson et al., 2011, Liba et al., 2013, Moniuszko et al., 2012, Moniuszko et al., 2014, Nordberg et al., 2011, Rupprecht et al., 2009).

2.5.2 *Treatment and prevention*

LB can be treated with antibiotics and, so far, antibiotic resistance has not been reported (Steere et al., 2016). According to Finnish guidelines and practices, EM can be treated with amoxicillin or doxycycline, and in the case of prolonged symptoms, ceftriaxone can also be used (Terveysportti: www.terveysportti.fi, accessed 26.7.2018)(Hytönen et al., 2008). Almost all of the patients recover after treatment but, for some reason, part of the patients have symptoms even after an antibiotic treatment (Steere et al., 2016). This condition is referred to as post-treatment Lyme disease syndrome. These patients do not have an ongoing active infection with live bacteria and, consequently, prolonged antibiotic treatment is of no value. The current understanding is that the ongoing symptoms are caused by immune dysregulation and autoimmune mechanisms (Lochhead et al., 2018, Steere et al., 2016).

There is no vaccine available for LB and, thus, the prevention of LB relies on avoiding contact with tick vectors (Steere et al., 2016). The best way to avoid contact is to wear long sleeves and trousers when outside in tick rich areas. Also, tick repellants can be used. Attached ticks should be removed from the skin immediately upon notice.

3 AIMS OF THE STUDY

It is not entirely understood how *Borrelia* migrate from the intial infection site to multiple distant organs and the laboratory diagnosis of LB requires development. To fill in some of the gaps in the knowledge of *Borrelia* pathogenesis and to develop and improve diagnostic methods, the following specific aims were set.

I. To study the pathogenesis of Lyme borreliosis, especially how *Borrelia* adhere to vascular wall and disseminate into distant tissues

II. To study the disseminated *Borrelia* infection in a live vertebrate host using *in vivo* imaging

III. To develop and evaluate new methods for laboratory diagnosis of Lyme borreliosis

4 MATERIALS AND METHODS

4.1 Bacterial strains and culture conditions (I-II)

All bacterial strains used in this study are listed in Table 2.

Wild type *Borrelia burgdorferi* N40 (studies I-II; kindly provided by Sven Bergström, University of Umeå, Sweden), *B. garinii* SBK40 (study I; isolated from skin biopsy), and *B. afzelii* A91 (study I; isolated from skin biopsy) were cultured in liquid Barbour-Stoenner-Kelly (BSK) II medium. Genetically modified *B. burgdorferi* B313 strains [study I; described in (Salo et al., 2011)] expressing the *dbpBA* operon (with the promoter sequence) of *B. burgdorferi* N40, *B. garinii* SBK40, or *B. afzelii* A91 were cultured in BSK II medium supplemented with 200 µg/ml kanamycin (Sigma, Steinheim, Germany). The growth phase of *Borrelia* was monitored by counting the bacterial cells in a Neubauer chamber and the experiments were performed when *Borrelia* were at a logarithmic growth phase. *Borrelia* from mouse tissue samples were cultured in BSK II medium supplemented with 50 µg/ml phosphomycin (Sigma) and 100 µg/ml rifampicin (Sigma) for six weeks and the growth was monitored every two weeks with a dark-field microscope. All *Borrelia* strains and samples were cultured in microaerophilic conditions at 33°C.

For cell adhesion assays, *Borrelia* were stained with carboxyfluorescein diacetate succinimidyl ester (CFSE; Molecular probes, Eugene, OR). *Borrelia* were washed once with phosphate buffered saline (PBS) and then labelled with 10 µM of CFSE in PBS in dark for 10 min at room temperature (RT). *Borrelia* were then washed with PBS containing 5% fetal bovine serum, counted in a Neubauer chamber and adjusted to 50 x 10^6 /ml in PBS containing 0.25% bovine serum albumin (BSA).

E. coli strains expressing recombinant *Borrelia* proteins are described elsewhere (Heikkilä et al., 2002a, Heikkilä et al., 2002b, Salo et al., 2011). *E. coli* BL21(DE3)pLysS used to overexpress recombinant DbpA and B proteins of *B. burgdorferi* N40 was cultured in lysogeny broth or agar supplemented with 34 µg/ml chloramphenicol (USB Corporation, Cleveland, OH) and 30 µg/ml kanamycin (Sigma) at 37°C. *E. coli* M15(pREP4) used to overexpress recombinant DbpA and B proteins of *B. garinii* SBK40 and *B. afzelii* A91 were cultured in lysogeny broth or agar supplemented with 25 µg/ml kanamycin (Sigma) and 34 µg/ml ampicillin (Sigma) at 37°C.

Table 2. Bacterial strains used in this study.

Bacterial strain	Genetic features / phenotype	Other special features	Reference
B. burgdorferi N40	cp26, lp54, lp17, lp25, lp28-2, lp28-4, lp28-5, lp36, lp38, cp9, cp32-4, cp32-5, cp32-7, cp32-9, cp32-10, cp32-12	isolated from a tick	BorreliaBase: www.borrelia-base.org; accessed 9.10.2018; Anderson et al., 1990
B. garinii SBK40	genome content not published, has at least lp54 (contains *dbpBA*)	isolated from the skin of a Finnish patient	Heikkilä et al., 2002a
B. afzelii A91	genome content not published, has at least lp54 (contains *dbpBA*)	isolated from the skin of a Finnish patient	Heikkilä et al., 2002a
B. burgdorferi B313	cp26, cp32-1, cp32-2, cp32-7, cp32-3, lp17	no lp54 (which contains *dbpBA*), high passage derivative of type strain B31, plasmids lost during prolonged *in vitro* cultivation	Zückert et al., 2004
B. burgdorferi B313 + pBSV2	cp26, cp32-1, cp32-2, cp32-7, cp32-3, lp17	transformed with pBSV2 (Km^r)	Salo et al., 2011
B. burgdorferi B313 + DbpAB/*B. garinii*	cp26, cp32-1, cp32-2, cp32-7, cp32-3, lp17	transformed with pBSV2 + *dbpBA*/*B. garinii* SBK40	Salo et al., 2011
B. burgdorferi B313 + DbpAB/*B. burgdorferi*	cp26, cp32-1, cp32-2, cp32-7, cp32-3, lp17	transformed with pBSV2 + *dbpBA*/*B. burgdorferi* N40	Salo et al., 2011
B. burgdorferi B313 + DbpAB/*B. afzelii*	cp26, cp32-1, cp32-2, cp32-7, cp32-3, lp17	transformed with pBSV2 + *dbpBA*/*B. afzelii* A91	Salo et al., 2011
E. coli BL21(DE3)pLysS + DbpA/*B. burgdorferi*	F$^-$ *ompT hsdS*$_B$(r_B^- m_B^-) *gal dcm* (DE3) pLysS (Cm^R)	transformed with pET-30 Ek/LIC + *dbpA*/*B. burgdorferi* N40 (Km^r)	Salo et al., 2011
E. coli BL21(DE3)pLysS + DbpB/*B. burgdorferi*	F$^-$ *ompT hsdS*$_B$(r_B^- m_B^-) *gal dcm* (DE3) pLysS (Cm^R)	transformed with pET-30 Ek/LIC + *dbpB*/*B. burgdorferi* N40 (Km^r)	Salo et al., 2011
E. coli M15(pREP4) + DbpA/*B.garinii*	F$^-$, Φ80ΔlacM15, thi, lac-, mtl-, recA+ , Km^R	transformed with pQE30 + *dbpA*/*B. garinii* SBK40 (Amp^r)	Heikkilä et al., 2002b
E. coli M15(pREP4) + DbpB/*B. garinii*	F$^-$, Φ80ΔlacM15, thi, lac-, mtl-, recA+ , Km^R	transformed with pQE30 + *dbpB*/*B. garinii* SBK40 (Amp^r)	Heikkilä et al., 2002a
E. coli M15(pREP4) + DbpA/*B. afzelii*	F$^-$, Φ80ΔlacM15, thi, lac-, mtl-, recA+ , Km^R	transformed with pQE30 + *dbpA*/*B. afzelii* A91(Amp^r)	Heikkilä et al., 2002b
E. coli M15(pREP4) + DbpB/*B. afzelii*	F$^-$, Φ80ΔlacM15, thi, lac-, mtl-, recA+ , Km^R	transformed with pQE30 + *dbpB*/*B. afzelii* A91 (Amp^r)	Heikkilä et al., 2002a

4.2 Cell lines (I)

All cell lines were collected and used following the ethical guidelines (see chapter 4.12).

4.2.1 *Human foreskin fibroblasts (I)*

The primary human foreskin fibroblasts (HFFs) were kindly provided by Docent Tytti Vuorinen (Institute of Biomedicine, University of Turku) and were cultured in Dublecco's modified Eagle's medium (Invitrogen, Waltham, MA) with 7% fetal calf serum (HyClone, Logan, UT) and gentamicin (Nalgene, Rochester, NY) in a cell culture incubator with 5% CO_2 at 37°C. The cells were passaged once a week.

4.2.2 *Human umbilical vein endothelial cells (I)*

Primary human umbilical vein endothelial cells (HUVECs) from individual donors were used in stationary adhesion studies and in the detection of proteoglycan expression, and were kindly provided by Professor Marko Salmi (Institute of Biomedicine, University of Turku). The cells were cultured in EGM™-Plus BulletKit™ medium (Lonza, Basel, Switzerland) with penicillin and streptomycin (Sigma). The primary HUVECs used in adhesion studies under flow conditions were pooled cells from multiple donors (Lonza). These cells were cultured in EGM™-2 medium supplemented with BulletKit™ (Lonza). All HUVECs were cultured in a cell culture incubator with 5% CO_2 at 37°C.

4.2.3 *Human brain microvascular endothelial cells*

Immortalized human brain microvascular endothelial cells (HBMECs) were kindly provided by Professor Tomomi Furihata (Chiba University, Chiba, Japan) and have been described elsewhere (Furihata et al., 2015, Kamiichi et al., 2012). The cells were cultured in Complete Medium with serum (Cell Systems, Kirkland, WA) supplemented with penicillin and streptomycin (Sigma) and 4 µg/ml Blasticidine S (Sigma) in a cell culture incubator with 5% CO_2 at 33°C. The cells were seeded and cultured in medium containing Cultureboost-R™ (Cell Systems) 1×10^5 /ml or 4×10^5 /ml on culture dishes and Costar™ Transwell™-COL inserts (Corning Incorporated, Corning, NY), respectively. The cells were grown for three days after which the medium was changed to Complete Medium with serum and antibiotics but no Cultureboost-R™. In addition, 180 nM of hydrocortisone

(Sigma) was added to the culture. The cells were then cultured for additional nine days (altogether 12 days post inoculation) and the medium was changed every other day to Complete Medium with serum, antibiotics, and hydrocortisone but no Cultureboost-R™. All experiments were performed 12 days post inoculation.

4.3 Tissue samples (I-IV)

All tissue samples were collected and used following the ethical guidelines (see chapter 4.12).

4.3.1 *Paraffin-embedded human tissues (I)*

Human tissue samples used in immunohistochemical stainings were kindly provided by Mirva Söderström (Department of Pathology, Turku University Hospital). Tissues were fixed with formalin for 24 hours, dehydrated, paraffin-embedded and sectioned.

4.3.2 *Cerebrospinal fluid samples (III-IV)*

Retrospectively identified CSF samples had been obtained from patients by lumbar puncture after which the samples were sent to the Clinical microbiology laboratory of Turku University Hospital at RT. The samples were stored at 4°C until the initial diagnostic assays were performed. After that, the samples were stored in -20°C.

In study III, the samples were obtained from 43 LNB patients, 19 non-LNB control subjects (samples sent to the Clinical microbiology laboratory of Turku University Hospital for *Borrelia* antibody analysis and found to be *Borrelia* antibody negative), 18 TBE patients, and 31 multiple sclerosis (MS) patients. Follow-up samples from 23 out of the 43 LNB patients obtained after the antibiotic treatment (6-380 days after intravenous ceftriaxone and /or oral doxycycline) were also analyzed. In study IV, the samples (n = 225) were from 220 individual patients with the final diagnosis available for 94 of them (13 LNB patients, 13 LB patients, 9 patients with suspected LNB, 9 TBE patients, and 50 *Borrelia* antibody negative patients).

4.3.3 *Histology of mouse joint samples (II)*

The tibio-tarsal joints of mice were formalin-fixed, demineralized, embedded in paraffin, sectioned, and stained with hematoxylin-eosin. Joint inflammation was analyzed from sagittal joint sections and scored on a scale from zero to six based on the evaluation of synovial proliferation and the signs of active and chronic inflammation. The researcher was unaware of the infection status of the mice.

4.4 Detection of proteoglycan expression of tissues and cells (I)

4.4.1 *Immunohistochemistry (I)*

For detection of decorin and biglycan from human tissues, sectioned tissue samples were incubated with monoclonal biglycan antibody clone 4E1-1G7 (dilution 1:1000; Abnova, Taipei, Taiwan) or monoclonal decorin antibody clone 9XX (dilution 1:300; Santa Cruz Biotechnology, Dallas, TX) for 1 hour at RT. Horseradish peroxidase (HRP) -labeled secondary antibody treatment and diaminobenzidine-based detection were performed with EnVision detection kit (Dako, Hamburg, Germany) using an automated staining machine (LabVision Corporation, Fremont, CA). After secondary antibody, epitope retrieval was performed in a microwave oven in Tris - ethylenediaminetetraacetic acid (EDTA) buffer (pH 9).

4.4.2 *Antibody staining of cultured cells (I)*

To detect biglycan and decorin expression on cultured HUVECs and HBMECs, the cells were grown on 8-well chamber slides (HUVECs: Nunc™ Lab-Tek™ Chamber Slides; HBMECs: Nunc™ Lab-Tek™ II CC2™ Chamber Slides; Thermo Fisher Scientific, Vantaa, Finland) until confluency (HUVECs) or for 12 days (HBMECs). The cells were fixed with acetone, washed twice with 0.05% Tween® 20 in PBS (PBS-T) and stained with monoclonal anti-biglycan clone 3E2 (HUVECs; dilution 1:50; Dako), monoclonal anti-biglycan clone 4E1-1G7 (HBMECs; dilution 1:50; Abnova) or monoclonal decorin antibody clone 9XX (dilution 1:50; Santa Cruz Biotechnology) for 1 h at 37°C. Unbound antibody was removed by washing the cells with PBS-T. HRP-labeled anti-mouse IgG (dilution 1:1000, Santa Cruz Biotechnology) was used as a secondary antibody and incubated with the cells for 1 hour at 37°C. After washing the cells, AEC substrate

[1mM 3-amino-9-ethylcarbazole, 5% (v/v) dimethylformamide, 0.1% (v/v) hydrogen peroxidase in acetate buffer (pH 5.5)] was used for detection. Cells without primary antibody served as controls.

4.4.3 *Western blot analysis (I)*

For detection of proteoglycans from HUVECs, the cells were washed once with serum containing growth medium and once with PBS. Washed cells were then lysed with lysis buffer (20% Triton X-100, 1.5 M NaCl, 0.1 M Tris-base, 15 mM $MgCl_2$) for 1 h on ice. Cell debris was removed by centrifugation and the supernatant fraction was collected for analysis.

To detect proteoglycans from HFFs, the growth medium of the cells near confluence was changed to starvation medium (medium without serum) and the incubation of the cells was continued overnight. Proteoglycans were detected in the starvation medium which was first concentrated ca. tenfold with centrifugal filters (Amicon Ultra-15 centrifugal filter unit 10000NMWL, Millipore, Cork, Ireland).

All samples were treated with chondroitinase ABC (Sigma) for 3 h at 37°C in chondroitinase ABC buffer (0.3 M Tris, 0.06% BSA, 30 mM NaAc, pH 8,0) before the Western blot analysis. To detect biglycan and decorin, the blot was stained with monoclonal anti-biglycan clone 3E2 (dilution 1:500; Santa Cruz Biotechnology) or monoclonal decorin antibody clone 9XX (dilution 1:500; Santa Cruz Biotechnology) and HRP-labeled anti-mouse IgG (dilution 1:10000; Santa Cruz Biotechnology). As a loading control, glyceraldehyde 3-phosphate dehydrogenase (GAPDH) detection was performed using monoclonal antibody clone 6C5 (dilution 1:20000; HyTest Ltd, Turku, Finland). Also controls without primary antibody were included in the analysis. Enhanced chemiluminescence (ECL) reagents (GE Healthcare, Buckinghamshire, UK) were used for detection.

4.4.4 *Flow cytometry analysis (I)*

HUVECs treated with small interfering RNA (siRNA) were detached using 5 mM EDTA. Biglycan expression was then detected using monoclonal biglycan antibody clone 4E1-1G7 (dilution 1:1000; Abnova) and adenylate kinase 1 antibody (in Vivo Biotech Services, Henningsdorf, Germany) was used as a negative control. R-phycoerythrin-conjugated goat anti-mouse IgG (Southern Biotech, Birmingham, AL) was used as a secondary antibody. The fluorescence was detected using FACSCalibur instrument (Becton-Dickinson, Franklin Lakes, NJ) and the

data were analyzed with FlowJo software (Tree Star, Ashland, OR). The percentage of positive cells was calculated by subtracting the values obtained with negative control antibody from the values obtained with the biglycan antibody. Geometric mean fluorescence intensities (MFIs) were calculated without subtracting the negative control antibody values.

HBMECs were detached from culture dish with 0.1% trypsin-EDTA. The cells were then washed once with serum containing culture medium and fixed for 5 min at 33°C with 4% paraformaldehyde (Santa Cruz Biotechnology). The fixative was removed by washing the cells three times with PBS. Unspecific protein-protein interactions were blocked by treating the cells with 0.1 M glycine in PBS for 5 min at RT. Proteoglycan expression was detected using monoclonal biglycan antibody clone 4E1-1G7 (dilution 10µg/ml; Abnova) or monoclonal decorin antibody clone 9XX (dilution 10µg/ml; Santa Cruz Biotechnology). Mouse IgG1 (1 µg; Caltag Laboratories, Carlsbad, CA) and mouse IgG2a κ clone eBM2a (1 µg; Thermo Fisher Scientific) were used as isotype control antibodies. Goat anti-mouse IgG Alexa Fluor 488 (1:1000; Invitrogen) was used as a secondary antibody. Also, as a control, a sample treated with the secondary antibody only was analyzed. The fluorescence was detected using Accuri™ C6 (Becton-Dickinson) or LSR II (Becton-Dickinson) and the data was analyzed with Flowing software 2 (version 2.5.1. by Perttu Terho, Turku Center for Biotechnology, University of Turku, Finland).

4.4.5 *Expression of proteoglycan mRNA by the cells*

RNA was extracted from HBMECs with RNeasy kit (Qiagen, Hilden, Germany) according to the manufacturer's instructions. Also, on-column DNA digestion was performed as instructed. Complementary DNA (cDNA) was created with QuantiTect® Reverse Transcription kit (Qiagen) by using extracted RNA samples as starting material. As a control, reactions without reverse transcription enzyme were also performed. The relative quantification of biglycan and decorin messenger RNA (mRNA) was performed using reverse transcription PCR (RT-PCR) with SYBR Green (Roche, Basel, Switzerland) and LightCycler® 480 (Roche) according to the manufacturer's instructions. Expression of GAPDH mRNA was used as a reference. The primer sequences and PCR conditions used are described in Table 3.

Table 3. Primers and PCR conditions used in this study.

Primers used in mRNA analysis	PCR conditions in mRNA analysis
Biglycan forward (based on sequence with accession number NM_001711.5): GGCCTACTACAACGGCATCAG Biglycan reverse (NM_001711.5): AAAGTGGCCGGCTGCA Decorin forward (BC005322.1): TCTGCCCACCTGGACACA Decorin reverse (BC005322.1): TGGACCGGGTTGCTGAAA GAPDH forward (BC025925.1): CTTAGCACCCCTGGCCAAG GAPDH reverse (BC025925.1): TGGTCATGAGTCCTTCCACG	1. 50°C 2 min 2. 95°C 10 min 3. 40 cycles: • 95°C 10 s • 60°C 10 s • 72°C 10 s 4. melt curve 5. 40°C
Primers used in quantitative PCR	**PCR conditions in quantitative PCR**
flaB forward (Jenkins et al., 2012): TCAAGAAATAATGCTATTAATGCTGCTAA *flaB* reverse (Jenkins et al., 2012): CCAGCAGCATCATCAGAAGCT	1. 90°C 5 min 2. 45 cycles: • 95°C 10 s • 58°C 10 s • 72°C 12 s 3. melt curve 4. 40°C

4.4.6 *Small interfering RNA silencing of biglycan expression (I)*

The cells were grown with EGM™-Plus BulletKit™ medium (Lonza) without antibiotics for 24 h before the mRNA expression of biglycan was silenced with ON-TARGET plus human biglycan smart pool siRNA (Thermo Fisher Scientific, Dharmacon, Vantaa, Finland). Biglycan siRNA or control siRNA were transfected into the cells with a lipofection kit (Lipofectamine RNAiMAX, Invitrogen, Thermo Fisher Scientific) according to the manufacturer's instructions. The cells were then grown for additional three days before further analyses.

4.5 Purification of recombinant proteins from *Escherichia coli* (I)

The recombinant His-tagged DbpA and B proteins were purified under native conditions from *E. coli* M15 and BL21 strains with Ni-NTA agarose (Qiagen). Isopropyl β-D-1-thiogalactopyranoside (IPTG) induced *E. coli* cultures were harvested and the cell suspension was resuspended in Na-phosphate buffer (pH 8). Benzonase (1 µl/ml; Merck Millipore, Burlington, MA) and 1 mM protease inhibitor phenylmethylsulfonyl fluoride (PMSF) were added to the suspension after which the bacterial cells were lysed by sonication. Cell debris was removed by

centrifugation and the supernatant lysate containing the recombinant proteins was collected. His-tagged recombinant proteins were then coupled with Ni-NTA agarose beads. The beads were washed and bound proteins were eluted with rising amounts of imidazole (up to 200 mM). The purity of the eluted proteins was verified by standard SDS-PAGE staining (SimplyBlue™ SafeStain; Invitrogen) after which the proteins were dialyzed against PBS. The concentrations of the dialyzed proteins were measured with Pierce™ BCA Protein Assay Kit (Thermo Fisher Scientific) according to the manufacturer's instructions.

4.6 Protein adhesion experiments (I)

4.6.1 *Adhesion of recombinant Dbps to proteoglycans in static conditions (I)*

Purified recombinant Dbp proteins were coated on enhanced binding microtiter plate strips (Thermo Fisher Scientific) 10 µg/ml 100 µl/well for 1 h at 37°C after which the wells were blocked with 1% BSA. Biotinylated biglycan (10 nM; Sigma, biotinylated with EZ-Link NHS-LC-Biotin (Pierce, Rockford) according to manufacturer's instructions)) was then allowed to adhere to the Dbps. Unbound biglycan was removed by washing the wells with PBS-T and the bound biglycan was detected using alkaline phosphatase conjugated to streptavidin (1 µg/ml; Pierce™, Thermo Fisher Scientific). The results were measured with Multiskan EX spectrophotometer (Thermo Fisher Scientific) and expressed as OD_{405} values subtracted with the average absorbance of wells without biotinylated proteoglycan.

To inhibit the adhesion of DbpB of *B. garinii* and DbpB of *B. burgdorferi* to biglycan, the inhibitors were incubated with the Dbps coated on microtiter plates for 1 h at 37°C. After the incubation, biotinylated biglycan was added to the reaction and allowed to adhere to the Dbps. Detection of bound biglycan was then performed as mentioned above. Dermatan sulphate (50 µg/ml, Sigma), chondroitin-4-suphate (50 µg/ml; Sigma), and chondroitin-6-sulphate (50 µg/ml, Sigma) were used as inhibitors. Biglycan (0.1 µM) and BSA fraction V (1 µM; Serological Proteins Inc., Kankakee, IL) were used as a positive and a negative control, respectively.

4.6.2 *Adhesion of recombinant Dbps to proteoglycans under flow (I)*

The affinity of Dbps to biglycan under liquid flow was analyzed by surface plasmon resonance assay with Biacore® X (GE Healthcare) according to the manufacturer's instructions with a flow rate of 10 µl/min. Purified and dialyzed Dbps were concentrated with centrifugal filters 4000 g 20 min at 4°C (Amicon Ultra-15 centrifugal filter unit 10000NMWL; Merck, Millipore) and immobilized on CM5 sensor chips (GE Healthcare) 50 µg/ml in 10 mM sodium acetate buffer (pH 5) by amine coupling (GE Healthcare) according to the manufacturer's instructions. Control cells in sensor chips were treated with the same sodium acetate buffer lacking the adhesins. Biglycan was diluted to 4-(2-hydroxyethyl)-1-piperazineethanesulfonic acid (HEPES) running buffer (GE Healthcare) and injected into the flow cells at concentrations of 0.1 µM, 0.5 µM, and 1 µM. BSA dissolved in running buffer (1 µM) was used as a negative control ligand. The data was analyzed using BIAevaluation software version 4.1 (GE Healthcare).

4.7 Adhesion of *Borrelia* to endothelial cells (I)

4.7.1 *Adhesion of Borrelia to endothelial cells under static conditions (I)*

For bacterial adhesion assays, HUVECs were cultured on Lab-Tek 8-well chamber slides (Nunc, Rockhester, NY) for two days and HBMECs were cultured on ViewPlate-96 Black plates (PerkinElmer, Waltham, MA) for 12 days. The cells were fixed with ice cold acetone for 15 min at RT. The fixative was removed by washing the cells twice with PBS-T. The nuclei of HBMECs were stained with 4',6-diamidino-2'-phenylindole dihydrochloride (DAPI; 2.5 µg/ml) for 5 min at RT and the actin cytoskeletons of HBMECs were stained with Alexa Fluor™ 568 Phalloidin (Thermo Fisher Scientific) for 60 min at RT. Unbound dyes were removed by washing the cells twice with PBS. CFSE-stained *Borrelia* (10^7 bacteria) were allowed to adhere to the cells for 60 min at 37°C. Unbound bacteria were removed by washing the wells twice with PBS. After the washes, 100µl of PBS was added to the wells of 96-well plates while the chamber slides were left to dry. *Borrelia* adhered to HUVECs were visualized with confocal microscope Zeiss LSM 780 (Oberkochen, Germany) and images of 5 to 10 random fields per well were recorded. *Borrelia* adhered to HBMECs were imaged with EVOS FL Auto Cell Imaging System (Thermo Fisher Scientific) and two random fields per well were recorded (ca. 400 cells/field). The data were analyzed with ImageJ software (developed at the National Institutes of Health, Bethesda, MD). Adhesion of *Borrelia* to

HUVECs is reported as bacteria per field and the adhesion of *Borrelia* to HBMECs is reported as bacteria per 100 cells.

4.7.2 *Inhibition of adhesion of Borrelia to endothelial cells (I)*

Inhibition assays were performed to find out the possible binding ligand of *Borrelia* in HUVECs. Biglycan (1 µM; from bovine cartilage, Sigma), dermatan sulphate (50 µg/ml; Sigma), and chondroitin-6-sulphate (50 µg/ml; Sigma) were used as inhibitors. The inhibitors were pre-incubated with CFSE-labelled *Borrelia* for one hour at 37°C. As a control, reactions without inhibitors were also perfomed. After the pre-incubation, the assay was carried out like the adhesion of *Borrelia* to HUVECs under static conditions.

Borrelia-HUVEC adhesion was also inhibited by removing the GAG chains from the endothelial cell layer with chondroitinase ABC (Sigma). The cells were grown for two days on Lab-Tek 8-well chamber slides (Nunc), washed twice with PBS, and treated with 10 mM chondroitinase ABC (diluted in enzyme buffer; 50 mM Tris Base, 5 mM sodium acetate, 0.01% BSA) in Roswell Park Memorial Institute medium (RPMI 1640; Thermo Fisher Scientific) for two hours at 37°C in a CO_2 incubator. The cells were then washed and CFSE-stained *Borrelia* were allowed to adhere to the cells as in the static adhesion experiment.

4.7.3 *Adhesion of Borrelia to endothelial cells under flow (I)*

Adhesion of *Borrelia* to HUVECs was analyzed under flow conditions. HUVECs were seeded on Ibidi 1 µ-SlideVI$^{0.4}$ ibiTreat flow chamber slides (Ibidi GmbH, Planegg, Martinsried, Germany) at a density of 1.8×10^6 /ml and grown to two days post-confluence. During the culture, the culture medium was changed daily. To verify the confluency of the cell layer, the cells were stained with CellMask™ Deed Red plasma membrane stain (Molecular Probes).

Borrelia were stained with fluorescent CellMask™ Orange plasma membrane stain (1:2000; Molecular Probes), adjusted to 10^8 bacteria/ml in Hanks's Balanced Salt Solution (HBSS) and transferred into 10 ml syringes. The syringes were then connected to flow chamber inlets using silicon tubing elbow adaptors (Ibidi GmbH) and placed in a syringe pump apparatus (Model: NE1000, New Era Pump Systems Inc., Farmingdale, NY). *Borrelia* were perfused through flow chamber channels at 1 dyne /cm^2 which corresponds the reported physiological shear stress of post-capillary venules (Ebady et al., 2016). Interactions between *Borrelia* and HUVECs were monitored by recording two-minute videos with a custom-built

spinning disk confocal microscope (Quorum Technologies Inc., Guelph, ON, Canada) equipped with a Zeiss Axiovert 200M inverted fluorescence microscope with an EMCCD camera at 15 frames /second (25 × objective). The videos were analyzed in Volocity software (PerkinElmer). Brightly fluorescent *Borrelia* which paused during flow through a 100 µm × 30 µm field of interest were counted and the results were expressed as bacteria per 120 seconds.

4.8 Transmigration of *Borrelia* across the endothelial cell layer

4.8.1 *Characterization of the permeability of HBMEC cell layer*

Before transmigration experiments, the permeability of HBMEC cell layer was analyzed with three different methods.

To analyze the free flow of ions across the cell layer, transendothelial electrical resistance (TEER) of the cells grown in transwell chambers was measured with EVOM2 Epithelial Volt/Ohm Meter (World Precision Instruments, Sarasota, FL) according to the manufacturer's instructions with an STX2 electrode (World Precision Instruments).

To measure whether small molecules can passively cross the HBMEC layer, the cells were incubated with small molecule compound Lucifer yellow (LY; 0,45kDa). The amount of LY that passed through the cellular layer during the incubation was measured. HBMECs were washed once with LY buffer (20 mM HEPES, 1.25 mM $CaCl_2$, 0.5 mM $MgCl_2$ in HBSS, pH 7.4) after which 670 µl of the buffer was added to the basolateral compartment and 150 µl of freshly dissolved LY in LY buffer (0.1 mg/ml; Sigma) was added on top of the cells to the apical compartment. Cells were then incubated at 33°C. At time points 2, 4, 6, 8, 15, 30, and 60 minutes a 10 µl sample was removed from the basolateral compartment, mixed with 90 µl of LY buffer and transferred into a 96-well plate (96F Nontreated White Microwell SI; Thermo Fisher Scientific). Also, a dilution series of LY was prepared and added to the 96-well plate to create a standard curve. The fluorescence of the samples was then measured with Infinite® 200 PRO (Tecan, Männedorf, Switzerland). The permeability coefficient was determined as described elsewhere (Takata et al., 2013).

To analyze the ability of HBMECs to form tight junctions, tight junction protein zonula occludens-1 (ZO-1) was stained with fluorescent antibody. The cells were grown on ViewPlate-96 Black plates (PerkinElmer) for 12 days. The cell culture medium was removed and the cells were fixed with 4% paraformaldehyde (PFA;

Santa Cruz Biotechnology) for 15 min after which the fixative was removed by washing the cells three times with PBS. The cells were permeabilized with 0.1% Triton™ X-100 in PBS for 15 min, washed and blocked with 3% BSA in PBS for 1 h. Fluorescent ZO-1 antibody (Thermo Fisher Scientific) was diluted in the blocking solution 1:500 and incubated with the cells for 3 h in the dark. Unbound antibodies were removed by washing the cells three times with PBS after which the nuclei of the cells were stained with 2.5 µg/ml of DAPI (Sigma) for 5 min. The cells were then washed with PBS and imaged with EVOS FL Auto Cell Imaging System (Thermo Fisher Scientific; 20x objective). All incubations were performed at room temperature.

4.8.2 *Transmigration analysis*

HBMECs were cultured on Costar™ Transwell™-COL inserts (Corning Incorporated) for 12 days after which the cells were washed with PBS and 10^7 *Borrelia* in cell culture medium were added to the apical side on top of the membranes. *Borrelia* were allowed to transmigrate for 5 h after which the medium containing transmigrated *Borrelia* was removed from the basolateral compartment. The amount of transmigrated *Borrelia* was analyzed by extracting the DNA from the medium samples with High Pure PCR Template Preparation kit (Roche) as instructed by the manufacturer. DNA was then used as a template in quantitative PCR (qPCR).

Quantitative PCR was performed by using the *flaB* gene as a target with SYBR Green (Roche) and LightCycler® 480 (Roche) according to the manufacturer's instructions. Standard curve was prepared by extracting DNA with High Pure PCR Template Preparation kit from a known number of spirochetes. A standard curve was prepared from each of the studied genospecies. The qPCR protocol and the primers are described in Table 3.

4.9 *In vivo* imaging of Lyme borreliosis (II)

4.9.1 *Experimental design (II)*

The experimental design is presented in Figure 8. *B. burgdorferi* N40 strain was used to infect twenty-two C3H/HeNhsd mice (Harlan Laboratories, Horst, the Netherlands). Before the infection, *Borrelia* were washed twice with PBS and adjusted to 10^7 bacteria/ml in PBS. Mice were infected intracutaneously in the lower back with a dose of 10^6 bacterial cells (100 µl). Four mice were injected only with

an equal volume of sterile PBS to serve as infection controls. After four weeks of infection, eight of the *Borrelia*-infected mice were treated with antibiotics by administrating 25 mg /kg of ceftriaxone (Rocephalin®; Roche, Espoo, Finland) subcutaneously twice a day for a total of five days. The joint swelling of each mouse was monitored once a week by measuring the mediolateral diameter of the hind tibio-tarsal joints. The measurer was unaware of the infection status of the mice.

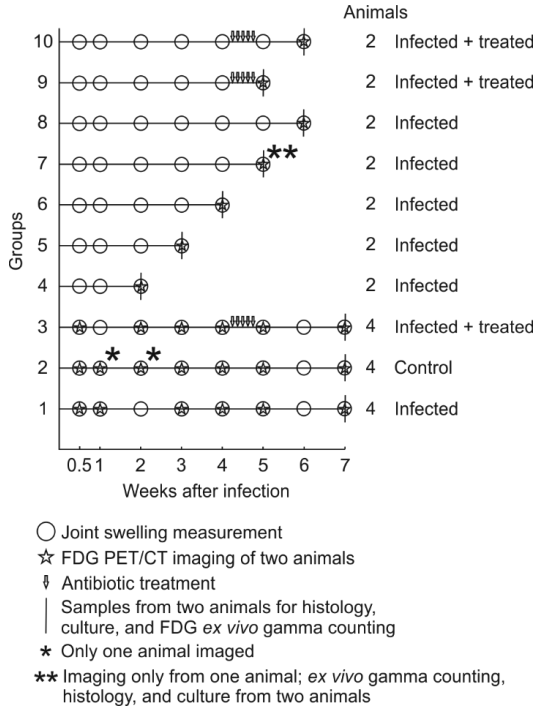

Figure 8. Experimental design of the *in vivo* imaging study. Twenty-two mice were infected with *Borrelia* and four mice were left as uninfected controls. Eight of the infected mice were treated with antibiotics four weeks after infection. Modified from the original publication II.

Two infected mice were imaged with combined positron emission tomography/computed tomography (PET/CT) and killed each week from two weeks up to seven weeks after infection. Whole blood, plasma, thymus, lungs, lymph nodes, liver, pancreas, spleen, kidney, small intestine, a piece of muscle, a bone sample from tibia, white adipose tissue, brown adipose tissue, brain, and urine were collected from the mice for *ex vivo* gamma counting. At the time of imaging, the more swollen hind tibio-tarsal joint was analyzed by *ex vivo* gamma counting and histology. The other hind tibio-tarsal joint, skin sample form ear, the bladder and the heart were also collected for *ex vivo* gamma counting and these tissues were also subjected to *Borrelia* culture.

Six mice (two infected, two infected and treated, and two controls) were followed throughout the experiment by imaging them first three days after infection and then once a week for a total of seven weeks. The mice were then killed and tissues collected for further analyses.

4.9.2 *Positron emission tomography/computed tomography (II)*

Mice were fasted for 4 h before PET/CT imaging. Anaesthetized mice were intravenously injected with [^{18}F]fluorodeoxyglucose ([^{18}F]FDG; 10 ± 0.28 MBq) via cannulated tail vein. A 20 min static PET imaging with Inveon Multimodality PET/CT (Siemens Medical Solutions, Knoxville, TN) was performed an hour after tracer injection. Before PET imaging, CT was performed for anatomical reference and for attenuation correction. This enabled defining regions of interest to specific organs so that quantitative PET analysis could be performed with Inveon Research Workplace 4.1 software (Siemens Medical Solutions, Malvern, PA). Quantitative PET data was analyzed from tibio-tarsal joints and axial and inguinal lymph nodes. Blood glucose concentrations of the mice were monitored with a glucometer (Bayer Contour, Bayer, Leverkusen, Germany) before the [^{18}F]FDG injection and again after the PET imaging. The tracer accumulation was expressed as standardized uptake values with blood glucose correction (*in vivo* SUV_{gluc}).

Ex vivo gamma counting was performed from excised tissues with a gamma counter (Triathler 3''; Hidex, Turku, Finland). The radioactivity measurements were corrected for the radionuclide decay to the time of the injection, weight of the tissue and animal, and blood glucose concentration. The results were expressed as *ex vivo* SUV_{gluc}.

4.10 Cytokine analyses (III-IV)

4.10.1 *Multiplex cytokine analysis (III)*

Cytokine levels of CSF samples were measured with a magnetic bead suspension array using the Bio-Plex Pro Human Cytokine 21- and 27-plex panels (Bio-Rad Laboratories, Hercules, CA) as previously described (Nieminen et al., 2014, Santalahti et al., 2016, Wang et al., 2016). Standard curves for each analyte were generated using recombinant cytokines included in the kit. Standards were analyzed in duplicates and human samples in one well. Individual concentration readings which remained below the measuring range of the assay were given a value

that corresponded to a half of the lowest standard concentration of the respective cytokine analysis. Concentrations over the detection range were given a value that was 1.5 times the value of the highest standard concentration.

4.10.2 *Measurement of CXCL13 concentration (III-IV)*

The concentration of cytokine CXCL13 was measured of the CSF (studies III- IV) and *Borrelia*-stimulated HBMEC culture supernatant samples with an ELISA-based human CXCL13 kit (Quantikine, R&D Systems, Minneapolis, MN) according to the manufacturer's instructions as previously described (Hytönen et al., 2014). Samples with a concentration below the standard curve of the assay were given a value that corresponded to a half of the value of the lowest point of the standard.

CXCL13 levels were also determined with a point-of-care (POC) test (study IV; ReaScan®; Reagena, Siilinjärvi, Finland) according to the manufacturer's instructions. Briefly, 100 µl of CSF was mixed with a conjugate and then transferred to the POC test cassette. The reaction was continued for 20 min after which the test cassette was placed in a cassette reader. The results were given in arbitrary ReaScan® values.

4.11 Statistical analyses (I-IV)

In all experiments (studies I, II, and IV), the normality of data was tested with the Shapiro-Wilk test. Statistical significance of differences in cell adhesion, transmigration, and microtiter plate assays was determined from at least three independent experiments by Analysis of Variance (ANOVA, IBM SPSS Statistics versions 21, 22, or 23). Also, the statistical analyses used to study the differences between the groups of mice (normally distributed data) were carried out with a two-tailed independent samples t-test or with ANOVA. In all ANOVA calculations, Post Hoc comparisons between means were done with Dunnett t-test whenever there was a clear control. Otherwise Tukey's honestly significant difference test was used. The correlations between normally distributed data were calculated with Pearson's method and correlations between skewed data were calculated with Spearman correlation method.

Bacterial binding to siRNA treated cells (study I) was analyzed with two independent experiments and two replicates in each experiment. Five random images were obtained from each replicate. The statistical significance of differences in bacterial

binding to siRNA treated HUVECs was determined with independent-samples t-test from a total of 20 images.

In multiplex analyses (study III), continuous variables were characterized using medians and range of values, and in case of categorical variables, frequencies and percents were used. Mann-Whitney U test was used to test the difference in age between the groups, and for sex, Pearson's chi-squared test was used. Differences in cytokine concentrations between patient groups (LNB, non-LNB controls, TBE, and MS) were tested using independent samples t-test for logarithmic transformed variables, and Bonferroni's method was used to correct the p values for multiplicity. To find the most important cytokines to distinguish the patient groups, the random forests method was used. The cytokines were ordered using variable importance, which is calculated by the mean decrease in the Gini coefficient. Paired samples t-test was used to test the difference in cytokine concentrations before and after treatment in LNB patients. Logarithmic transformation was made for the data. Nine cytokines with the smallest p values were presented using box-plots. In all cytokine analyses, the natural logarithmic transformation was used to achieve the normality of the distributions and all of the results and figures are presented using transformed variables. Statistical analyses were carried out using SAS System for Windows, version 9.4 (SAS Institute Inc., Cary, NC).

4.12 Ethics (I-IV)

All tissues of human origin were handled following strict anonymity practices.

Primary HUVECs (study I) were isolated from human umbilical cords. Fresh umbilical cords were recovered from healthy females at the Obstetrics and Gynecology Department of Turku University Hospital. The donors provided informed consent before donating the tissues. Paraffin-embedded human tissues (study I) were collected from archives of the Department of Pathology and Forensic Medicine at the University of Turku and Turku University Hospital. No information was collected from the umbilical cord donors and paraffin-embedded tissue samples did not include any patient information.

CSF samples (studies III-IV) were collected as a part of routine clinical practice from patients who were suspected to have a neurological disease. An informed consent was obtained from the patients before the procedure. According to the Finnish Medical Research Act (No. 488/1999), Chapter 1, Sections 1, 2, and 3, the research made with human CSF samples is not medical research, and thus, a separate approval from the local Ethics committee was not required. The study IV was

approved by The Hospital District of Southwest Finland (Decision number T240/2017).

All mouse experiments (study II) were approved by the National Animal Experiment Board of the Regional State Administrative Agency for Southern Finland (permission numbers ESAVI/5507/04.10.07/2014 and ESAVI/3006/04.10.07/2014) and conducted in accordance with the Finnish Act on the Use of Animals for Experimental Purposes and the relevant European Union directive.

5 RESULTS

5.1 Adhesion of *Borrelia* to vascular endothelium

5.1.1 *Adherence of wild type Borrelia strains to human endothelial cells*

To study whether representative strains of different *Borrelia* genospecies are able to adhere to endothelial cells, fluorescently labelled wild type *B. burgdorferi* sensu stricto N40, *B. garinii* SBK40, and *B. afzelii* A91 were allowed to interact with HUVECs and HBMECs. As a control, surface protein deficient *B. burgdorferi* sensu stricto B313 strain was also included in the experiments. The binding of *Borrelia* to endothelial cells showed great variability between the individual experiments, and the only statistically significant difference was seen in binding of *B. garinii* SBK40 to HUVECs (Figure 9A). However, although not reaching statistical significance, it seemed that all of the studied wild type *Borrelia* strains could adhere to the endothelial cells better than the surface protein deficient B313 strain (Figure 9A-B).

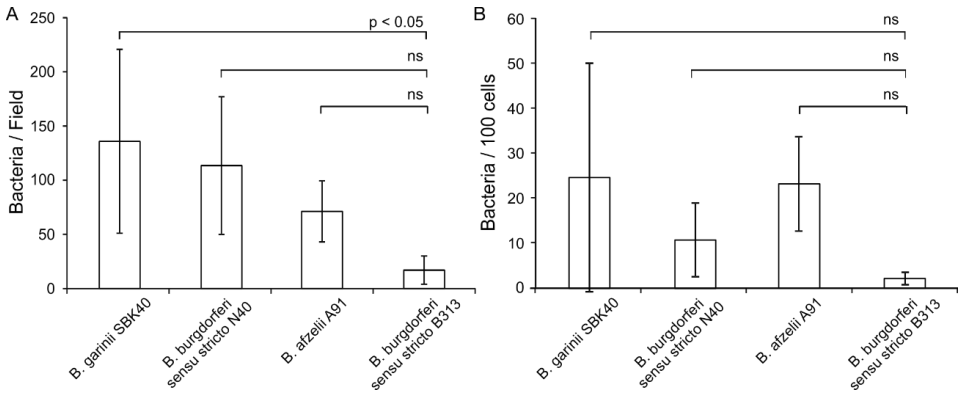

Figure 9. Binding of wild type *Borrelia* to endothelial cells. (A) The adherence of different *Borrelia* genospecies to HUVECs is expressed as an average of bacteria per field in three independent experiments. (B) The adherence of different *Borrelia* genospecies to HBMECs is expressed as an average of bacteria per 100 endothelial cells in at least three independent experiments. ns = not significant. Modified from the original publication I.

5.1.2 *Proteoglycan expression in endothelial cells and human tissues*

Because *Borrelia* are known to adhere to decorin, the expression of decorin in HUVECs and HBMECs was analyzed. Moreover, because biglycan resembles decorin and belongs to the same family of small leucine-rich proteoglycans, also the expression of biglycan on endothelial cells was analyzed. As a result, HUVECs did not seem to express decorin while biglycan expression could be demonstrated (I, Figure 2A, 2B, and 3C). In contrast, HBMECs clearly expressed both of these proteoglycans (Figure 10). However, biglycan RNA was produced more abundantly (ΔCt 2.68 ± 0.70) than decorin RNA (ΔCt 14.25 ± 0.46) in relation to the housekeeping gene GAPDH.

To further expand the knowledge of decorin and biglycan expression patterns in different human tissues, immunohistochemical analyses were performed on skin, heart, and brain samples. Decorin expression was observed in dermal fibroblasts but not in the blood vessel wall or endothelial cells of the skin, the heart, or the brain (I, Supplementary Figure 3). Biglycan expression, on the other hand, could be demonstrated in vascular endothelial cells and the blood vessel wall in human brain tissue, dermal blood vessels, and vascular endothelial cells and blood vessel pericytes of heart tissue (I, Figure 2C; I, Supplementary Figure 2).

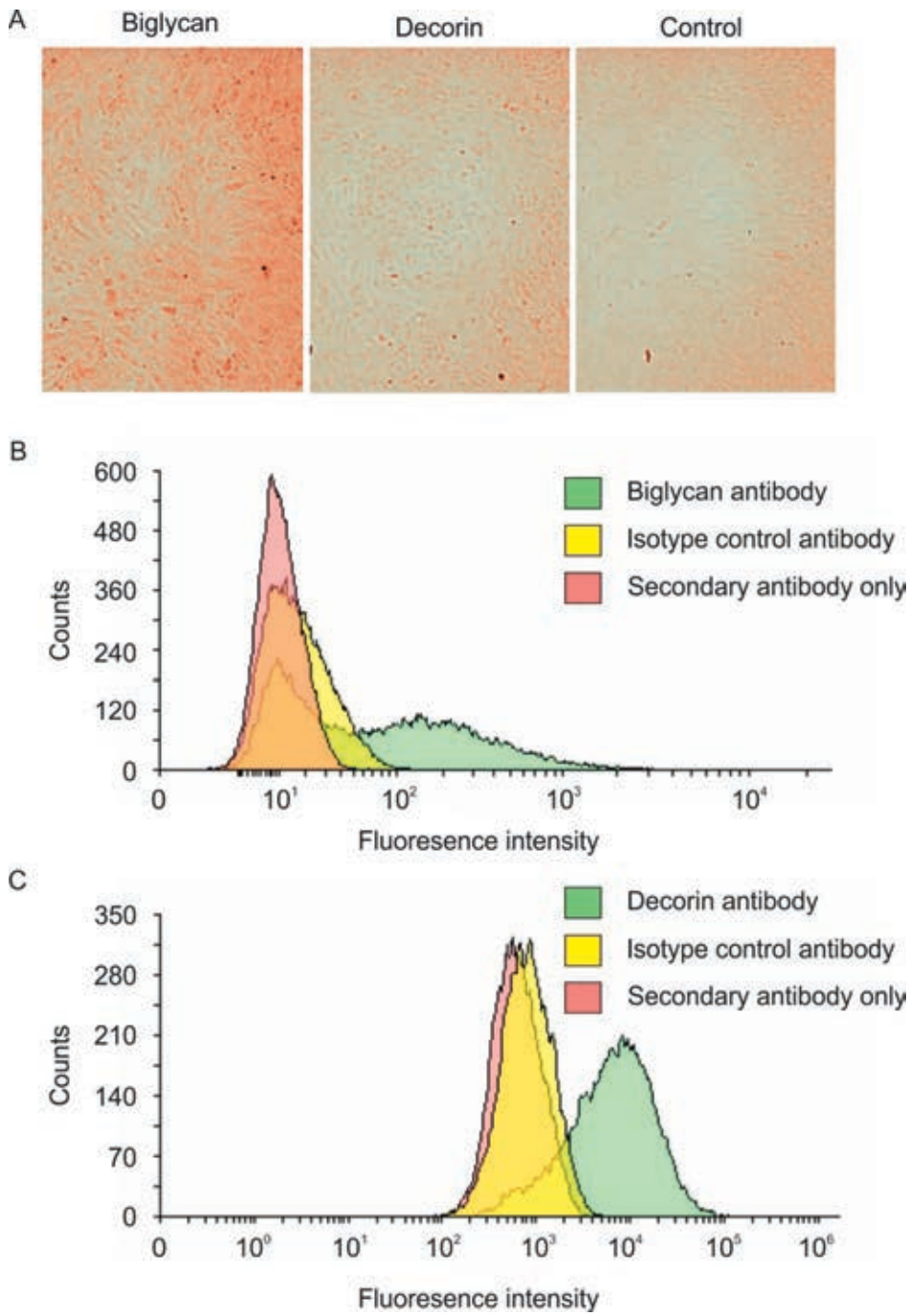

Figure 10. Biglycan and decorin expression in HBMECs. (A) The expression of biglycan and decorin on HBMECs was studied by culturing the cells on chamber slides and staining the proteoglycans with monoclonal antibodies and a peroxidase-conjugated secondary antibody. (B) The expression of biglycan was studied by flow cytometry with LSR II. (C) The expression of decorin was studied by flow cytometry with Accuri™ C6.

5.1.3 *The role of Dbps in endothelial adhesion*

To study the role of Dbps in endothelial adhesion, fluorescently labelled *B. burgdorferi* B313 strains expressing Dbps of different genospecies were allowed to interact with the endothelial cells in static conditions. The strains expressing Dbps of *B. garinii* and *B. burgdorferi* sensu stricto adhered to HUVECs significantly more efficiently than the negative control strain (transformed with the expression plasmid pBSV2) (Figure 11; I, Figure 1B). However, when these same Dbp-expressing *Borrelia* strains were allowed to adhere to HBMECs, the strains did not bind to the cells any better than the strain used as a negative control (Figure 11). Moreover, Dbps of *B. afzelii* did not mediate adhesion to neither of the endothelial cell lines (Figure 11; I, Figure 1B). When the Dbp-expressing *Borrelia* strains were allowed to interact with HUVECs under flow conditions, only the strain expressing Dbps of *B. garinii* bound to the endothelium significantly more than the control strain (I, Figure 5A).

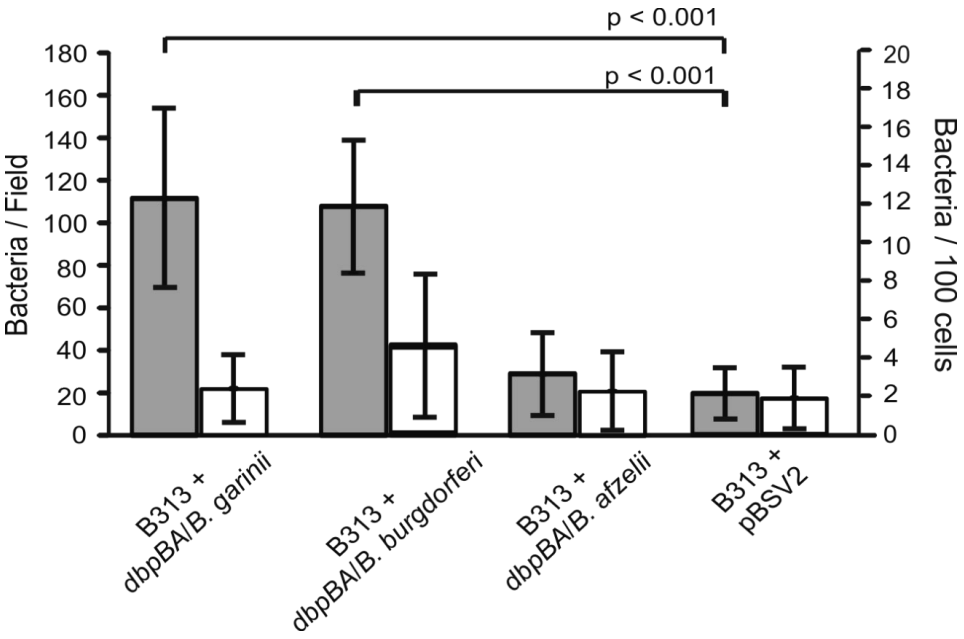

Figure 11. Binding of B313 strains expressing Dbp proteins of different *Borrelia* genospecies to endothelial cells. Binding to HUVECs is presented in grey bars as an average of bound bacteria per field in three independent experiments. Binding to HBMECs is presented in white bars as an average of bound bacteria per 100 endothelial cells in three independent experiments. The differences in binding when compared with the B313 + pBSV2 negative control strain are not statistically significant unless otherwise indicated. Modified from the original publication I.

5.1.4 *Biglycan as the binding ligand on endothelial cells*

To study whether biglycan serves as a ligand for Dbps in HUVEC adhesion, the adherence of *Borrelia* to the cells was inhibited 1) by pretreating the bacteria expressing Dbps of *B. garinii* and Dbps of *B. burgdorferi* sensu stricto with biglycan, dermatan sulphate, and chondroitin-6-sulphate before the adhesion experiment, 2) by pretreating the HUVECs with GAG-degrading chondroitinase ABC enzyme before the adhesion experiment, and 3) by silencing biglycan expression of HUVECs with siRNA before the adhesion experiments. All these studies demonstrated diminished binding of Dbp-expressing *Borrelia* strains to HUVECs when compared with uninhibited conditions (I, Figures 3A, 3B, 3D, and Supplementary Figure 4).

The role of biglycan and /or dermatan sulphate as an adhesion ligand of Dbps in vascular endothelial cells was further confirmed by studying the binding of recombinant Dbps to biglycan. Interestingly, when recombinant DbpA of *B. garinii* was allowed to interact with biglycan in static conditions, no binding could be observed (I, Figure 4A) but when the same interaction was studied under flow conditions, there was a clear interaction (I, Figures 4B-C). DbpB of *B. garinii* and DbpB of *B. burgdorferi* sensu stricto adhered to biglycan both in static and in flow conditions (I, Figures 4A-C). Moreover, the binding could be inhibited with biglycan, dermatan sulphate, chondroitin-6-sulphate, and chondroitin-4-sulphate (I, Supplementary Figure 6). The binding of DbpA and B of *B. garinii* and the binding of DbpB of *B. burgdorferi* sensu stricto to biglycan was dose dependent (I, Supplementary Figure 7B).

5.2 Dissemination of *Borrelia* into distant tissues

5.2.1 *Transmigration of Borrelia across HBMEC cell layer*

To analyze the ability of HBMECs to form a BBB –type of cell layer, the barrier properties of HBMEC layer were characterized by a LY assay, TEER-measurement, and by antibody staining of ZO-1 tight junction molecules. Tight junction protein ZO-1 was detected in endothelial cell junctions of HBMECs although the staining pattern was not constant all over the cell layer (Figure 12A). Permeability coefficient for a small molecule dye LY (0,45 kDa) was $2.7 \times 10^{-3} \pm 1.76 \times 10^{-3}$ cm /min and the measured TEER was $3.5 \pm 1.6\ \Omega cm^2$.

The ability of wild type *Borrelia* strains to transmigrate across the endothelial cell layer was analyzed by culturing HBMECs in transwell chambers and incubating

Borrelia on the apical side of the wells while analyzing the number of transmigrated *Borrelia* in the medium on the basolateral compartments under the cells. As a result, all tested strains seemed to be able to cross the cell layer equally well after 5 hour incubation (Figure 12B). Moreover, when *Borrelia* were left to transmigrate overnight, no differences between the strains could be seen (data not shown).

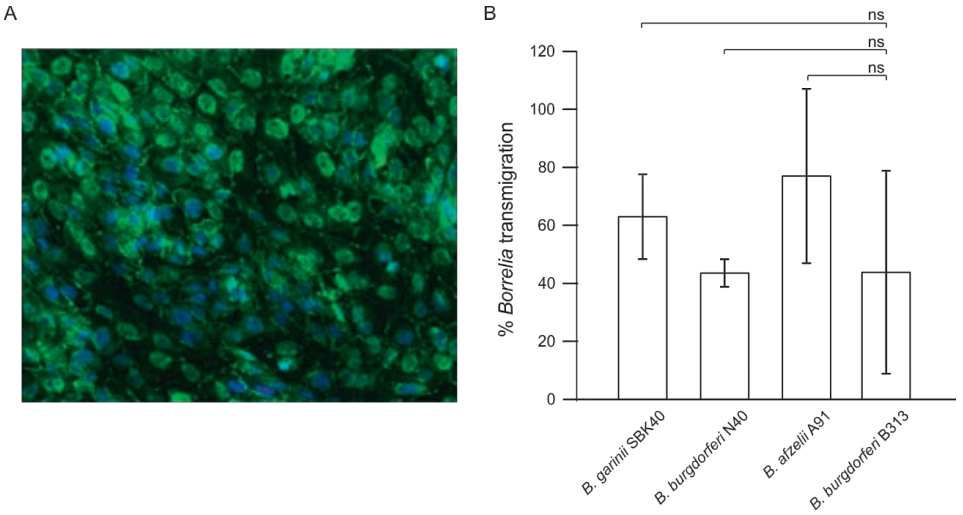

Figure 12. Zonula occludens-1 staining and transmigration of different *Borrelia* genospecies across HBMEC layer. (A) Zonula occludens-1 (ZO-1) tight junction protein was stained with fluorescent antibody (green) and the nuclei of HBMECs were stained with DAPI (blue). ZO-1 localized to the cell borders but the staining was not even. Also the nuclei gave strong background signal. 20x objective. (B) *Borrelia* that had transmigrated across the HBMEC layer in 5 hours were quantified with qPCR. Transmigration is expressed as a percentage of the number of *Borrelia* crossing the transwell membrane with HBMECs relative to the number of *Borrelia* crossing the transwell membrane without HBMECs. ns = not significant

5.2.2 *Dissemination of Borrelia in vivo*

Mice infected with *Borrelia* and uninfected control mice were PET/CT imaged with [^{18}F]FDG tracer once a week to longitudinally monitor the dissemination of infection and the degree of inflammation. The sensitivity and resolution of the imaging technique were high enough to visualize inflamed tissues (Figure 13; II, Figure 2A-B). The tracer accumulated to the sites of high glucose metabolism (the brain, the eyes, the heart) and to the excretory system (the bladder and the kidneys) in all imaged mice at every time point. However, unlike in uninfected control mice, the tracer accumulated also to the joints, the spleen, and the axillary and inguinal lymph nodes of *Borrelia* infected mice. Interestingly the stifle joints of infected

mice showed tracer accumulation one week after infection while the tracer generally accumulated to the tibio-tarsal joints 3-5 weeks post infection.

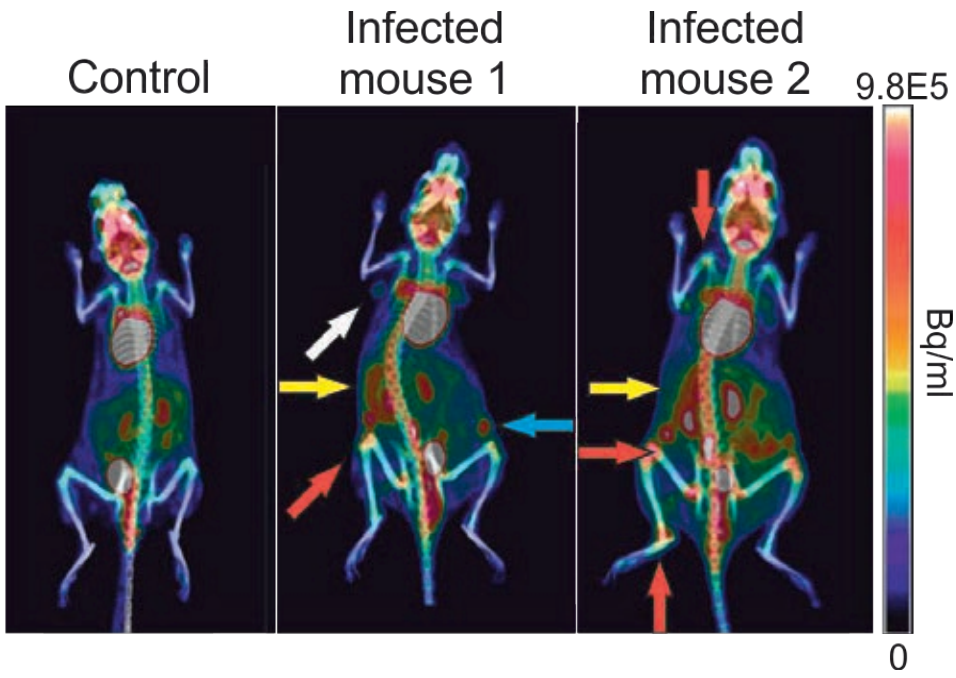

Figure 13. PET/CT imaging of one uninfected control mouse and two *Borrelia*-infected mice one week after infection. Mice were PET/CT imaged with an [18F]FDG tracer. Red arrows indicate different inflamed joints, yellow arrows indicate the tracer uptake in the spleen, and white and blue arrows indicate tracer accumulation in axillary and inguinal lymph nodes. Scale bar shows the intensity of the signal per volume as Bq /ml. Modified from the original publication II.

More precise examination of the tracer accumulation in the tibio-tarsal joints of infected mice revealed that the peak inflammation appeared four weeks after infection after which the tracer signal started to diminish and reached the level of the signal in the tibio-tarsal joints of control mice (II, Figure 3A). The result was also confirmed by *ex vivo* gamma counting (II, Figure 4A). When the tracer accumulation in tibio-tarsal joints was compared to other inflammation markers (*ex vivo* gamma counting, joint swelling, and histology), good or excellent correlations between the parameters were observed (II, Figure 4C).

In inguinal and axillary lymph nodes of infected mice, the peak tracer accumulation was observed one and two weeks after infection, respectively (II, Figure 3B-C). At week 6, the tracer signal in the axillary lymph nodes of infected mice diminished to the level observed in uninfected control mice. The signal of the tracer in inguinal lymph nodes, however, was elevated when compared with the control animals even at the last imaging time point seven weeks after infection. The similar

phenomenon could be observed in *ex vivo* gamma counting of pooled axillary and cervical lymph nodes (II, Figure 4B). The tracer accumulation was the highest two weeks after infection but remained elevated even at the last time point of the experiment (7 weeks post infection) when compared with the pooled lymph nodes of uninfected control mice.

5.3 Cytokines in the CSF of Lyme neuroborreliosis patients

5.3.1 *Characteristic cytokine profile of Lyme neuroborreliosis patients*

To characterize the cytokine profile of CSF, the concentrations of 49 different cytokines were quantified of the CSF samples of LNB patients, TBE patients, MS patients, and control patients. The nine best cytokines to differentiate all studied patient groups from each other were CXCL13, interleukin (IL) -6, IL-10, granulocyte-colony stimulating factor (G-CSF), IL-1 receptor antagonist (IL-1ra), TNF-α, CXCL10, interferon gamma (IFN-γ), and IL-8 (III, Figure 1). Pairwise comparisons between the different groups, on the other hand, demonstrated that there were only ten cytokines that could not distinguish LNB patients from the control patients (III, Figure 2A). All other studied cytokines were significantly elevated in the CSF of LNB patients when compared with the control patients. In addition, the cytokine profile of LNB patients was highly different when compared with the cytokine profile of MS patients as only ten cytokines were unable to separate these groups from each other (III, Figure 2B). TBE patients, on the other hand, seemed to have the strongest cytokine secretion among the studied patient groups. There were 15 cytokines that differentiated TBE patients from the LNB patients and the majority of these were more elevated in the TBE group (III, Figure 2C). Chemokine CXCL13 was the only cytokine marker in the CSF of LNB patients the concentration of which was highly elevated and, importantly, showed no overlap between the other patient groups (III, Figure 3).

To find out whether endothelial cells could be responsible for the high CXCL13 secretion, the ability of HBMECs to produce CXCL13 was studied by stimulating the cells with *Borrelia*. However, no CXCL13 production could be detected (data not shown).

5.3.2 *The performance of a point-of-care test measuring CSF CXCL13 levels*

To study whether a newly developed POC test measuring CSF CXCL13 levels could be used in place of a more laborious ELISA-based method, CXCL13 concentrations of 225 patient CSF samples were analyzed with both the ELISA and the POC test. The results correlated well with each other (IV, Figure 1). However, a few CSF samples obtained from TBE patients gave relatively high CXCL13 values with the POC test even though the concentrations remained low in the ELISA.

5.4 Effect of antibiotic treatment on immune mediators

5.4.1 *Inflammation in antibiotic treated mice*

To study the feasibility of PET/CT imaging in monitoring the effect of antibiotics on inflammation, subgroups of *Borrelia*-infected mice were treated with antibiotics four weeks post infection. Antibiotic treatment was efficient as all the tissues collected and cultured from ceftriaxone treated mice were *Borrelia* culture negative. Also, the joint swelling diminished and the signs of inflammation in histological samples disappeared in treated mice by the end of the experiment (II, Figure 6A-B). Moreover, the [^{18}F]FDG tracer accumulation to the tibio-tarsal joints diminished to the level of control mice right after the treatment (II, Figure 6C-D). The same decline in inflammation parameters was also observed in untreated *Borrelia* infected mice. However, at week 7, the tracer signal in the joints of untreated mice started to rise again. In addition, at week 7, the treated mice had no histological signs of inflammation in the joints while the untreated mice still had an ongoing infection according to histology (II, Figure 6B).

5.4.2 *Cytokine profile of antibiotic treated Lyme neuroborreliosis patients*

To study whether cytokines can serve as biomarkers that distinguish LNB patients with active disease from those that have received antibiotic treatment, the levels of 49 different cytokines were measured of the CSF samples of LNB patients treated with antibiotics. The results were compared to the cytokine levels measured of the CSF obtained from these same patients before the treatment. Forty-two of the studied cytokines were significantly more elevated in the untreated LNB patient samples when compared with the treated LNB patient samples (III, Figure 4). Nine best markers to differentiate these two groups from each other were IL-1ra,

CXCL13, CXCL9, TNF-α, IL-10, IFN-γ, IL-6, beta nerve growth factor (β-NGF), and IL-8 (III, Figures 4-5).

6 DISCUSSION

6.1 Vascular dissemination of *Borrelia*

Previous studies have shown that *Borrelia* disseminate via the blood vasculature into distant tissues in a living host (Moriarty et al., 2008, Norman et al., 2008). The first step in this process is the interaction with and the adhesion to the vascular endothelium. Because there is a constant flow of blood in the vasculature, the effect of the liquid flow on adhesion needs to be considered when characterizing adhesins that bind to vascular endothelium. To cause a systemic infection, bacteria have to adhere firmly to the endothelium although the blood-flow continuously creates a preventive force for many interactions (Lemichez et al., 2010). Firm adhesion usually involves initial adhesion of bacteria to endothelium, and as a following step, reorganization of the endothelial membrane.

Borrelia are known to bind vascular endothelial cells which is in accordance with the results of this study. However, in this study, the overall binding of wild type *Borrelia* strains to the endothelial cells remains rather modest. It is known that flow can induce the expression of proteins that are used as adhesion ligands by *Borrelia* (e.g. integrins) on vascular endothelium (Cucullo et al., 2011). In our studies, the binding experiments with wild type strains were, however, done in static conditions. Thus, it can be speculated whether the binding would have increased if the experiments had been performed under flow.

The knowledge of the molecular level interactions in vascular adhesion of *Borrelia* has been limited. Moreover, only few studies have been done in flow conditions (Ebady et al., 2016, Moriarty et al., 2008, Moriarty et al., 2012, Niddam et al., 2017, Norman et al., 2008). The results of our study demonstrate that the Dbp-adhesins of *Borrelia* mediate binding to primary endothelial cells (HUVECs) in a flow dependent manner. Dbps have previously been shown to bind decorin (Benoit et al., 2011, Salo et al., 2011) but our results show that a potentially more relevant ligand on vascular endothelium is biglycan. Decorin is not expressed by HUVECs while biglycan expression can be demonstrated. Also the other endothelial cell line studied (HBMEC) seems to express biglycan more than decorin.

Recombinant DbpA of *B. garinii* acts in a flow dependent manner binding biglycan only under shear stress. Moreover, Dbps of *B. garinii* are also flow tolerant adhesins when expressed on the surface of *Borrelia* since they mediate interaction of *Borrelia* with HUVECs under flow. These results suggest that Dbps of *B. garinii* have a key role in *in vivo* endothelial adhesion in the blood vasculature. The results

support the previous observations of the importance of Dbps in the early dissemination of *Borrelia* (Imai et al., 2013, Weening et al., 2008). Before this study, BBK32, which binds fibronectin and GAGs, was the only adhesin of *Borrelia* that had been shown to mediate binding to vascular endothelium under flow conditions (Moriarty et al., 2012, Norman et al., 2008).

The reason behind the flow dependency of DbpA of *B. garinii* is not known. However, it is likely that the protein changes its conformation under liquid flow. Such adhesins have been characterized also previously. For example, FimH protein of fimbriae of *E. coli* changes its conformation under shear stress which then leads to formation of catch-bonds with mannose (Thomas et al., 2004). Unlike many other interactions between adhesins and their ligands, catch-bonds become stronger under liquid flow.

B. afzelii A91 and B. *burgdorferi* N40 strains are infectious and, as a consequence, even though the Dbps of these strains do not seem to mediate binding to endothelium under flow, they are likely to have other adhesins which contribute to vascular adhesion under shear stress. In addition, the rate of blood flow is heterogeneous and in some specific locations in microvasculature the flow can even stop for a moment (Mairey et al., 2006). This creates an opportunity for adhesins, which are not able to bind under flow, to interact with their ligand. When the blood flow starts again, stationary adhesions may already have been formed. In fact, although not measured accurately, it seemed that, at least in some flow experiments, B313 strain expressing Dbps of *B. burgdorferi* N40 adhered to HUVECs before the pump apparatus creating the liquid flow was turned on. When the liquid flow started, the spirochetes that had already adhered to the cells resisted the flow and remained adhered.

It is not known why all Dbps do not bind decorin and biglycan as efficiently. All Dbps studied in this thesis contain the critical lysine amino acid residues shown to contribute to adhesion (Brown et al., 1999, Fortune et al., 2014, Pikas et al., 2003). However, when the structures of mature Dbps were compared, it was noted that even the small differences in amino acid composition lead to varying tertiary structures of the proteins and hindered accessibility to the GAG binding site (Morgan et al., 2015, Morgan and Wang, 2015).

Despite adhering to HUVECs, Dbp-expressing strains seem to fail in binding to HBMECs although these cells clearly express both biglycan and decorin. The reason for this is unclear. It can be speculated that the proteoglycans on HBMECs are not necessarily glycosylated. Indeed, proteoglycans are known to sometimes be expressed on endothelium in their unglycosylated forms (Valiyaveettil et al., 2004). Another explanation could be that the GAGs are present but they are of

such a type (e.g. chondroitin-6-sulphate) that Dbps are not able to bind so efficiently. Yet another possible explanation could be that biglycan, decorin, and their GAGs are somehow covered with other types of molecules expressed on HBMECs and, thus, the specific binding sites are not available to Dbps.

After adhesion to the vascular endothelium, the next step in dissemination process is transmigration of *Borrelia* across the endothelium. *In vivo* imaging of GFP-expressing *Borrelia* has demonstrated that *Borrelia* transmigrate from the blood into tissues and that the process is relatively fast, ca. 10 min (Moriarty et al., 2008). Transmigration has been studied mainly with *B. burgdorferi* sensu stricto strains while studies with *B. afzelii* or *B. garinii* genospecies have not been performed. According to the results of the present study, representative wild type *Borrelia* strains from all these three major genospecies are able to transmigrate across the HBMEC cell layer. However, transmigration seems to be as efficient also with the B313 laboratory strain.

Only a few molecules of *Borrelia* have been shown to have a role in transmigration process. OspA [encoded in plasmid lp54 (BorreliaBase: www.borreliabase.org; accessed 30.7.2018)] is needed for transmigration across the endothelium (Pulzova et al., 2011). Another protein shown to be important in transmigration of *Borrelia*, P66 (Kumar et al., 2015), is encoded by the chromosomal gene *p66* (BorreliaBase: www.borreliabase.org; accessed 30.7.2018). BbHtrA is a protein which degrades the components of ECM (including decorin and biglycan) and cell junction proteins, and consequently, most likely has a role in transmigration of *Borrelia* (Russell et al., 2013). Like P66, it is also encoded by a chromosomal gene (BorreliaBase: www.borreliabase.org; accessed 30.7.2018). B313 strain is lacking the plasmid lp54 so it does not encode OspA (Exner et al., 2000). Chromosomal genes *p66* and *bbHtrA* are most likely expressed. This may explain why B313 strain is able to cross the HBMEC layer equally well as the wild type strains. In addition, it has to be noted that the barrier properties of the used HBMECs are not optimal as demonstrated by the low TEER values, disconnected ZO-1 staining, and suboptimal permeability coefficient (Eigenmann et al., 2013).

6.2 *In vivo* imaging of disseminated *Borrelia* infection and *Borrelia*-induced inflammation

Mice are widely used experimental animals in *Borrelia*-infection studies and especially in LA research. Traditional techniques for studying disseminated *Borrelia* infection include 1) *Borrelia*-culture or PCR of mouse tissues, 2) histology, 3) serology, and in the case of arthritis, 4) the measurement of the diameter of tibiotarsal joints. These methods are either imprecise (diameter measurement) or the

animals must be killed to obtain tissues for the analyses. *In vivo* imaging would, thus, be a helpful tool for *Borrelia* research. Imaging of *Borrelia* infection is possible with genetically modified GFP- or luciferase-expressing *Borrelia* (Bockenstedt et al., 2012, Hyde et al., 2011, Moriarty et al., 2008, Norman et al., 2008, Skare et al., 2016). Spinning disc intravital imaging and multiphoton laser scanning microscopy detection of GFP can be used only for studying specific organs. Bioluminescent imaging detecting luciferase expressing *Borrelia* can be used to image whole animals but using this approach, the resolution for imaging specific organs in live mice is not sufficient. The results of the present study show that these drawbacks can be overcome by using PET/CT imaging with the [^{18}F]FDG tracer. With this imaging technique, whole animals can be imaged and the inflammation caused by infection with genetically unmodified *Borrelia* can be detected in specific organs. Thus, PET/CT imaging of *Borrelia* infection enables targeted tissue sampling when the mice are sacrificed diminishing the number of mice needed for an experiment. Previously, other types of bacterial infections have also been studied by PET/CT imaging in rodent models. These include e.g. diseases caused by *Grimontia hollisae*, *Staphylococcus aureus*, *E. coli*, and *Mycobacterium tuberculosis* (Lin et al., 2013, Mokaleng et al., 2015, Takemiya et al., 2018, Weinstein et al., 2012, Weinstein et al., 2014).

[^{18}F]FDG accumulation can be seen in the joints, the spleen, and the lymph nodes of *Borrelia*-infected mice. Interestingly, since the tracer accumulates to the lymph nodes, and because lymph nodes of mice have been shown to be *Borrelia* culture positive (Hyde et al., 2011, Imai et al., 2013), it seems possible that, in addition to the blood vasculature, *Borrelia* might exploit the lymphatic circulation in dissemination. PET/CT imaging has potential as an imaging technique to study this process.

Also the kinetics of *Borrelia* infection can be monitored with PET/CT as demonstrated by the finding that tissues closer to the primary infection focus (stifle joints and inguinal lymph nodes) have tracer accumulation and, thus, inflammation, before more distant tibio-tarsal joints and axillary lymph nodes. In addition, individual variation in infection kinetics between different animals can be observed with PET/CT. Moreover, the results show that the inflammation focus in the joints fluctuates from one tibio-tarsal joint to the other, a phenomenon known to occur also in human LB patients (Steere et al., 2016). PET/CT seems to be a useful tool to monitor also this process.

[^{18}F]FDG is a marker for high glucose metabolism and, as a consequence, it is not *Borrelia* specific (Basu et al., 2011, Basu et al., 2014). Indeed, [^{18}F]FDG PET/CT imaging method visualizes *Borrelia*-induced metabolic activity of the mouse immune response, like glucose uptake of neutrophils and macrophages (Matsui et al.,

2009, Rennen et al., 2001), but not the bacteria themselves. To develop PET/CT imaging of *Borrelia* infection further, a *Borrelia* specific tracer should be designed. A few studies have been published where such pathogen-specific immunotracers have successfully been used in PET/CT imaging of infection (Rolle et al., 2016, Santangelo et al., 2015).

Currently, there are no imaging techniques available for the diagnostics of LB in human patients although a few studies and case reports have been published on the subject (Aigelsreiter et al., 2005, Flemming et al., 2014, Kalina et al., 2005, Logigian et al., 1997, Newberg et al., 2002, Plotkin et al., 2005). However, if a *Borrelia*-specific tracer could be developed, PET/CT imaging might have potential also as a method to image and diagnose LB patients. PET/CT imaging has already proven to be useful in diagnostics of human patients with other types of infections such as infections of pacemakers and spinal infections (Beadsmoore et al., 2015, Hess et al., 2014, Vaidyanathan et al., 2015).

Recently, another tracer, [^{68}Ga]DOTA-Siglec-9, was used to study *Borrelia*-induced arthritis in mice (Siitonen et al., 2017). The tracer accumulated to the joints of *Borrelia*-infected mice but not to the joints of uninfected control animals. However, like [^{18}F]FDG, this tracer is not *Borrelia*-specific. [^{68}Ga]DOTA-Siglec-9 binds to vascular adhesion protein-1 which is expressed by endothelial cells under inflammatory conditions. Thus, the tracer detects inflammation rather than live *Borrelia*.

6.3 Cytokines as diagnostic markers for Lyme neuroborreliosis

Once *Borrelia* eventually disseminate into the CNS, the immune system of the host starts secreting cytokines into the CSF in response to the invading organism. To analyze which cytokines are produced and whether they could be used as diagnostic markers, a multiplex analysis of CSF samples collected from LNB patients, MS patients, TBE patients, and control patients was performed. The results show that many of the studied cytokines are clearly elevated in the CSF of LNB patients when compared with the other patient groups. However, CXCL13 is the only cytokine the concentration of which shows no overlap between LNB patients and other patient groups in this study. This result is in accordance with other reports demonstrating the potential of CSF CXCL13 as a diagnostic marker for LNB both in adult and child patients (van Burgel et al., 2011, Eckman et al., 2018, Henningsson et al., 2016, Hytönen et al., 2014, Markowicz et al., 2018, Remy et al., 2017, Schmidt et al., 2011, Senel et al., 2010, Sillanpää et al., 2013, Skogman et al., 2017, Tjernberg et al., 2011, Wagner et al., 2017, Wutte et al., 2011).

Some laboratories in Europe, and also in Finland, have already started to use CSF CXCL13 measurement for diagnostic purposes. The only controversy concerning the use of CXCL13 as a biomarker for LNB is that, currently, there is no consensus on the optimal cut-off value which would lead to highest possible specificity without compromising sensitivity. However, a recent meta-analysis evaluating the optimal cut-off value suggested 162 pg/ml as the optimal (Rupprecht et al., 2018). Further, combining CXCL13 concentration result with the CSF cell count of the same patient has been suggested to improve specificity (Markowicz et al., 2018). Nonetheless, correlation between CSF cell count and CXCL13 concentration needs to be further verified by other studies since correlation was not observed e.g. in Finnish patient material (Hytönen et al., 2014).

Even though LNB patients have high concentrations of CXCL13 in their CSF, the cell type responsible for the production of CXCL13 remains unclear. Two studies have been published demonstrating that PBMCs secrete CXCL13 in response to *Borrelia* stimulation, and monocyte derived DC population among the PBMCs is the specific cell type responsible for the production (Narayan et al., 2005, Rupprecht et al., 2007). However, leucocytes in the CSF of a healthy person are mainly T cells (90%) (Ransohoff and Engelhardt, 2012). B cells and monocytes both account for 5% and DCs less than 1% of the cells in the CSF. Also other cell types in the CSF have been shown to produce CXCL13 in response to different stimuli. For example, CXCL13 has been shown to be localized on brain vascular endothelium (Brunn et al., 2007, Smith et al., 2003). Moreover, some studies report microglia as the cells producing CXCL13 in *Borrelia* infection (Ramesh et al., 2009). To further study the cell type responsible for the high CXCL13 production in LNB patients, we also stimulated many different cell types (HBMECs, primary human microglia, immortalized human astrocytes, PBMCs, primary human macrophages differentiated from PBMCs, primary human DCs differentiated from PBMCs, immortalized human B cells) with *Borrelia* in order to find out the cellular source for CXCL13. Undifferentiated PBMCs were the only cell population that, also in our studies, produced CXCL13 upon stimulation (unpublished observations). It can be speculated that CXCL13 production in LNB is actually a result of activation of many different cell types and all these cell types together would be responsible for the high CXCL13 concentration observed in the CSF of LNB patients. For example, if resident microglia in the CSF interacted with invading *Borrelia* and introduced the antigens to T cells, T cells would then start producing proinflammatory cytokines and, as a consequence, CXCL13 secretion by DCs and /or other cell types could be initiated.

6.4 Point-of-care testing for CXCL13

CSF CXCL13 concentration is typically measured with ELISA or Luminex-based methods. Moreover, the measurement is often performed as an additional step in LNB diagnostic workflow (Koedel et al., 2015). However, because high CXCL13 concentration is a good biomarker for LNB, both the clinicians and the patients would benefit from a fast-to-be-performed laboratory test that could be used to measure CXCL13 concentration right after the lumbar puncture.

In general, POC tests are increasingly used in diagnostics (St John and Price, 2014). The advantage of POC testing over typical laboratory testing is e.g. the rapid availability of the results, which leads to more rapid and targeted initiation of treatment (Price, 2001). In the field of clinical microbiology, POC tests are usually based on lateral flow immunoassay principal (Kozel and Burnham-Marusich, 2017). They are available e.g. for infections caused by group A *Streptococcus*, *Helicobacter pylori*, and influenza viruses. There is also a POC test available for detecting *Borrelia* specific IgM and IgG antibodies in human blood samples, as well as a POC test for *Borrelia* diagnostics in veterinary medicine (Kozel and Burnham-Marusich, 2017, Schvartz et al., 2015). In addition, new POC tests for LB diagnostics are constantly being developed (Nayak et al., 2016).

Recently, a POC test that measures CSF CXCL13 levels in less than an hour was developed and brought to the market. According to the results of the present study, the POC test performs equally well as an ELISA based method in recognizing high CXCL13 concentrations of CSF samples. The results of these two different methods correlate very well with each other. The POC test, however, gave high CXCL13 values for a few CSF samples of TBE patients although the concentrations of these same samples remained low in ELISA measurement. This contradiction warrants more research.

Based on the good performance of CXCL13 as a biomarker for LNB and due to the availability of the POC test for CXCL13 measurement, a change in the current LNB diagnostic workup is proposed. With the POC test, CSF CXCL13 concentration can be measured right after the lumbar puncture. It has been reported that the earlier LNB patients are diagnosed and treated, the less they have residual symptoms after the treatment (Knudtzen et al., 2017). This highlights the need for fast diagnosis and early initiation of antibiotics for LNB patients. However, also more targeted use of antibiotics is extremely important in the battle against increasing antibiotic resistance of microbes. The results of the POC CXCL13 measurement, together with the clinical picture and pleocytosis, could guide clinicians to start

targeted antibiotic treatment for LNB patients soon after the lumbar puncture. After CXCL13 POC test (and also after / in parallel with ELISA), *Borrelia* specific antibodies should still be measured to confirm the diagnosis.

6.5 Effect of antibiotic treatment on inflammation and cytokine secretion

Treatment of *Borrelia*-infected mice with ceftriaxone has been shown to eradicate cultivable spirochetes (Salo et al., 2015). However, after antibiotic treatment, *Borrelia* DNA, RNA, proteins, and even intact but attenuated *Borrelia* have been detected in mouse tissues (Bockenstedt et al., 2012, Bockenstedt et al., 2002, Hodzic et al., 2008, Hodzic et al., 2014, Salo et al., 2015, Yrjänäinen et al., 2010). In the *in vivo* imaging study, the mice were administered with ceftriaxone four weeks after infection. After antibiotic treatment, joint swelling started to resolve, histological signs of inflammation started to disappear and [^{18}F]FDG tracer accumulation declined. However, at the same time, the same phenomena were also seen in untreated *Borrelia*-infected mice. Seven weeks post infection, signs of inflammation started to appear again in untreated mice while no increase in inflammation parameters was seen in antibiotic treated mice. This indicates that PET/CT imaging could also be used to study the effect of antibiotic treatment on *Borrelia*-induced inflammation. If the mouse experiment had been continued longer, most likely, more significant rise in all inflammation parameters in untreated mice would have been observed. This assumption is based the our previous reports show-ing a two-peaked joint swelling pattern in *Borrelia*-infected mice followed up for 15 weeks after infection (Salo et al., 2015).

Borrelia-specific antibodies can persist in the CSF of LNB patients for months or even years after treatment without protecting from reinfections (Steere et al., 2016). Thus, patients suspected to have a reinfection are a challenge for serology based diagnostics of LB. To study the effect of antibiotics on cytokine concentrations and to find out whether cytokines can be used as diagnostic biomarkers also in reinfected patients, we performed a multiplex cytokine analysis with follow-up CSF samples obtained from LNB patients after antibiotic treatment. According to the results, out of 49 analyzed cytokines, the concentrations of 42 decline significantly after the treatment. The results show that, in addition to CXCL13, also IL-1ra might have potential as a biomarker of successful antibiotic treatment. There are no other cytokines besides CXCL13 which have previously been proposed to have value as biomarkers of LNB treatment response. However, because the overall performance of CXCL13 as a biomarker exceeds the performance of IL-1ra, the use of IL-1ra alone as a biomarker for LNB treatment response is not supported.

7 CONCLUSIONS

Borrelia have multiple surface-exposed lipoproteins which mediate binding to various components of the ECM and to endothelial cells. However, in order to escape the blood vasculature and to reach distant tissues, adhesins must overcome the shear stress caused by the flowing blood. Before this study, only one *Borrelia* adhesin mediating flow-tolerant interactions with the vascular endothelium was characterized. The present study identified Dbp adhesins as additional flow-tolerant molecules of *Borrelia*. They were shown to mediate binding to vascular endothelial cells in a flow-tolerant manner through interaction with biglycan.

After adhesion to the vascular wall, *Borrelia* transmigrate across the endothelium to invade distant tissues. *B. burgdorferi* sensu stricto strains have previously been shown to transmigrate across the endothelial layer. This study showed that also strains representing *B. afzelii* and *B. garinii* are able to cross the endothelial cell layer. This study also showed that PET/CT imaging can be used to study disseminated LB infection caused by wild type *Borrelia in vivo* in mice.

When spirochetes disseminate into the CNS, patients develop LNB. This study demonstrated that LNB causes the secretion of multiple cytokines into the CSF. While IL-ra could potentially be used as a diagnostic marker of LNB treatment response, CXCL13 is clearly the best cytokine that can be used both as a diagnostic marker for LNB and for the verification of treatment response. This study also demonstrated that the concentration of CXCL13 can be measured with a POC test and, thus, we suggest a reorganization of the current diagnostic work-flow.

The main findings of this study are presented in Figure 14. Altogether, the results give important information on how *Borrelia* disseminate into distant tissues to cause a multisystem infection and how new methods can be exploited to improve current LB diagnostics. The results are useful for infection research and for healthcare professionals involved in LB diagnostics and treatment.

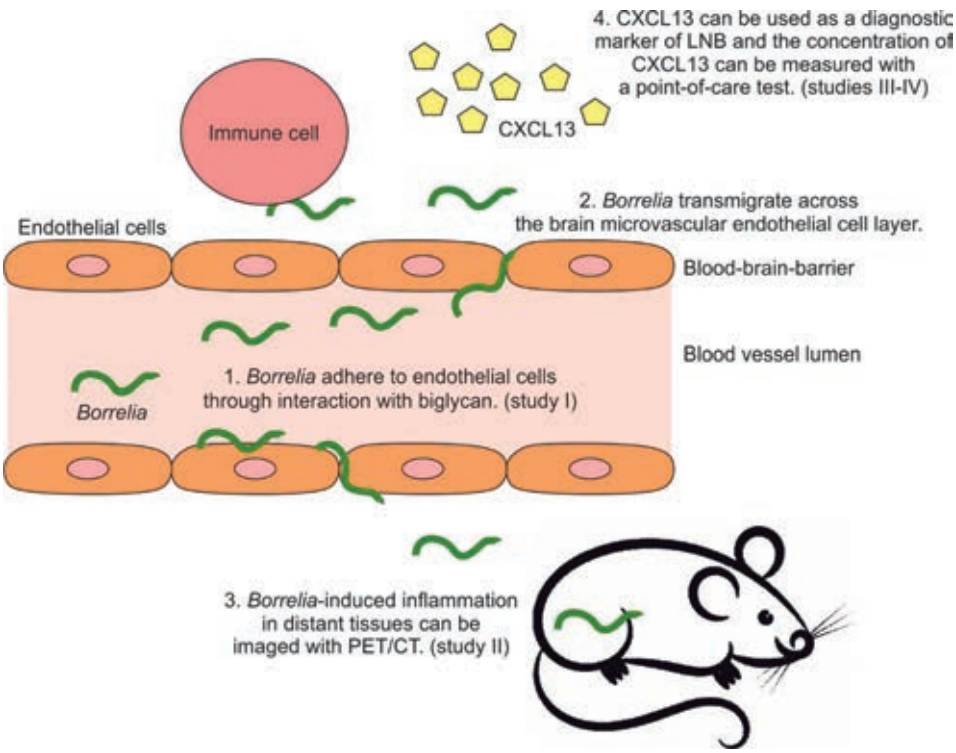

Figure 14. Conclusions of the studies. *Borrelia* adhere to human endothelial cells under flow through interaction with biglycan. After adhesion, *Borrelia* transmigrate across the endothelial cell layer into deeper tissues. Disseminated *Borrelia* infection can be imaged *in vivo* in mice with [18F]FDG PET/CT imaging. If *Borrelia* transmigrate across the BBB, human immune defense starts producing high concentrations of CXCL13. CXCL13 can be used as a diagnostic marker for LNB and the concentration of CXCL13 in CSF samples can be measured with a point-of-care test.

ACKNOWLEDGEMENTS

This study was conducted at the Institute of Biomedicine (Medical Microbiology and Immunology), Faculty of Medicine, University of Turku.

First and foremost, I want to thank my excellent supervisor Associate Professor Jukka Hytönen. Thank you for guiding me during the years and for teaching me how important it is to consider the medical relevance of scientific questions. Thank you also for introducing me to the world of clinical microbiology and diagnostics of infectious diseases, a subject I am much interested in.

Professors Jaana Vuopio and Pentti Huovinen, as the heads of Medical Microbiology and Immunology, you are thanked for creating such a warm atmosphere to our working environment.

I am grateful to my follow-up committee members Docent Kaisa Auvinen and Docent Arto Pulliainen who at each of our meetings showed genuine interest in my work. You gave me valuable comments and suggestions during the years which undoubtedly improved my research.

During the years I have had a great opportunity to conduct projects and write papers with brilliant scientists and amazing co-authors. Thank you Kaisa Auvinen, Rhodaba Ebady, Olli Eskola, Saija Hurme, Jukka Hytönen, Tommi Kauko, Heidi Liljenbäck, Mikael Maksimow, Tara Moriarty, Jarmo Oksi, Anne Roivainen, Marko Salmi, Jemiina Salo, Riikka Siitonen, Mirva Söderström, and Matti Viljanen. Moreover, Tara and Rhodaba, thank you for hosting me in Toronto. I will never forget that experience.

The pre-examiners of my thesis, Docent Anne Jääskeläinen and Docent Benita Westerlund-Wikström are thanked for excellent and constructive feedback. Your comments were of great value.

A thousand thanks to all the co-workers at Mikro 3.rd floor and MedisiinaD 7.th floor and especially the former and present members of Borrelia research group (Julia Cuellar, Heli Elovaara, Eeva Feuth, Otto Glader, Anna Karvonen, Elisa Kortela, Maija Laaksonen, Tuula Rantasalo, Julia Rask, Meri Rouhiainen, Jemiina Salo). Thank you for the peer support and taking my mind away from research. You made it enjoyable to come to work every single day.

I am grateful for all the technical assistance I have received for my lab experiments from Heidi Isokääntä, Teija Kanasuo, Anna Karvonen, Tiina Mäkilä, Erica Nyman, Tuula Rantasalo, Riikka Sjöroos, Kirsi Sundholm-Heino, Sari Uuppo, Marika Vesalainen, and Tiina Virtanen. Aake Honkaniemi is thanked for operating the PET instrument and Jouko Sandholm is thanked for helping me with flow cytometry and confocal microscopy issues. Thank you also Tiina Haarala, Anna Karvonen, and Kaisa Leppänen for all the reagent orders and practicalities.

My friends outside work, Heidi, Tiina, Laura and the whole Hottis crew: you have kept me sane during all these years. Thank you for all the joyable moments we have shared. Life has been a wonderful journey with you!

I want to thank also my parents and my brother. You have supported me in everything I have ever done, believed in me, and gently pushed me forward. Thank you!

Finally, I want to thank my family. AP, you are the reason why we moved to Turku in the first place and I started this thesis project. You have been extremely supportive. I am forever grateful to you for taking care of Onni while I was taking care of endothelial cells or mice. AP and Onni, I love you!

This research was financially supported by the Academy of Finland, Turku Doctoral Programme of Molecular Medicine (TuDMM), Turku University Foundation, The Emil Aaltonen Foundation, Orion Research Foundation sr, and The Scientific Foundation of Microbiologists in Turku.

Turku, November 2018

Annukka Pietikäinen

REFERENCES

ABERER, E. & DURAY, P. H. 1991. Morphology of Borrelia burgdorferi: structural patterns of cultured borreliae in relation to staining methods. *J Clin Microbiol,* 29**,** 764-72.

ADEOLU, M. & GUPTA, R. S. 2014. A phylogenomic and molecular marker based proposal for the division of the genus Borrelia into two genera: the emended genus Borrelia containing only the members of the relapsing fever Borrelia, and the genus Borreliella gen. nov. containing the members of the Lyme disease Borrelia (Borrelia burgdorferi sensu lato complex). *Antonie Van Leeuwenhoek,* 105**,** 1049-72.

AGUERO-ROSENFELD, M. E., NOWAKOWSKI, J., BITTKER, S., COOPER, D., NADELMAN, R. B. & WORMSER, G. P. 1996. Evolution of the serologic response to Borrelia burgdorferi in treated patients with culture-confirmed erythema migrans. *J Clin Microbiol,* 34**,** 1-9.

AIGELSREITER, A., PUMP, A., BUCHHÄUSL, W., SCHÖNFELDER, M., BEHAM-SCHMID, C., CERRONI, L., BERTHA, G., DIMAI, H. P., STELZL, E., DAGHOFER, E. & WENISCH, C. 2005. Successful antibiotic treatment of Borreliosis associated pseudolymphomatous systemic infiltrates. *J Infect,* 51**,** e203-6.

AIRD, W. C. 2007. Phenotypic heterogeneity of the endothelium: I. Structure, function, and mechanisms. *Circ Res,* 100**,** 158-73.

ALEXOPOULOU, L., THOMAS, V., SCHNARE, M., LOBET, Y., ANGUITA, J., SCHOEN, R. T., MEDZHITOV, R., FIKRIG, E. & FLAVELL, R. A. 2002. Hyporesponsiveness to vaccination with Borrelia burgdorferi OspA in humans and in TLR1- and TLR2-deficient mice. *Nat Med,* 8**,** 878-84.

AMFT, N., CURNOW, S. J., SCHEEL-TOELLNER, D., DEVADAS, A., OATES, J., CROCKER, J., HAMBURGER, J., AINSWORTH, J., MATHEWS, J., SALMON, M., BOWMAN, S. J. & BUCKLEY, C. D. 2001. Ectopic expression of the B cell-attracting chemokine BCA-1 (CXCL13) on endothelial cells and within lymphoid follicles contributes to the establishment of germinal center-like structures in Sjögren's syndrome. *Arthritis Rheum,* 44**,** 2633-41.

ANDERSON, J. F., BARTHOLD, S. W. & MAGNARELLI, L. A. 1990. Infectious but nonpathogenic isolate of Borrelia burgdorferi. *J Clin Microbiol,* 28**,** 2693-9.

BACON, R. M., KUGELER, K. J., MEAD, P. S. & (CDC), C. F. D. C. A. P. 2008. Surveillance for Lyme disease--United States, 1992-2006. *MMWR Surveill Summ,* 57**,** 1-9.

BADAWI, A. 2017. The Potential of Omics Technologies in Lyme Disease Biomarker Discovery and Early Detection. *Infect Dis Ther,* 6**,** 85-102.

BARBOUR, A. G. 1988. Laboratory aspects of Lyme borreliosis. *Clin Microbiol Rev,* 1**,** 399-414.

BARBOUR, A. G. 1989. The molecular biology of Borrelia. *Rev Infect Dis,* 11 Suppl 6**,** S1470-4.

BARBOUR, A. G., ADEOLU, M. & GUPTA, R. S. 2017. Division of the genus Borrelia into two genera (corresponding to Lyme disease and relapsing fever groups) reflects their genetic and phenotypic distinctiveness and will lead to a better understanding of these two groups of microbes (Margos et al. (2016) There is inadequate evidence to support the division of the genus Borrelia. Int. J. Syst. Evol. Microbiol. doi: 10.1099/ijsem.0.001717). *Int J Syst Evol Microbiol,* 67**,** 2058-2067.

BARBOUR, A. G., BURGDORFER, W., GRUNWALDT, E. & STEERE, A. C. 1983. Antibodies of patients with Lyme disease to components of the Ixodes dammini spirochete. *J Clin Invest,* 72**,** 504-15.

BARBOUR, A. G. & HAYES, S. F. 1986. Biology of Borrelia species. *Microbiol Rev,* 50**,** 381-400.

BARSTAD, B., TVEITNES, D., NORAAS, S., SELVIK ASK, I., SAEED, M., BOSSE, F., VIGEMYR, G., HUBER, I. & ØYMAR, K. 2017. Cerebrospinal Fluid B-lymphocyte Chemoattractant CXCL13 in the Diagnosis of Acute Lyme Neuroborreliosis in Children. *Pediatr Infect Dis J,* 36**,** e286-e292.

BARTHOLD, S. W., BECK, D. S., HANSEN, G. M., TERWILLIGER, G. A. & MOODY, K. D. 1990. Lyme borreliosis in selected strains and ages of laboratory mice. *J Infect Dis,* 162**,** 133-8.

BARTHOLD, S. W., MOODY, K. D., TERWILLIGER, G. A., DURAY, P. H., JACOBY, R. O. & STEERE, A. C. 1988. Experimental Lyme arthritis in rats infected with Borrelia burgdorferi. *J Infect Dis,* 157**,** 842-6.

BARTHOLD, S. W., PERSING, D. H., ARMSTRONG, A. L. & PEEPLES, R. A. 1991. Kinetics of Borrelia burgdorferi dissemination and evolution of disease after intradermal inoculation of mice. *Am J Pathol,* 139**,** 263-73.

BASU, S., HESS, S., NIELSEN BRAAD, P. E., OLSEN, B. B., INGLEV, S. & HØILUND-CARLSEN, P. F. 2014. The Basic Principles of FDG-PET/CT Imaging. *PET Clin,* 9**,** 355-70, v.

BASU, S., KWEE, T. C., SURTI, S., AKIN, E. A., YOO, D. & ALAVI, A. 2011. Fundamentals of PET and PET/CT imaging. *Ann N Y Acad Sci,* 1228**,** 1-18.

BAXTER, R. H., CONTET, A. & KRUEGER, K. 2017. Arthropod Innate Immune Systems and Vector-Borne Diseases. *Biochemistry,* 56**,** 907-918.

BEADSMOORE, C., NEWMAN, D., MACIVER, D. & PAWAROO, D. 2015. Positron Emission Tomography Computed Tomography: A Guide for the General Radiologist. *Can Assoc Radiol J*.

BECKER, N. S., MARGOS, G., BLUM, H., KREBS, S., GRAF, A., LANE, R. S., CASTILLO-RAMÍREZ, S., SING, A. & FINGERLE, V. 2016. Recurrent evolution of host and vector association in bacteria of the Borrelia burgdorferi sensu lato species complex. *BMC Genomics,* 17**,** 734.

BENACH, J. L., BOSLER, E. M., HANRAHAN, J. P., COLEMAN, J. L., HABICHT, G. S., BAST, T. F., CAMERON, D. J., ZIEGLER, J. L., BARBOUR, A. G., BURGDORFER, W., EDELMAN, R. & KASLOW, R. A. 1983. Spirochetes isolated from the blood of two patients with Lyme disease. *N Engl J Med,* 308**,** 740-2.

BENOIT, V. M., FISCHER, J. R., LIN, Y. P., PARVEEN, N. & LEONG, J. M. 2011. Allelic variation of the Lyme disease spirochete adhesin DbpA influences spirochetal binding to decorin, dermatan sulfate, and mammalian cells. *Infect Immun,* 79**,** 3501-9.

BERENDE, A., OOSTING, M., KULLBERG, B. J., NETEA, M. G. & JOOSTEN, L. A. 2010. Activation of innate host defense mechanisms by Borrelia. *Eur Cytokine Netw,* 21**,** 7-18.

BERGER, B. W., JOHNSON, R. C., KODNER, C. & COLEMAN, L. 1994. Cultivation of Borrelia burgdorferi from the blood of two patients with erythema migrans lesions lacking extracutaneous signs and symptoms of Lyme disease. *J Am Acad Dermatol,* 30**,** 48-51.

BERNARD, S. C., SIMPSON, N., JOIN-LAMBERT, O., FEDERICI, C., LARAN-CHICH, M. P., MAÏSSA, N., BOUZINBA-SÉGARD, H., MORAND, P. C., CHRETIEN, F., TAOUJI, S., CHEVET, E., JANEL, S., LAFONT, F., COUREUIL, M., SEGURA, A., NIEDERGANG, F., MARULLO, S., COURAUD, P. O., NASSIF, X. & BOURDOULOUS, S. 2014. Pathogenic Neisseria meningitidis utilizes CD147 for vascular colonization. *Nat Med,* 20**,** 725-31.

BERNARDINO, A. L., MYERS, T. A., ALVAREZ, X., HASEGAWA, A. & PHILIPP, M. T. 2008. Toll-like receptors: insights into their possible role in the pathogenesis of lyme neuroborreliosis. *Infect Immun,* 76**,** 4385-95.

BIANCO, P., FISHER, L. W., YOUNG, M. F., TERMINE, J. D. & ROBEY, P. G. 1990. Expression and localization of the two small proteoglycans biglycan and decorin in developing human skeletal and non-skeletal tissues. *J Histochem Cytochem,* 38**,** 1549-63.

BOCKENSTEDT, L. K., GONZALEZ, D. G., HABERMAN, A. M. & BELPERRON, A. A. 2012. Spirochete antigens persist near cartilage after murine Lyme borreliosis therapy. *J Clin Invest,* 122**,** 2652-60.

BOCKENSTEDT, L. K., MAO, J., HODZIC, E., BARTHOLD, S. W. & FISH, D. 2002. Detection of attenuated, noninfectious spirochetes in Borrelia burgdorferi-infected mice after antibiotic treatment. *J Infect Dis,* 186**,** 1430-7.

BOUQUET, J., SOLOSKI, M. J., SWEI, A., CHEADLE, C., FEDERMAN, S., BILLAUD, J. N., REBMAN, A. W., KABRE, B., HALPERT, R., BOORGULA, M., AUCOTT, J. N. & CHIU, C. Y. 2016. Longitudinal Transcriptome Analysis Reveals a Sustained Differential Gene Expression Signature in Patients Treated for Acute Lyme Disease. *MBio,* 7**,** e00100-16.

BRANDT, F. C., ERTAS, B., FALK, T. M., METZE, D. & BÖER-AUER, A. 2014. Genotyping of Borrelia from formalin-fixed paraffin-embedded skin biopsies of cutaneous borreliosis and tick bite reactions by assays targeting the intergenic spacer region, ospA and ospC genes. *Br J Dermatol,* 171**,** 528-43.

BRANDT, M. E., RILEY, B. S., RADOLF, J. D. & NORGARD, M. V. 1990. Immunogenic integral membrane proteins of Borrelia burgdorferi are lipoproteins. *Infect Immun,* 58**,** 983-91.

BREMELL, D., MATTSSON, N., EDSBAGGE, M., BLENNOW, K., ANDREASSON, U., WIKKELSÖ, C., ZETTERBERG, H. & HAGBERG, L. 2013. Cerebrospinal fluid CXCL13 in Lyme neuroborreliosis and asymptomatic HIV infection. *BMC Neurol,* 13**,** 2.

BRISSETTE, C. A. & GAULTNEY, R. A. 2014. That's my story, and I'm sticking to it--an update on B. burgdorferi adhesins. *Front Cell Infect Microbiol,* 4**,** 41.

BRITES-NETO, J., DUARTE, K. M. & MARTINS, T. F. 2015. Tick-borne infections in human and animal population worldwide. *Vet World,* 8**,** 301-15.

BROWN, E. L., GUO, B. P., O'NEAL, P. & HÖÖK, M. 1999. Adherence of Borrelia burgdorferi. Identification of critical lysine residues in DbpA required for decorin binding. *J Biol Chem,* 274**,** 26272-8.

BROWN, E. L., WOOTEN, R. M., JOHNSON, B. J., IOZZO, R. V., SMITH, A., DOLAN, M. C., GUO, B. P., WEIS, J. J. & HÖÖK, M. 2001. Resistance to Lyme disease in decorin-deficient mice. *J Clin Invest,* 107**,** 845-52.

BRUNN, A., MONTESINOS-RONGEN, M., STRACK, A., REIFENBERGER, G., MAWRIN, C., SCHALLER, C. & DECKERT, M. 2007. Expression pattern and cellular sources of chemokines in primary central nervous system lymphoma. *Acta Neuropathol,* 114**,** 271-6.

BURGDORFER, W., BARBOUR, A. G., HAYES, S. F., BENACH, J. L., GRUNWALDT, E. & DAVIS, J. P. 1982. Lyme disease-a tick-borne spirochetosis? *Science,* 216**,** 1317-9.

CAIMANO, M. J. 2018. Generation of Mammalian Host-Adapted Borrelia burgdorferi by Cultivation in Peritoneal Dialysis Membrane Chamber Implantation in Rats. *Methods Mol Biol,* 1690**,** 35-45.

CARRASCO, S. E., TROXELL, B., YANG, Y., BRANDT, S. L., LI, H., SANDUSKY, G. E., CONDON, K. W., SEREZANI, C. H. & YANG, X. F. 2015. Outer surface protein OspC is an antiphagocytic factor that protects Borrelia burgdorferi from phagocytosis by macrophages. *Infect Immun,* 83**,** 4848-60.

CASJENS, S., PALMER, N., VAN VUGT, R., HUANG, W. M., STEVENSON, B., ROSA, P., LATHIGRA, R., SUTTON, G., PETERSON, J., DODSON, R. J., HAFT, D., HICKEY, E., GWINN, M., WHITE, O. & FRASER, C. M. 2000. A bacterial genome in flux: the twelve linear and nine circular extrachromosomal DNAs in an infectious isolate of the Lyme disease spirochete Borrelia burgdorferi. *Mol Microbiol,* 35**,** 490-516.

CASJENS, S. R., DI, L., AKTHER, S., MONGODIN, E. F., LUFT, B. J., SCHUTZER, S. E., FRASER, C. M. & QIU, W. G. 2018. Primordial origin and diversification of plasmids in Lyme disease agent bacteria. *BMC Genomics,* 19**,** 218.

CASJENS, S. R., GILCREASE, E. B., VUJADINOVIC, M., MONGODIN, E. F., LUFT, B. J., SCHUTZER, S. E., FRASER, C. M. & QIU, W. G. 2017. Plasmid diversity and phylogenetic consistency in the Lyme disease agent Borrelia burgdorferi. *BMC Genomics,* 18**,** 165.

CASJENS, S. R., MONGODIN, E. F., QIU, W. G., LUFT, B. J., SCHUTZER, S. E., GILCREASE, E. B., HUANG, W. M., VUJADINOVIC, M., ARON, J. K., VARGAS, L. C., FREEMAN, S., RADUNE, D., WEIDMAN, J. F., DIMITROV, G. I., KHOURI, H. M., SOSA, J. E., HALPIN, R. A., DUNN, J. J. & FRASER, C. M. 2012. Genome stability of Lyme disease spirochetes: comparative genomics of Borrelia burgdorferi plasmids. *PLoS One,* 7**,** e33280.

CASSATT, D. R., PATEL, N. K., ULBRANDT, N. D. & HANSON, M. S. 1998. DbpA, but not OspA, is expressed by Borrelia burgdorferi during spirochetemia and is a target for protective antibodies. *Infect Immun,* 66**,** 5379-87.

CEPOK, S., ZHOU, D., VOGEL, F., ROSCHE, B., GRUMMEL, V., SOMMER, N. & HEMMER, B. 2003. The immune response at onset and during recovery from Borrelia burgdorferi meningoradiculitis. *Arch Neurol,* 60**,** 849-55.

CERAR, T., OGRINC, K., LOTRIC-FURLAN, S., KOBAL, J., LEVICNIK-STEZINAR, S., STRLE, F. & RUZIĆ-SABLJIC, E. 2013. Diagnostic value of cytokines and chemokines in lyme neuroborreliosis. *Clin Vaccine Immunol,* 20**,** 1578-84.

CERAR, T., STRLE, F., STUPICA, D., RUZIC-SABLJIC, E., MCHUGH, G., STEERE, A. C. & STRLE, K. 2016. Differences in Genotype, Clinical Features, and Inflammatory Potential of Borrelia burgdorferi sensu stricto Strains from Europe and the United States. *Emerg Infect Dis,* 22**,** 818-27.

CHANG, Y. C., WANG, Z., FLAX, L. A., XU, D., ESKO, J. D., NIZET, V. & BARON, M. J. 2011. Glycosaminoglycan binding facilitates entry of a bacterial pathogen into central nervous systems. *PLoS Pathog,* 7**,** e1002082.

CLAES, J., VANASSCHE, T., PEETERMANS, M., LIESENBORGHS, L., VANDENBRIELE, C., VANHOORELBEKE, K., MISSIAKAS, D., SCHNEEWIND, O., HOYLAERTS, M. F., HEYING, R. & VERHAMME, P. 2014. Adhesion of Staphylococcus aureus to the vessel wall under flow is mediated by von Willebrand factor-binding protein. *Blood,* 124**,** 1669-76.

CLARK, K. L., LEYDET, B. F. & THRELKELD, C. 2014. Geographical and genospecies distribution of Borrelia burgdorferi sensu lato DNA detected in humans in the USA. *J Med Microbiol,* 63**,** 674-84.

COBURN, J., LEONG, J. & CHACONAS, G. 2013. Illuminating the roles of the Borrelia burgdorferi adhesins. *Trends Microbiol,* 21**,** 372-9.

COBURN, J., MAGOUN, L., BODARY, S. C. & LEONG, J. M. 1998. Integrins alpha(v)beta3 and alpha5beta1 mediate attachment of lyme disease spirochetes to human cells. *Infect Immun,* 66**,** 1946-52.

COIPAN, E. C., JAHFARI, S., FONVILLE, M., OEI, G. A., SPANJAARD, L., TAKUMI, K., HOVIUS, J. W. & SPRONG, H. 2016. Imbalanced presence of Borrelia burgdorferi s.l. multilocus sequence types in clinical manifestations of Lyme borreliosis. *Infect Genet Evol,* 42**,** 66-76.

COLEMAN, J. L., SELLATI, T. J., TESTA, J. E., KEW, R. R., FURIE, M. B. & BENACH, J. L. 1995. Borrelia burgdorferi binds plasminogen, resulting in enhanced penetration of endothelial monolayers. *Infect Immun,* 63**,** 2478-84.

COLLARES-PEREIRA, M., COUCEIRO, S., FRANCA, I., KURTENBACH, K., SCHÄFER, S. M., VITORINO, L., GONÇALVES, L., BAPTISTA, S., VIEIRA, M. L. & CUNHA, C. 2004. First isolation of Borrelia lusitaniae from a human patient. *J Clin Microbiol,* 42**,** 1316-8.

COMSTOCK, L. E. & THOMAS, D. D. 1989. Penetration of endothelial cell monolayers by Borrelia burgdorferi. *Infect Immun,* 57**,** 1626-8.

COMSTOCK, L. E. & THOMAS, D. D. 1991. Characterization of Borrelia burgdorferi invasion of cultured endothelial cells. *Microb Pathog,* 10**,** 137-48.

COOK, M. J. 2015. Lyme borreliosis: a review of data on transmission time after tick attachment. *Int J Gen Med,* 8**,** 1-8.

COUREUIL, M., LÉCUYER, H., BOURDOULOUS, S. & NASSIF, X. 2017. A journey into the brain:

insight into how bacterial pathogens cross blood-brain barriers. *Nat Rev Microbiol,* 15**,** 149-159.

COURTIOUX, B., PERVIEUX, L., VATUNGA, G., MARIN, B., JOSENANDO, T., JAUBERTEAU-MARCHAN, M. O., BOUTEILLE, B. & BISSER, S. 2009. Increased CXCL-13 levels in human African trypanosomiasis meningo-encephalitis. *Trop Med Int Health,* 14**,** 529-34.

CUCULLO, L., HOSSAIN, M., PUVENNA, V., MARCHI, N. & JANIGRO, D. 2011. The role of shear stress in Blood-Brain Barrier endothelial physiology. *BMC Neurosci,* 12**,** 40.

CYSTER, J. G., ANSEL, K. M., REIF, K., EKLAND, E. H., HYMAN, P. L., TANG, H. L., LUTHER, S. A. & NGO, V. N. 2000. Follicular stromal cells and lymphocyte homing to follicles. *Immunol Rev,* 176**,** 181-93.

DANDO, S. J., MACKAY-SIM, A., NORTON, R., CURRIE, B. J., ST JOHN, J. A., EKBERG, J. A., BATZLOFF, M., ULETT, G. C. & BEACHAM, I. R. 2014. Pathogens penetrating the central nervous system: infection pathways and the cellular and molecular mechanisms of invasion. *Clin Microbiol Rev,* 27**,** 691-726.

DE TAEYE, S. W., KREUK, L., VAN DAM, A. P., HOVIUS, J. W. & SCHUIJT, T. J. 2013. Complement evasion by Borrelia burgdorferi: it takes three to tango. *Trends Parasitol,* 29**,** 119-28.

DERSCH, R., HOTTENROTT, T., SENEL, M., LEHMENSIEK, V., TUMANI, H., RAUER, S. & STICH, O. 2015. The chemokine CXCL13 is elevated in the cerebrospinal fluid of patients with neurosyphilis. *Fluids Barriers CNS,* 12**,** 12.

DESSAU, R. B., VAN DAM, A. P., FINGERLE, V., GRAY, J., HOVIUS, J., HUNFELD, K. P., JAULHAC, B., KAHL, O., KRISTOFERITSCH, W., LINDGREN, P. E., MARKOWICZ, M., MAVIN, S., ORNSTEIN, K., RUPPRECHT, T., STANEK, G. & STRLE, F. 2017. To test or not to test? Laboratory support for the diagnosis of Lyme borreliosis. *Clin Microbiol Infect*.

DI, L., PAGAN, P. E., PACKER, D., MARTIN, C. L., AKTHER, S., RAMRATTAN, G., MONGODIN, E. F., FRASER, C. M., SCHUTZER, S. E., LUFT, B. J., CASJENS, S. R. & QIU, W. G. 2014. BorreliaBase: a phylogeny-centered browser of Borrelia genomes. *BMC Bioinformatics,* 15**,** 233.

DIVAN, A., CASSELLI, T., NARAYANAN, S. A., MUKHERJEE, S., ZAWIEJA, D. C., WATT, J. A., BRISSETTE, C. A. & NEWELL-ROGERS, M. K. 2018. Borrelia burgdorferi adhere to blood vessels in the dura mater and are associated with increased meningeal T cells during murine disseminated borreliosis. *PLoS One,* 13**,** e0196893.

EBADY, R., NIDDAM, A. F., BOCZULA, A. E., KIM, Y. R., GUPTA, N., TANG, T. T., ODISHO, T., ZHI, H., SIMMONS, C. A., SKARE, J. T. & MORIARTY, T. J. 2016. Biomechanics of Borrelia burgdorferi Vascular Interactions. *Cell Rep,* 16**,** 2593-604.

ECKMAN, E. A., PACHECO-QUINTO, J., HERDT, A. R. & HALPERIN, J. J. 2018. Neuroimmunomodulators in neuroborreliosis and Lyme encephalopathy. *Clin Infect Dis*.

EDWARDS, I. J. 2012. Proteoglycans in prostate cancer. *Nat Rev Urol,* 9**,** 196-206.

EIGENMANN, D. E., XUE, G., KIM, K. S., MOSES, A. V., HAMBURGER, M. & OUFIR, M. 2013. Comparative study of four immortalized human brain capillary endothelial cell lines, hCMEC/D3, hBMEC, TY10, and BB19, and optimization of culture conditions, for an in vitro blood-brain barrier model for drug permeability studies. *Fluids Barriers CNS,* 10**,** 33.

EISEN, L. 2018. Pathogen transmission in relation to duration of attachment by Ixodes scapularis ticks. *Ticks Tick Borne Dis,* 9**,** 535-542.

ENGELHARDT, B., CARARE, R. O., BECHMANN, I., FLÜGEL, A., LAMAN, J. D. & WELLER, R. O. 2016. Vascular, glial, and lymphatic immune gateways of the central nervous system. *Acta Neuropathol,* 132**,** 317-38.

ERMERT, D. & LAABEI, M. 2018. Catch Me if You Can: Streptococcus pyogenes Complement Evasion Strategies. *J Innate Immun***,** 1-10.

EXNER, M. M., WU, X., BLANCO, D. R., MILLER, J. N. & LOVETT, M. A. 2000. Protection elicited by native outer membrane protein Oms66 (p66) against host-adapted Borrelia burgdorferi: conformational nature of bactericidal epitopes. *Infect Immun,* 68**,** 2647-54.

FECHTNER, T., STALLMANN, S., MOELLEKEN, K., MEYER, K. L. & HEGEMANN, J. H. 2013. Characterization of the interaction between the chlamydial adhesin OmcB and the human host cell. *J Bacteriol,* 195**,** 5323-33.

FEENSTRA, T., THØGERSEN, M. S., WIESER, E., PESCHEL, A., BALL, M. J., BRANDES, R., SATCHELL, S. C., STOCKNER, T., AARESTRUP, F. M., REES, A. J. & KAIN, R. 2017. Adhesion of Escherichia coli under flow conditions reveals potential novel effects of FimH mutations. *Eur J Clin Microbiol Infect Dis,* 36**,** 467-478.

FENG, W. & WANG, X. 2015. Structure of decorin binding protein B from Borrelia burgdorferi and its interactions with glycosaminoglycans. *Biochim Biophys Acta,* 1854**,** 1823-32.

FERDOWS, M. S. & BARBOUR, A. G. 1989. Megabase-sized linear DNA in the bacterium Borrelia burgdorferi, the Lyme disease agent. *Proc Natl Acad Sci U S A,* 86**,** 5969-73.

FERNÁNDEZ, F. J., GÓMEZ, S. & VEGA, M. C. 2017. Pathogens' toolbox to manipulate human complement. *Semin Cell Dev Biol*.

FINGERLE, V., SCHULTE-SPECHTEL, U. C., RUZIC-SABLJIC, E., LEONHARD, S., HOFMANN, H.,

WEBER, K., PFISTER, K., STRLE, F. & WILSKE, B. 2008. Epidemiological aspects and molecular characterization of Borrelia burgdorferi s.l. from southern Germany with special respect to the new species Borrelia spielmanii sp. nov. *Int J Med Microbiol,* 298**,** 279-90.

FISHER, L. W., TERMINE, J. D. & YOUNG, M. F. 1989. Deduced protein sequence of bone small proteoglycan I (biglycan) shows homology with proteoglycan II (decorin) and several nonconnective tissue proteins in a variety of species. *J Biol Chem,* 264**,** 4571-6.

FLEMMING, D. J., HASH, T. W., BERNARD, S. A. & BRIAN, P. S. 2014. MR imaging assessment of arthritis of the knee. *Magn Reson Imaging Clin N Am,* 22**,** 703-24.

FORTUNE, D. E., LIN, Y. P., DEKA, R. K., GROSHONG, A. M., MOORE, B. P., HAGMAN, K. E., LEONG, J. M., TOMCHICK, D. R. & BLEVINS, J. S. 2014. Identification of lysine residues in the Borrelia burgdorferi DbpA adhesin required for murine infection. *Infect Immun,* 82**,** 3186-98.

FRASER, C. M., CASJENS, S., HUANG, W. M., SUTTON, G. G., CLAYTON, R., LATHIGRA, R., WHITE, O., KETCHUM, K. A., DODSON, R., HICKEY, E. K., GWINN, M., DOUGHERTY, B., TOMB, J. F., FLEISCHMANN, R. D., RICHARDSON, D., PETERSON, J., KERLAVAGE, A. R., QUACKENBUSH, J., SALZBERG, S., HANSON, M., VAN VUGT, R., PALMER, N., ADAMS, M. D., GOCAYNE, J., WEIDMAN, J., UTTERBACK, T., WATTHEY, L., MCDONALD, L., ARTIACH, P., BOWMAN, C., GARLAND, S., FUJI, C., COTTON, M. D., HORST, K., ROBERTS, K., HATCH, B., SMITH, H. O. & VENTER, J. C. 1997. Genomic sequence of a Lyme disease spirochaete, Borrelia burgdorferi. *Nature,* 390**,** 580-6.

FREVERT, C. W., FELGENHAUER, J., WYGRECKA, M., NASTASE, M. V. & SCHAEFER, L. 2017. Danger-Associated Molecular Patterns Derived From the Extracellular Matrix Provide Temporal Control of Innate Immunity. *J Histochem Cytochem***,** 22155417740880.

FREY, H., SCHROEDER, N., MANON-JENSEN, T., IOZZO, R. V. & SCHAEFER, L. 2013. Biological interplay between proteoglycans and their innate immune receptors in inflammation. *FEBS J.*

FURIHATA, T., KAWAMATSU, S., ITO, R., SAITO, K., SUZUKI, S., KISHIDA, S., SAITO, Y., KAMIICHI, A. & CHIBA, K. 2015. Hydrocortisone enhances the barrier properties of HBMEC/ciβ, a brain microvascular endothelial cell line, through mesenchymal-to-endothelial transition-like effects. *Fluids Barriers CNS,* 12**,** 7.

GARCIA-MONCO, J. C. & BENACH, J. L. 2013. A disconnect between the neurospirochetoses in humans and rodent models of disease. *PLoS Pathog,* 9**,** e1003288.

GARKOWSKI, A., ZAJKOWSKA, J., ZAJKOWSKA, A., KUŁAKOWSKA, A., ZAJKOWSKA, O., KUBAS, B., JURGILEWICZ, D., HŁADUŃSKI, M. & ŁEBKOWSKA, U. 2017. Cerebrovascular Manifestations of Lyme Neuroborreliosis-A Systematic Review of Published Cases. *Front Neurol,* 8**,** 146.

GASIC, G. & GASIC, T. 1962. Removal of sialic acid from the cell coat in tumor cells and vascular endothelium, and its effects on metastasis. *Proc Natl Acad Sci U S A,* 48**,** 1172-7.

GLICKSTEIN, L. J. & COBURN, J. L. 2006. Short report: Association of macrophage inflammatory response and cell death after in vitro Borrelia burgdorferi infection with arthritis resistance. *Am J Trop Med Hyg,* 75**,** 964-7.

GOLDSTEIN, S. F., BUTTLE, K. F. & CHARON, N. W. 1996. Structural analysis of the Leptospiraceae and Borrelia burgdorferi by high-voltage electron microscopy. *J Bacteriol,* 178**,** 6539-45.

GRAB, D. J., NYARKO, E., NIKOLSKAIA, O. V., KIM, Y. V. & DUMLER, J. S. 2009. Human brain microvascular endothelial cell traversal by Borrelia burgdorferi requires calcium signaling. *Clin Microbiol Infect,* 15**,** 422-6.

GRAB, D. J., PERIDES, G., DUMLER, J. S., KIM, K. J., PARK, J., KIM, Y. V., NIKOLSKAIA, O., CHOI, K. S., STINS, M. F. & KIM, K. S. 2005. Borrelia burgdorferi, host-derived proteases, and the blood-brain barrier. *Infect Immun,* 73**,** 1014-22.

GRUSELL, M., WIDHE, M. & EKERFELT, C. 2002. Increased expression of the Th1-inducing cytokines interleukin-12 and interleukin-18 in cerebrospinal fluid but not in sera from patients with Lyme neuroborreliosis. *J Neuroimmunol,* 131**,** 173-8.

GRYGORCZUK, S., PANCEWICZ, S., ZAJKOWSKA, J., KONDRUSIK, M., RWIERZBIŃSKA, R. & HERMANOWSKA-SZPAKOWICZ, T. 2004. Concentrations of macrophage inflammatory proteins MIP-1alpha and MIP-1beta and interleukin 8 (il-8) in lyme borreliosis. *Infection,* 32**,** 350-5.

GUNN, M. D., NGO, V. N., ANSEL, K. M., EKLAND, E. H., CYSTER, J. G. & WILLIAMS, L. T. 1998. A B-cell-homing chemokine made in lymphoid follicles activates Burkitt's lymphoma receptor-1. *Nature,* 391**,** 799-803.

GUO, B. P., BROWN, E. L., DORWARD, D. W., ROSENBERG, L. C. & HÖÖK, M. 1998. Decorin-binding adhesins from Borrelia burgdorferi. *Mol Microbiol,* 30**,** 711-23.

GUPTA, R. S., MAHMOOD, S. & ADEOLU, M. 2013. A phylogenomic and molecular signature based approach for characterization of the phylum Spirochaetes and its major clades: proposal for a

taxonomic revision of the phylum. *Front Microbiol,* 4**,** 217.

GYLLEMARK, P., FORSBERG, P., ERNERUDH, J. & HENNINGSSON, A. J. 2017. Intrathecal Th17- and B cell-associated cytokine and chemokine responses in relation to clinical outcome in Lyme neuroborreliosis: a large retrospective study. *J Neuroinflammation,* 14**,** 27.

HAGMAN, K. E., LAHDENNE, P., POPOVA, T. G., PORCELLA, S. F., AKINS, D. R., RADOLF, J. D. & NORGARD, M. V. 1998. Decorin-binding protein of Borrelia burgdorferi is encoded within a two-gene operon and is protective in the murine model of Lyme borreliosis. *Infect Immun,* 66**,** 2674-83.

HALPERIN, J. J. 2017. Neuroborreliosis. *J Neurol,* 264**,** 1292-1297.

HATCHETTE, T. F., JOHNSTON, B. L., SCHLEIHAUF, E., MASK, A., HALDANE, D., DREBOT, M., BAIKIE, M., COLE, T. J., FLEMING, S., GOULD, R. & LINDSAY, R. 2015. Epidemiology of Lyme Disease, Nova Scotia, Canada, 2002-2013. *Emerg Infect Dis,* 21**,** 1751-8.

HEIKKILÄ, T., SEPPÄLÄ, I., SAXEN, H., PANELIUS, J., PELTOMAA, M., HUPPERTZ, H. I. & LAHDENNE, P. 2002a. Cloning of the gene encoding the decorin-binding protein B (DbpB) in Borrelia burgdorferi sensu lato and characterisation of the antibody responses to DbpB in Lyme borreliosis. *J Med Microbiol,* 51**,** 641-8.

HEIKKILÄ, T., SEPPÄLÄ, I., SAXEN, H., PANELIUS, J., YRJÄNÄINEN, H. & LAHDENNE, P. 2002b. Species-specific serodiagnosis of Lyme arthritis and neuroborreliosis due to Borrelia burgdorferi sensu stricto, B. afzelii, and B. garinii by using decorin binding protein A. *J Clin Microbiol,* 40**,** 453-60.

HEINEGÅRD, D. & OLDBERG, A. 1989. Structure and biology of cartilage and bone matrix noncollagenous macromolecules. *FASEB J,* 3**,** 2042-51.

HENNINGSSON, A. J., GYLLEMARK, P., LAGER, M., SKOGMAN, B. H. & TJERNBERG, I. 2016. Evaluation of two assays for CXCL13 analysis in cerebrospinal fluid for laboratory diagnosis of Lyme neuroborreliosis. *APMIS,* 124**,** 985-990.

HENNINGSSON, A. J., TJERNBERG, I., MALMVALL, B. E., FORSBERG, P. & ERNERUDH, J. 2011. Indications of Th1 and Th17 responses in cerebrospinal fluid from patients with Lyme neuroborreliosis: a large retrospective study. *J Neuroinflammation,* 8**,** 36.

HESS, S., HANSSON, S. H., PEDERSEN, K. T., BASU, S. & HØILUND-CARLSEN, P. F. 2014. FDG-PET/CT in Infectious and Inflammatory Diseases. *PET Clin,* 9**,** 497-519, vi-vii.

HIRSCHFELD, M., KIRSCHNING, C. J., SCHWANDNER, R., WESCHE, H., WEIS, J. H., WOOTEN, R. M. & WEIS, J. J. 1999. Cutting edge: inflammatory signaling by Borrelia burgdorferi lipoproteins is mediated by toll-like receptor 2. *J Immunol,* 163**,** 2382-6.

HOCKING, A. M., STRUGNELL, R. A., RAMAMURTHY, P. & MCQUILLAN, D. J. 1996. Eukaryotic expression of recombinant biglycan. Post-translational processing and the importance of secondary structure for biological activity. *J Biol Chem,* 271**,** 19571-7.

HODZIC, E., FENG, S., FREET, K. J. & BARTHOLD, S. W. 2003. Borrelia burgdorferi population dynamics and prototype gene expression during infection of immunocompetent and immunodeficient mice. *Infect Immun,* 71**,** 5042-55.

HODZIC, E., FENG, S., HOLDEN, K., FREET, K. J. & BARTHOLD, S. W. 2008. Persistence of Borrelia burgdorferi following antibiotic treatment in mice. *Antimicrob Agents Chemother,* 52**,** 1728-36.

HODZIC, E., IMAI, D., FENG, S. & BARTHOLD, S. W. 2014. Resurgence of persisting non-cultivable Borrelia burgdorferi following antibiotic treatment in mice. *PLoS One,* 9**,** e86907.

HOFHUIS, A., VAN DE KASSTEELE, J., SPRONG, H., VAN DEN WIJNGAARD, C. C., HARMS, M. G., FONVILLE, M., DOCTERS VAN LEEUWEN, A., SIMÕES, M. & VAN PELT, W. 2017. Predicting the risk of Lyme borreliosis after a tick bite, using a structural equation model. *PLoS One,* 12**,** e0181807.

HOVIUS, J. W., DE JONG, M. A., DEN DUNNEN, J., LITJENS, M., FIKRIG, E., VAN DER POLL, T., GRINGHUIS, S. I. & GEIJTENBEEK, T. B. 2008. Salp15 binding to DC-SIGN inhibits cytokine expression by impairing both nucleosome remodeling and mRNA stabilization. *PLoS Pathog,* 4**,** e31.

HUPPERTZ, H. I., BÖHME, M., STANDAERT, S. M., KARCH, H. & PLOTKIN, S. A. 1999. Incidence of Lyme borreliosis in the Würzburg region of Germany. *Eur J Clin Microbiol Infect Dis,* 18**,** 697-703.

HYDE, J. A. 2017. Borrelia burgdorferi Keeps Moving and Carries on: A Review of Borrelial Dissemination and Invasion. *Front Immunol,* 8**,** 114.

HYDE, J. A., WEENING, E. H., CHANG, M., TRZECIAKOWSKI, J. P., HÖÖK, M., CIRILLO, J. D. & SKARE, J. T. 2011. Bioluminescent imaging of Borrelia burgdorferi in vivo demonstrates that the fibronectin-binding protein BBK32 is required for optimal infectivity. *Mol Microbiol,* 82**,** 99-113.

HYTÖNEN, J., HARTIALA, P., OKSI, J. & VILJANEN, M. K. 2008. Borreliosis: recent research, diagnosis, and management. *Scand J Rheumatol,* 37**,** 161-72.

HYTÖNEN, J., KORTELA, E., WARIS, M., PUUSTINEN, J., SALO, J. & OKSI, J. 2014. CXCL13 and neopterin concentrations in cerebrospinal fluid of patients with Lyme neuroborreliosis and other diseases that cause neuroinflammation. *J Neuroinflammation,* 11**,** 103.

IMAI, D. M., SAMUELS, D. S., FENG, S., HODZIC, E., OLSEN, K. & BARTHOLD, S. W. 2013. The Early Dissemination Defect Attributed to Disruption of Decorin-binding Proteins is Abolished in Chronic Murine Lyme Borreliosis. *Infect Immun*.

JAVID, A., ZLOTNIKOV, N., PĚTROŠOVÁ, H., TANG, T. T., ZHANG, Y., BANSAL, A. K., EBADY, R., PARIKH, M., AHMED, M., SUN, C., NEWBIGGING, S., KIM, Y. R., SANTANA SOSA, M., GLOGAUER, M. & MORIARTY, T. J. 2016. Hyperglycemia Impairs Neutrophil-Mediated Bacterial Clearance in Mice Infected with the Lyme Disease Pathogen. *PLoS One,* 11**,** e0158019.

JENKINS, A., HVIDSTEN, D., MATUSSEK, A., LINDGREN, P. E., STUEN, S. & KRISTIANSEN, B. E. 2012. Borrelia burgdorferi sensu lato in Ixodes ricinus ticks from Norway: evaluation of a PCR test targeting the chromosomal flaB gene. *Exp Appl Acarol,* 58**,** 431-9.

JIANG, B. C., CAO, D. L., ZHANG, X., ZHANG, Z. J., HE, L. N., LI, C. H., ZHANG, W. W., WU, X. B., BERTA, T., JI, R. R. & GAO, Y. J. 2016. CXCL13 drives spinal astrocyte activation and neuropathic pain via CXCR5. *J Clin Invest,* 126**,** 745-61.

JÄRVELÄINEN, H., SAINIO, A. & WIGHT, T. N. 2015. Pivotal role for decorin in angiogenesis. *Matrix Biol,* 43**,** 15-26.

JÄRVELÄINEN, H. T., KINSELLA, M. G., WIGHT, T. N. & SANDELL, L. J. 1991. Differential expression of small chondroitin/dermatan sulfate proteoglycans, PG-I/biglycan and PG-II/decorin, by vascular smooth muscle and endothelial cells in culture. *J Biol Chem,* 266**,** 23274-81.

KALINA, P., DECKER, A., KORNEL, E. & HALPERIN, J. J. 2005. Lyme disease of the brainstem. *Neuroradiology,* 47**,** 903-7.

KAMIICHI, A., FURIHATA, T., KISHIDA, S., OHTA, Y., SAITO, K., KAWAMATSU, S. & CHIBA, K. 2012. Establishment of a new conditionally immortalized cell line from human brain microvascular endothelial cells: a promising tool for human blood-brain barrier studies. *Brain Res,* 1488**,** 113-22.

KAO, W. A., PĚTROŠOVÁ, H., EBADY, R., LITHGOW, K. V., ROJAS, P., ZHANG, Y., KIM, Y. E., KIM, Y. R., ODISHO, T., GUPTA, N., MOTER, A., CAMERON, C. E. & MORIARTY, T. J. 2017. Identification of Tp0751 (Pallilysin) as a Treponema pallidum Vascular Adhesin by Heterologous Expression in the Lyme disease Spirochete. *Sci Rep,* 7**,** 1538.

KAZRAGIS, R. J., DEVER, L. L., JORGENSEN, J. H. & BARBOUR, A. G. 1996. In vivo activities of ceftriaxone and vancomycin against Borrelia spp. in the mouse brain and other sites. *Antimicrob Agents Chemother,* 40**,** 2632-6.

KELLER, A., GRAEFEN, A., BALL, M., MATZAS, M., BOISGUERIN, V., MAIXNER, F., LEIDINGER, P., BACKES, C., KHAIRAT, R., FORSTER, M., STADE, B., FRANKE, A., MAYER, J., SPANGLER, J., MCLAUGHLIN, S., SHAH, M., LEE, C., HARKINS, T. T., SARTORI, A., MORENO-ESTRADA, A., HENN, B., SIKORA, M., SEMINO, O., CHIARONI, J., ROOTSI, S., MYRES, N. M., CABRERA, V. M., UNDERHILL, P. A., BUSTAMANTE, C. D., VIGL, E. E., SAMADELLI, M., CIPOLLINI, G., HAAS, J., KATUS, H., O'CONNOR, B. D., CARLSON, M. R., MEDER, B., BLIN, N., MEESE, E., PUSCH, C. M. & ZINK, A. 2012. New insights into the Tyrolean Iceman's origin and phenotype as inferred by whole-genome sequencing. *Nat Commun,* 3**,** 698.

KENEDY, M. R., LENHART, T. R. & AKINS, D. R. 2012. The role of Borrelia burgdorferi outer surface proteins. *FEMS Immunol Med Microbiol,* 66**,** 1-19.

KERN, A., SCHNELL, G., BERNARD, Q., BŒUF, A., JAULHAC, B., COLLIN, E., BARTHEL, C., EHRET-SABATIER, L. & BOULANGER, N. 2015. Heterogeneity of Borrelia burgdorferi Sensu Stricto Population and Its Involvement in Borrelia Pathogenicity: Study on Murine Model with Specific Emphasis on the Skin Interface. *PLoS One,* 10**,** e0133195.

KIKUCHI, A., TOMOYASU, H., KIDO, I., TAKAHASHI, K., TANAKA, A., NONAKA, I., IWAKAMI, N. & KAMO, I. 2000. Haemopoietic biglycan produced by brain cells stimulates growth of microglial cells. *J Neuroimmunol,* 106**,** 78-86.

KINSELLA, M. G. & WIGHT, T. N. 1988. Isolation and characterization of dermatan sulfate proteoglycans synthesized by cultured bovine aortic endothelial cells. *J Biol Chem,* 263**,** 19222-31.

KITAYA, K. & YASUO, T. 2009. Dermatan sulfate proteoglycan biglycan as a potential selectin L/CD44 ligand involved in selective recruitment of peripheral blood CD16(-) natural killer cells into human endometrium. *J Leukoc Biol,* 85**,** 391-400.

KNUDTZEN, F. C., ANDERSEN, N. S., JENSEN, T. G. & SKARPHÉDINSSON, S. 2017. Characteristics and Clinical Outcome of Lyme Neuroborreliosis in a High Endemic Area, 1995-2014: A Retrospective Cohort Study in Denmark. *Clin Infect Dis,* 65**,** 1489-1495.

KOCK, R. A. 2015. Vertebrate reservoirs and secondary epidemiological cycles of vector-borne diseases. *Rev Sci Tech,* 34**,** 151-63.

KOEDEL, U., FINGERLE, V. & PFISTER, H. W. 2015. Lyme neuroborreliosis-epidemiology, diagnosis and management. *Nat Rev Neurol,* 11**,** 446-56.

KORTELA, E., HYTÖNEN, J., NUMMINEN, J., OVERMYER, M., SAXEN, H. & OKSI, J. 2017. Cerebral vasculitis and intracranial multiple aneurysms in a child with Lyme neuroborreliosis. *JMM Case Rep,* 4**,** e005090.

KOWARIK, M. C., CEPOK, S., SELLNER, J., GRUMMEL, V., WEBER, M. S., KORN, T., BERTHELE, A. & HEMMER, B. 2012. CXCL13 is the major determinant for B cell recruitment to the CSF during neuroinflammation. *J Neuroinflammation,* 9**,** 93.

KOZEL, T. R. & BURNHAM-MARUSICH, A. R. 2017. Point-of-Care Testing for Infectious Diseases: Past, Present, and Future. *J Clin Microbiol,* 55**,** 2313-2320.

KUMAR, D., RISTOW, L. C., SHI, M., MUKHERJEE, P., CAINE, J. A., LEE, W. Y., KUBES, P., COBURN, J. & CHACONAS, G. 2015. Intravital Imaging of Vascular Transmigration by the Lyme Spirochete: Requirement for the Integrin Binding Residues of the B. burgdorferi P66 Protein. *PLoS Pathog,* 11**,** e1005333.

KUNG, F., ANGUITA, J. & PAL, U. 2013. Borrelia burgdorferi and tick proteins supporting pathogen persistence in the vector. *Future Microbiol,* 8**,** 41-56.

LAABEI, M., LIU, G., ERMERT, D., LAMBRIS, J. D., RIESBECK, K. & BLOM, A. M. 2018. Short Leucine-Rich Proteoglycans Modulate Complement Activity and Increase Killing of the Respiratory Pathogen. *J Immunol*.

LAAKSONEN, M., KLEMOLA, T., FEUTH, E., SORMUNEN, J. J., PUISTO, A., MÄKELÄ, S., PENTTINEN, R., RUOHOMÄKI, K., HÄNNINEN, J., SÄÄKSJÄRVI, I. E., VUORINEN, I., SPRONG, H., HYTÖNEN, J. & VESTERINEN, E. J. 2018. Tick-borne pathogens in Finland: comparison of Ixodes ricinus and I. persulcatus in sympatric and parapatric areas. *Parasit Vectors,* 11**,** 556.

LAAKSONEN, M., SAJANTI, E., SORMUNEN, J. J., PENTTINEN, R., HÄNNINEN, J., RUOHOMÄKI, K., SÄÄKSJÄRVI, I., VESTERINEN, E. J., VUORINEN, I., HYTÖNEN, J. & KLEMOLA, T. 2017. Crowdsourcing-based nationwide tick collection reveals the distribution of Ixodes ricinus and I. persulcatus and associated pathogens in Finland. *Emerg Microbes Infect,* 6**,** e31.

LEMICHEZ, E., LECUIT, M., NASSIF, X. & BOURDOULOUS, S. 2010. Breaking the wall: targeting of the endothelium by pathogenic bacteria. *Nat Rev Microbiol,* 8**,** 93-104.

LEONG, J. M., WANG, H., MAGOUN, L., FIELD, J. A., MORRISSEY, P. E., ROBBINS, D., TATRO, J. B., COBURN, J. & PARVEEN, N. 1998. Different classes of proteoglycans contribute to the attachment of Borrelia burgdorferi to cultured endothelial and brain cells. *Infect Immun,* 66**,** 994-9.

LIANG, F. T., BROWN, E. L., WANG, T., IOZZO, R. V. & FIKRIG, E. 2004a. Protective niche for Borrelia burgdorferi to evade humoral immunity. *Am J Pathol,* 165**,** 977-85.

LIANG, F. T., YAN, J., MBOW, M. L., SVIAT, S. L., GILMORE, R. D., MAMULA, M. & FIKRIG, E. 2004b. Borrelia burgdorferi changes its surface antigenic expression in response to host immune responses. *Infect Immun,* 72**,** 5759-67.

LIBA, Z., KAYSEROVA, J. & KOMAREK, V. 2013. Th1 and Th17 but no Th2-related cytokine spectrum in the cerebrospinal fluid of children with Borrelia-related facial nerve palsy. *Fluids Barriers CNS,* 10**,** 30.

LIN, T., GAO, L., ZHANG, C., ODEH, E., JACOBS, M. B., COUTTE, L., CHACONAS, G., PHILIPP, M. T. & NORRIS, S. J. 2012. Analysis of an ordered, comprehensive STM mutant library in infectious Borrelia burgdorferi: insights into the genes required for mouse infectivity. *PLoS One,* 7**,** e47532.

LIN, Y. P., BENOIT, V., YANG, X., MARTÍNEZ-HERRANZ, R., PAL, U. & LEONG, J. M. 2014. Strain-specific variation of the decorin-binding adhesin DbpA influences the tissue tropism of the lyme disease spirochete. *PLoS Pathog,* 10**,** e1004238.

LIN, Y. R., CHEN, Y. L., WANG, K. B., WU, Y. F., WANG, Y. K., HUANG, S. C., LIU, T. A., NAYAK, M., YIP, B. S. & WU, T. K. 2013. The thermostable direct hemolysin from Grimontia hollisae causes acute hepatotoxicity in vitro and in vivo. *PLoS One,* 8**,** e56226.

LJUBIMOVA, J. Y., SUN, T., MASHOUF, L., LJUBIMOV, A. V., ISRAEL, L. L., LJUBIMOV, V. A., FALAHATIAN, V. & HOLLER, E. 2017. Covalent nano delivery systems for selective imaging and treatment of brain tumors. *Adv Drug Deliv Rev,* 113**,** 177-200.

LOCHHEAD, R. B., ARVIKAR, S. L., AVERSA, J. M., SADREYEV, R. I., STRLE, K. & STEERE, A. C. 2018. Robust interferon signature and suppressed tissue repair gene expression in synovial tissue from patients with post-infectious, Borrelia burgdorferi-induced Lyme arthritis. *Cell Microbiol***,** e12954.

LOGIGIAN, E. L., JOHNSON, K. A., KIJEWSKI, M. F., KAPLAN, R. F., BECKER, J. A., JONES, K. J., GARADA, B. M., HOLMAN, B. L. & STEERE, A. C. 1997. Reversible cerebral hypoperfusion in Lyme encephalopathy. *Neurology,* 49**,** 1661-70.

MA, Y., STURROCK, A. & WEIS, J. J. 1991. Intracellular localization of Borrelia burgdorferi within human endothelial cells. *Infect Immun,* 59**,** 671-8.

MADIGAN, M. T., MARTINKO, J. M., DUNLAP, P. V. & CLARK, D. P. 2009. *Brock Biology of Microorganisms,* San Francisco, CA, Pearson Benjamin Cummings.

MAIREY, E., GENOVESIO, A., DONNADIEU, E., BERNARD, C., JAUBERT, F., PINARD, E., SEYLAZ, J., OLIVO-MARIN, J. C., NASSIF, X. & DUMÉNIL, G. 2006. Cerebral microcirculation shear stress levels determine Neisseria meningitidis attachment sites along the blood-brain barrier. *J Exp Med,* 203**,** 1939-50.

MARGOS, G., HEPNER, S., MANG, C., MAROSEVIC, D., REYNOLDS, S. E., KREBS, S., SING, A., DERDAKOVA, M., REITER, M. A. & FINGERLE, V. 2017a. Lost in plasmids: next generation sequencing and the complex genome of the tick-borne pathogen Borrelia burgdorferi. *BMC Genomics,* 18**,** 422.

MARGOS, G., MAROSEVIC, D., CUTLER, S., DERDAKOVA, M., DIUK-WASSER, M., EMLER, S., FISH, D., GRAY, J., HUNFELDT, K. P., JAULHAC, B., KAHL, O., KOVALEV, S., KRAICZY, P., LANE, R. S., LIENHARD, R., LINDGREN, P. E., OGDEN, N., ORNSTEIN, K., RUPPRECHT, T., SCHWARTZ, I., SING, A., STRAUBINGER, R. K., STRLE, F., VOORDOUW, M., RIZZOLI, A., STEVENSON, B. & FINGERLE, V. 2017b. There is inadequate evidence to support the division of the genus Borrelia. *Int J Syst Evol Microbiol,* 67**,** 1081-1084.

MARKOWICZ, M., SCHÖTTA, A. M., KUNDI, M., BOGOVIČ, P., OGRINC, K., STRLE, F. & STANEK, G. 2018. CXCL13 concentrations in cerebrospinal fluid of patients with Lyme neuroborreliosis and other neurological disorders determined by Luminex and ELISA. *Ticks Tick Borne Dis*.

MARQUES, A. R. 2015. Laboratory diagnosis of Lyme disease: advances and challenges. *Infect Dis Clin North Am,* 29**,** 295-307.

MARRA, C. M., TANTALO, L. C., SAHI, S. K., MAXWELL, C. L. & LUKEHART, S. A. 2010. CXCL13 as a cerebrospinal fluid marker for neurosyphilis in HIV-infected patients with syphilis. *Sex Transm Dis,* 37**,** 283-7.

MASON, L. M., WAGEMAKERS, A., VAN 'T VEER, C., OEI, A., VAN DER POT, W. J., AHMED, K., VAN DER POLL, T., GEIJTENBEEK, T. B. & HOVIUS, J. W. 2016. Borrelia burgdorferi Induces TLR2-Mediated Migration of Activated Dendritic Cells in an Ex Vivo Human Skin Model. *PLoS One,* 11**,** e0164040.

MATSUI, T., NAKATA, N., NAGAI, S., NAKATANI, A., TAKAHASHI, M., MOMOSE, T., OHTOMO, K. & KOYASU, S. 2009. Inflammatory cytokines and hypoxia contribute to 18F-FDG uptake by cells involved in pannus formation in rheumatoid arthritis. *J Nucl Med,* 50**,** 920-6.

MCLOUGHLIN, A., ROCHFORT, K. D., MCDONNELL, C. J., KERRIGAN, S. W. & CUMMINS, P. M. 2017. Staphylococcus aureus-mediated blood-brain barrier injury: an in vitro human brain microvascular endothelial cell model. *Cell Microbiol,* 19.

MEAD, P. S. 2015. Epidemiology of Lyme disease. *Infect Dis Clin North Am,* 29**,** 187-210.

MIDDLETON, J., NEIL, S., WINTLE, J., CLARK-LEWIS, I., MOORE, H., LAM, C., AUER, M., HUB, E. & ROT, A. 1997. Transcytosis and surface presentation of IL-8 by venular endothelial cells. *Cell,* 91**,** 385-95.

MIDDLETON, J., PATTERSON, A. M., GARDNER, L., SCHMUTZ, C. & ASHTON, B. A. 2002. Leukocyte extravasation: chemokine transport and presentation by the endothelium. *Blood,* 100**,** 3853-60.

MIKATY, G., SOYER, M., MAIREY, E., HENRY, N., DYER, D., FOREST, K. T., MORAND, P., GUADAGNINI, S., PRÉVOST, M. C., NASSIF, X. & DUMÉNIL, G. 2009. Extracellular bacterial pathogen induces host cell surface reorganization to resist shear stress. *PLoS Pathog,* 5**,** e1000314.

MILLER, J. C., MA, Y., CRANDALL, H., WANG, X. & WEIS, J. J. 2008. Gene expression profiling provides insights into the pathways involved in inflammatory arthritis development: murine model of Lyme disease. *Exp Mol Pathol,* 85**,** 20-7.

MOHAN, H., KRUMBHOLZ, M., SHARMA, R., EISELE, S., JUNKER, A., SIXT, M., NEWCOMBE, J., WEKERLE, H., HOHLFELD, R., LASSMANN, H. & MEINL, E. 2010. Extracellular matrix in multiple sclerosis lesions: Fibrillar collagens, biglycan and decorin are upregulated and associated with infiltrating immune cells. *Brain Pathol,* 20**,** 966-75.

MOKALENG, B. B., EBENHAN, T., RAMESH, S., GOVENDER, T., KRUGER, H. G., PARBOOSING, R., HAZARI, P. P., MISHRA, A. K., MARJANOVIC-PAINTER, B., ZEEVAART, J. R. & SATHEKGE, M. M. 2015. Synthesis, 68Ga-radiolabeling, and preliminary in vivo assessment of a depsipeptide-derived compound as a potential PET/CT infection imaging agent. *Biomed Res Int,* 2015**,** 284354.

MOLINS, C. R., ASHTON, L. V., WORMSER, G. P., HESS, A. M., DELOREY, M. J., MAHAPATRA, S., SCHRIEFER, M. E. & BELISLE, J. T. 2015. Development of a metabolic biosignature for detection of early Lyme disease. *Clin Infect Dis,* 60**,** 1767-75.

MONIUSZKO, A., CZUPRYNA, P., PANCEWICZ, S., RUTKOWSKI, K., ZAJKOWSKA, O., SWIERZBIŃSKA, R., GRYGORCZUK, S.,

KONDRUSIK, M., OWŁASIUK, P. & ZAJKOWSKA, J. 2014. Evaluation of CXCL8, CXCL10, CXCL11, CXCL12 and CXCL13 in serum and cerebrospinal fluid of patients with neuroborreliosis. *Immunol Lett,* 157**,** 45-50.

MONIUSZKO, A., PANCEWICZ, S., CZUPRYNA, P., GRYGORCZUK, S., ŚWIERZBIŃSKA, R., KONDRUSIK, M., PENZA, P. & ZAJKOWSKA, J. 2012. ssICAM-1, IL-21 and IL-23 in patients with tick borne encephalitis and neuroborreliosis. *Cytokine,* 60**,** 468-72.

MORETH, K., BRODBECK, R., BABELOVA, A., GRETZ, N., SPIEKER, T., ZENG-BROUWERS, J., PFEILSCHIFTER, J., YOUNG, M. F., SCHAEFER, R. M. & SCHAEFER, L. 2010. The proteoglycan biglycan regulates expression of the B cell chemoattractant CXCL13 and aggravates murine lupus nephritis. *J Clin Invest,* 120**,** 4251-72.

MORGAN, A., SEPURU, K. M., FENG, W., RAJARATHNAM, K. & WANG, X. 2015. Flexible Linker Modulates Glycosaminoglycan Affinity of Decorin Binding Protein A. *Biochemistry,* 54**,** 5113-9.

MORGAN, A. & WANG, X. 2013. The novel heparin-binding motif in decorin-binding protein A from strain B31 of Borrelia burgdorferi explains the higher binding affinity. *Biochemistry,* 52**,** 8237-45.

MORGAN, A. M. & WANG, X. 2015. Structural mechanisms underlying sequence-dependent variations in GAG affinities of decorin binding protein A, a Borrelia burgdorferi adhesin. *Biochem J,* 467**,** 439-51.

MORIARTY, T. J., NORMAN, M. U., COLARUSSO, P., BANKHEAD, T., KUBES, P. & CHACONAS, G. 2008. Real-time high resolution 3D imaging of the lyme disease spirochete adhering to and escaping from the vasculature of a living host. *PLoS Pathog,* 4**,** e1000090.

MORIARTY, T. J., SHI, M., LIN, Y. P., EBADY, R., ZHOU, H., ODISHO, T., HARDY, P. O., SALMAN-DILGIMEN, A., WU, J., WEENING, E. H., SKARE, J. T., KUBES, P., LEONG, J. & CHACONAS, G. 2012. Vascular binding of a pathogen under shear force through mechanistically distinct sequential interactions with host macromolecules. *Mol Microbiol,* 86**,** 1116-31.

MOTHAPO, K. M., VERBEEK, M. M., VAN DER VELDEN, L. B., ANG, C. W., KOOPMANS, P. P., VAN DER VEN, A. & STELMA, F. 2015. Has CXCL13 an added value in diagnosis of neurosyphilis? *J Clin Microbiol,* 53**,** 1693-6.

MUEHLENBACHS, A., BOLLWEG, B. C., SCHULZ, T. J., FORRESTER, J. D., DELEON CARNES, M., MOLINS, C., RAY, G. S., CUMMINGS, P. M., RITTER, J. M., BLAU, D. M., ANDREW, T. A., PRIAL, M., NG, D. L., PRAHLOW, J. A., SANDERS, J. H., SHIEH, W. J., PADDOCK, C. D., SCHRIEFER, M. E., MEAD, P. & ZAKI, S. R. 2016. Cardiac Tropism of Borrelia burgdorferi: An Autopsy Study of Sudden Cardiac Death Associated with Lyme Carditis. *Am J Pathol,* 186**,** 1195-205.

MYGLAND, A., LJØSTAD, U., FINGERLE, V., RUPPRECHT, T., SCHMUTZHARD, E., STEINER, I. & SOCIETIES, E. F. O. N. 2010. EFNS guidelines on the diagnosis and management of European Lyme neuroborreliosis. *Eur J Neurol,* 17**,** 8-16, e1-4.

MÜLLEGGER, R. R., MCHUGH, G., RUTHAZER, R., BINDER, B., KERL, H. & STEERE, A. C. 2000. Differential expression of cytokine mRNA in skin specimens from patients with erythema migrans or acrodermatitis chronica atrophicans. *J Invest Dermatol,* 115**,** 1115-23.

NADELMAN, R. B. 2015. Erythema migrans. *Infect Dis Clin North Am,* 29**,** 211-39.

NARAYAN, K., DAIL, D., LI, L., CADAVID, D., AMRUTE, S., FITZGERALD-BOCARSLY, P. & PACHNER, A. R. 2005. The nervous system as ectopic germinal center: CXCL13 and IgG in lyme neuroborreliosis. *Ann Neurol,* 57**,** 813-23.

NAYAK, S., SRIDHARA, A., MELO, R., RICHER, L., CHEE, N. H., KIM, J., LINDER, V., STEINMILLER, D., SIA, S. K. & GOMES-SOLECKI, M. 2016. Microfluidics-based point-of-care test for serodiagnosis of Lyme Disease. *Sci Rep,* 6**,** 35069.

NELIMARKKA, L., KAINULAINEN, V., SCHÖNHERR, E., MOISANDER, S., JORTIKKA, M., LAMMI, M., ELENIUS, K., JALKANEN, M. & JÄRVELÄINEN, H. 1997. Expression of small extracellular chondroitin/dermatan sulfate proteoglycans is differentially regulated in human endothelial cells. *J Biol Chem,* 272**,** 12730-7.

NELSON, C. A., SAHA, S., KUGELER, K. J., DELOREY, M. J., SHANKAR, M. B., HINCKLEY, A. F. & MEAD, P. S. 2015. Incidence of Clinician-Diagnosed Lyme Disease, United States, 2005-2010. *Emerg Infect Dis,* 21**,** 1625-31.

NEWBERG, A., HASSAN, A. & ALAVI, A. 2002. Cerebral metabolic changes associated with Lyme disease. *Nucl Med Commun,* 23**,** 773-7.

NIDDAM, A. F., EBADY, R., BANSAL, A., KOEHLER, A., HINZ, B. & MORIARTY, T. J. 2017. Plasma fibronectin stabilizes Borrelia burgdorferi-endothelial interactions under vascular shear stress by a catch-bond mechanism. *Proc Natl Acad Sci U S A,* 114**,** E3490-E3498.

NIEMINEN, A., MAKSIMOW, M., MENTULA, P., KYHÄLÄ, L., KYLÄNPÄÄ, L., PUOLAKKAINEN, P., KEMPPAINEN, E., REPO, H. & SALMI, M. 2014. Circulating cytokines in predicting development of severe acute pancreatitis. *Crit Care,* 18**,** R104.

NORDBERG, M., FORSBERG, P., JOHANSSON, A., NYMAN, D., JANSSON, C., ERNERUDH, J. & EKERFELT, C. 2011. Cytotoxic mechanisms may play a role in the local immune response in the central nervous system in neuroborreliosis. *J Neuroimmunol,* 232**,** 186-93.

NORMAN, M. U., MORIARTY, T. J., DRESSER, A. R., MILLEN, B., KUBES, P. & CHACONAS, G. 2008. Molecular mechanisms involved in vascular interactions of the Lyme disease pathogen in a living host. *PLoS Pathog,* 4**,** e1000169.

NYARKO, E., GRAB, D. J. & DUMLER, J. S. 2006. Anaplasma phagocytophilum-infected neutrophils enhance transmigration of Borrelia burgdorferi across the human blood brain barrier in vitro. *Int J Parasitol,* 36**,** 601-5.

OBERMEIER, B., DANEMAN, R. & RANSOHOFF, R. M. 2013. Development, maintenance and disruption of the blood-brain barrier. *Nat Med,* 19**,** 1584-96.

OLIVER, J. H., OWSLEY, M. R., HUTCHESON, H. J., JAMES, A. M., CHEN, C., IRBY, W. S., DOTSON, E. M. & MCLAIN, D. K. 1993. Conspecificity of the ticks Ixodes scapularis and I. dammini (Acari: Ixodidae). *J Med Entomol,* 30**,** 54-63.

OOSTING, M., KERSTHOLT, M., TER HORST, R., LI, Y., DEELEN, P., SMEEKENS, S., JAEGER, M., LACHMANDAS, E., VRIJMOETH, H., LUPSE, M., FLONTA, M., CRAMER, R. A., KULLBERG, B. J., KUMAR, V., XAVIER, R., WIJMENGA, C., NETEA, M. G. & JOOSTEN, L. A. 2016. Functional and Genomic Architecture of Borrelia burgdorferi-Induced Cytokine Responses in Humans. *Cell Host Microbe,* 20**,** 822-833.

OOSTING, M., TER HOFSTEDE, H., STURM, P., ADEMA, G. J., KULLBERG, B. J., VAN DER MEER, J. W., NETEA, M. G. & JOOSTEN, L. A. 2011a. TLR1/TLR2 heterodimers play an important role in the recognition of Borrelia spirochetes. *PLoS One,* 6**,** e25998.

OOSTING, M., TER HOFSTEDE, H., VAN DE VEERDONK, F. L., STURM, P., KULLBERG, B. J., VAN DER MEER, J. W., NETEA, M. G. & JOOSTEN, L. A. 2011b. Role of interleukin-23 (IL-23) receptor signaling for IL-17 responses in human Lyme disease. *Infect Immun,* 79**,** 4681-7.

ORNSTEIN, K., BERGLUND, J., NILSSON, I., NORRBY, R. & BERGSTRÖM, S. 2001. Characterization of Lyme borreliosis isolates from patients with erythema migrans and neuroborreliosis in southern Sweden. *J Clin Microbiol,* 39**,** 1294-8.

PACHNER, A. R., CADAVID, D., SHU, G., DAIL, D., PACHNER, S., HODZIC, E. & BARTHOLD, S. W. 2001a. Central and peripheral nervous system infection, immunity, and inflammation in the NHP model of Lyme borreliosis. *Ann Neurol,* 50**,** 330-8.

PACHNER, A. R., DAIL, D., LI, L., GUREY, L., FENG, S., HODZIC, E. & BARTHOLD, S. 2002. Humoral immune response associated with lyme borreliosis in nonhuman primates: analysis by immunoblotting and enzyme-linked immunosorbent assay with sonicates or recombinant proteins. *Clin Diagn Lab Immunol,* 9**,** 1348-55.

PACHNER, A. R., DELANEY, E. & O'NEILL, T. 1995a. Neuroborreliosis in the nonhuman primate: Borrelia burgdorferi persists in the central nervous system. *Ann Neurol,* 38**,** 667-9.

PACHNER, A. R., DELANEY, E., O'NEILL, T. & MAJOR, E. 1995b. Inoculation of nonhuman primates with the N40 strain of Borrelia burgdorferi leads to a model of Lyme neuroborreliosis faithful to the human disease. *Neurology,* 45**,** 165-72.

PACHNER, A. R., GELDERBLOM, H. & CADAVID, D. 2001b. The rhesus model of Lyme neuroborreliosis. *Immunol Rev,* 183**,** 186-204.

PACHNER, A. R. & STEINER, I. 2007. Lyme neuroborreliosis: infection, immunity, and inflammation. *Lancet Neurol,* 6**,** 544-52.

PAGE, C., ROSE, M., YACOUB, M. & PIGOTT, R. 1992. Antigenic heterogeneity of vascular endothelium. *Am J Pathol,* 141**,** 673-83.

PAPAIOANNOU, T. G. & STEFANADIS, C. 2005. Vascular wall shear stress: basic principles and methods. *Hellenic J Cardiol,* 46**,** 9-15.

PARVEEN, N., CAIMANO, M., RADOLF, J. D. & LEONG, J. M. 2003. Adaptation of the Lyme disease spirochaete to the mammalian host environment results in enhanced glycosaminoglycan and host cell binding. *Mol Microbiol,* 47**,** 1433-44.

PETNICKI-OCWIEJA, T. & KERN, A. 2014. Mechanisms of Borrelia burgdorferi internalization and intracellular innate immune signaling. *Front Cell Infect Microbiol,* 4**,** 175.

PETZKE, M. & SCHWARTZ, I. 2015. Borrelia burgdorferi Pathogenesis and the Immune Response. *Clin Lab Med,* 35**,** 745-64.

PHILIPP, M. T., AYDINTUG, M. K., BOHM, R. P., COGSWELL, F. B., DENNIS, V. A., LANNERS, H. N., LOWRIE, R. C., ROBERTS, E. D., CONWAY, M. D., KARAÇORLU, M., PEYMAN, G. A., GUBLER, D. J., JOHNSON, B. J., PIESMAN, J. & GU, Y. 1993. Early and early disseminated phases of Lyme disease in the rhesus monkey: a model for infection in humans. *Infect Immun,* 61**,** 3047-59.

PICHERT, A., SAMSONOV, S. A., THEISGEN, S., THOMAS, L., BAUMANN, L., SCHILLER, J., BECK-SICKINGER, A. G., HUSTER, D. & PISABARRO, M. T. 2012. Characterization of the interaction of interleukin-8 with hyaluronan, chondroitin sulfate, dermatan sulfate and their sulfated derivatives by spectroscopy and molecular modeling. *Glycobiology,* 22**,** 134-45.

PICKEN, R. N., CHENG, Y., STRLE, F. & PICKEN, M. M. 1996. Patient isolates of Borrelia burgdorferi sensu lato with genotypic and phenotypic similarities of strain 25015. *J Infect Dis,* 174**,** 1112-5.

PIESMAN, J. 1995. Dispersal of the Lyme disease spirochete Borrelia burgdorferi to salivary glands of feeding nymphal Ixodes scapularis (Acari: Ixodidae). *J Med Entomol,* 32**,** 519-21.

PIESMAN, J., MATHER, T. N., SINSKY, R. J. & SPIELMAN, A. 1987. Duration of tick attachment and Borrelia burgdorferi transmission. *J Clin Microbiol,* 25**,** 557-8.

PIKAS, D. S., BROWN, E. L., GURUSIDDAPPA, S., LEE, L. Y., XU, Y. & HÖÖK, M. 2003. Decorin-binding sites in the adhesin DbpA from Borrelia burgdorferi: a synthetic peptide approach. *J Biol Chem,* 278**,** 30920-6.

PLOTKIN, M., HAUTZEL, H., KRAUSE, B. J., MOHR, S., LANGEN, K. J. & MÜLLER, H. W. 2005. Fluorine-18-labeled fluorodeoxyglucose-positron emission tomography studies of acute brainstem Lyme neuroborreliosis [corrected] Case report. *J Neurosurg,* 102**,** 927-9.

PRICE, C. P. 2001. Point of care testing. *BMJ,* 322**,** 1285-8.

PRIES, A. R., SECOMB, T. W. & GAEHTGENS, P. 1995. Design principles of vascular beds. *Circ Res,* 77**,** 1017-23.

PRITT, B. S. & PETERSEN, J. M. 2016. Borrelia mayonii: prying open Pandora's box of spirochetes - Authors' reply. *Lancet Infect Dis,* 16**,** 637-638.

PULZOVA, L., KOVAC, A., MUCHA, R., MLYNARCIK, P., BENCUROVA, E., MADAR, M., NOVAK, M. & BHIDE, M. 2011. OspA-CD40 dyad: ligand-receptor interaction in the translocation of neuroinvasive Borrelia across the blood-brain barrier. *Sci Rep,* 1**,** 86.

PURSER, J. E. & NORRIS, S. J. 2000. Correlation between plasmid content and infectivity in Borrelia burgdorferi. *Proc Natl Acad Sci U S A,* 97**,** 13865-70.

PÍCHA, D., MORAVCOVÁ, L. & SMÍŠKOVÁ, D. 2016. Prospective study on the chemokine CXCL13 in neuroborreliosis and other aseptic neuroinfections. *J Neurol Sci,* 368**,** 214-20.

PĚTROŠOVÁ, H., ESHGHI, A., ANJUM, Z., ZLOTNIKOV, N., CAMERON, C. E. & MORIARTY, T. J. 2017. Diet-Induced Obesity Does Not Alter Tigecycline Treatment Efficacy in Murine Lyme Disease. *Front Microbiol,* 8**,** 292.

RADOLF, J. D., CAIMANO, M. J., STEVENSON, B. & HU, L. T. 2012. Of ticks, mice and men: understanding the dual-host lifestyle of Lyme disease spirochaetes. *Nat Rev Microbiol,* 10**,** 87-99.

RAMAMOORTHI, N., NARASIMHAN, S., PAL, U., BAO, F., YANG, X. F., FISH, D., ANGUITA, J., NORGARD, M. V., KANTOR, F. S., ANDERSON, J. F., KOSKI, R. A. & FIKRIG, E. 2005. The Lyme disease agent exploits a tick protein to infect the mammalian host. *Nature,* 436**,** 573-7.

RAMESH, G., BORDA, J. T., GILL, A., RIBKA, E. P., MORICI, L. A., MOTTRAM, P., MARTIN, D. S., JACOBS, M. B., DIDIER, P. J. & PHILIPP, M. T. 2009. Possible role of glial cells in the onset and progression of Lyme neuroborreliosis. *J Neuroinflammation,* 6**,** 23.

RAMESH, G., DIDIER, P. J., ENGLAND, J. D., SANTANA-GOULD, L., DOYLE-MEYERS, L. A., MARTIN, D. S., JACOBS, M. B. & PHILIPP, M. T. 2015. Inflammation in the pathogenesis of lyme neuroborreliosis. *Am J Pathol,* 185**,** 1344-60.

RANSOHOFF, R. M. & ENGELHARDT, B. 2012. The anatomical and cellular basis of immune surveillance in the central nervous system. *Nat Rev Immunol,* 12**,** 623-35.

REED, K. D. 2002. Laboratory testing for Lyme disease: possibilities and practicalities. *J Clin Microbiol,* 40**,** 319-24.

REITSMA, S., SLAAF, D. W., VINK, H., VAN ZANDVOORT, M. A. & OUDE EGBRINK, M. G. 2007. The endothelial glycocalyx: composition, functions, and visualization. *Pflugers Arch,* 454**,** 345-59.

REMY, M. M., SCHÖBI, N., KOTTANATTU, L., PFISTER, S., DUPPENTHALER, A. & SUTER-RINIKER, F. 2017. Cerebrospinal fluid CXCL13 as a diagnostic marker of neuroborreliosis in children: a retrospective case-control study. *J Neuroinflammation,* 14**,** 173.

RENNEN, H. J., BOERMAN, O. C., OYEN, W. J. & CORSTENS, F. H. 2001. Imaging infection/inflammation in the new millennium. *Eur J Nucl Med,* 28**,** 241-52.

RIJPKEMA, S. G., TAZELAAR, D. J., MOLKENBOER, M. J., NOORDHOEK, G. T., PLANTINGA, G., SCHOULS, L. M. & SCHELLEKENS, J. F. 1997. Detection of Borrelia afzelii, Borrelia burgdorferi sensu stricto, Borrelia garinii and group VS116 by PCR in skin biopsies of patients with erythema migrans and acrodermatitis chronica atrophicans. *Clin Microbiol Infect,* 3**,** 109-116.

RINKER, D. C., PITTS, R. J. & ZWIEBEL, L. J. 2016. Disease vectors in the era of next generation sequencing. *Genome Biol,* 17**,** 95.

RIZZOLI, A., HAUFFE, H., CARPI, G., VOURC H, G., NETELER, M. & ROSA, R. 2011. Lyme borreliosis in Europe. *Euro Surveill,* 16.

ROBERTS, E. D., BOHM, R. P., LOWRIE, R. C., HABICHT, G., KATONA, L., PIESMAN, J. & PHILIPP, M. T. 1998a. Pathogenesis of Lyme neuroborreliosis in the rhesus monkey: the early disseminated and chronic phases of disease in the peripheral nervous system. *J Infect Dis,* 178**,** 722-32.

ROBERTS, W. C., MULLIKIN, B. A., LATHIGRA, R. & HANSON, M. S. 1998b. Molecular analysis of

sequence heterogeneity among genes encoding decorin binding proteins A and B of Borrelia burgdorferi sensu lato. *Infect Immun,* 66**,** 5275-85.

ROGOVSKYY, A. S. & BANKHEAD, T. 2013. Variable VlsE is critical for host reinfection by the Lyme disease spirochete. *PLoS One,* 8**,** e61226.

ROLLE, A. M., HASENBERG, M., THORNTON, C. R., SOLOUK-SARAN, D., MÄNN, L., WESKI, J., MAURER, A., FISCHER, E., SPYCHER, P. R., SCHIBLI, R., BOSCHETTI, F., STEGEMANN-KONISZEWSKI, S., BRUDER, D., SEVERIN, G. W., AUTENRIETH, S. E., KRAPPMANN, S., DAVIES, G., PICHLER, B. J., GUNZER, M. & WIEHR, S. 2016. ImmunoPET/MR imaging allows specific detection of Aspergillus fumigatus lung infection in vivo. *Proc Natl Acad Sci U S A,* 113**,** E1026-33.

ROLLEND, L., FISH, D. & CHILDS, J. E. 2013. Transovarial transmission of Borrelia spirochetes by Ixodes scapularis: a summary of the literature and recent observations. *Ticks Tick Borne Dis,* 4**,** 46-51.

ROSA, P. A., TILLY, K. & STEWART, P. E. 2005. The burgeoning molecular genetics of the Lyme disease spirochaete. *Nat Rev Microbiol,* 3**,** 129-43.

ROUGHLEY, P. J. 2006. The structure and function of cartilage proteoglycans. *Eur Cell Mater,* 12**,** 92-101.

RUBENSTEIN, J. L., WONG, V. S., KADOCH, C., GAO, H. X., BARAJAS, R., CHEN, L., JOSEPHSON, S. A., SCOTT, B., DOUGLAS, V., MAITI, M., KAPLAN, L. D., TRESELER, P. A., CHA, S., HWANG, J. H., CINQUE, P., CYSTER, J. G. & LOWELL, C. 2013. CXCL13 plus interleukin 10 is highly specific for the diagnosis of CNS lymphoma. *Blood,* 121**,** 4740-8.

RUDENKO, N., GOLOVCHENKO, M., GRUBHOFFER, L. & OLIVER, J. H. 2011. Updates on Borrelia burgdorferi sensu lato complex with respect to public health. *Ticks Tick Borne Dis,* 2**,** 123-8.

RUDENKO, N., GOLOVCHENKO, M., MOKRÁCEK, A., PISKUNOVÁ, N., RUZEK, D., MALLATOVÁ, N. & GRUBHOFFER, L. 2008. Detection of Borrelia bissettii in cardiac valve tissue of a patient with endocarditis and aortic valve stenosis in the Czech Republic. *J Clin Microbiol,* 46**,** 3540-3.

RUPPRECHT, T. A., KIRSCHNING, C. J., POPP, B., KASTENBAUER, S., FINGERLE, V., PFISTER, H. W. & KOEDEL, U. 2007. Borrelia garinii induces CXCL13 production in human monocytes through Toll-like receptor 2. *Infect Immun,* 75**,** 4351-6.

RUPPRECHT, T. A., KOEDEL, U., FINGERLE, V. & PFISTER, H. W. 2008. The pathogenesis of lyme neuroborreliosis: from infection to inflammation. *Mol Med,* 14**,** 205-12.

RUPPRECHT, T. A., MANZ, K. M., FINGERLE, V., LECHNER, C., KLEIN, M., PFIRRMANN, M. & KOEDEL, U. 2018. Diagnostic value of cerebrospinal fluid CXCL13 for acute Lyme neuroborreliosis. A systematic review and meta-analysis. *Clin Microbiol Infect*.

RUPPRECHT, T. A., PLATE, A., ADAM, M., WICK, M., KASTENBAUER, S., SCHMIDT, C., KLEIN, M., PFISTER, H. W. & KOEDEL, U. 2009. The chemokine CXCL13 is a key regulator of B cell recruitment to the cerebrospinal fluid in acute Lyme neuroborreliosis. *J Neuroinflammation,* 6**,** 42.

RUSSELL, T. M., DELOREY, M. J. & JOHNSON, B. J. 2013. Borrelia burgdorferi BbHtrA degrades host ECM proteins and stimulates release of inflammatory cytokines in vitro. *Mol Microbiol,* 90**,** 241-51.

RYFFEL, K., PÉTER, O., RUTTI, B., SUARD, A. & DAYER, E. 1999. Scored antibody reactivity determined by immunoblotting shows an association between clinical manifestations and presence of Borrelia burgdorferi sensu stricto, B. garinii, B. afzelii, and B. Valaisiana in humans. *J Clin Microbiol,* 37**,** 4086-92.

SADZIENE, A., THOMAS, D. D., BUNDOC, V. G., HOLT, S. C. & BARBOUR, A. G. 1991. A flagella-less mutant of Borrelia burgdorferi. Structural, molecular, and in vitro functional characterization. *J Clin Invest,* 88**,** 82-92.

SAJANTI, E., VIRTANEN, M., HELVE, O., KUUSI, M., LYYTIKÄINEN, O., HYTÖNEN, J. & SANE, J. 2017. Lyme Borreliosis in Finland, 1995-2014. *Emerg Infect Dis,* 23**,** 1282-1288.

SALAZAR, J. C., POPE, C. D., SELLATI, T. J., FEDER, H. M., KIELY, T. G., DARDICK, K. R., BUCKMAN, R. L., MOORE, M. W., CAIMANO, M. J., POPE, J. G., KRAUSE, P. J., RADOLF, J. D. & NETWORK, L. D. 2003. Coevolution of markers of innate and adaptive immunity in skin and peripheral blood of patients with erythema migrans. *J Immunol,* 171**,** 2660-70.

SALO, J., JAATINEN, A., SÖDERSTRÖM, M., VILJANEN, M. K. & HYTÖNEN, J. 2015. Decorin binding proteins of Borrelia burgdorferi promote arthritis development and joint specific post-treatment DNA persistence in mice. *PLoS One,* 10**,** e0121512.

SALO, J., LOIMARANTA, V., LAHDENNE, P., VILJANEN, M. K. & HYTÖNEN, J. 2011. Decorin binding by DbpA and B of Borrelia garinii, Borrelia afzelii, and Borrelia burgdorferi sensu Stricto. *J Infect Dis,* 204**,** 65-73.

SANCHEZ, J. L. 2015. Clinical Manifestations and Treatment of Lyme Disease. *Clin Lab Med,* 35**,** 765-78.

SANTALAHTI, K., MAKSIMOW, M., AIROLA, A., PAHIKKALA, T., HUTRI-KÄHÖNEN, N., JALKANEN, S., RAITAKARI, O. T. & SALMI, M. 2016. Circulating Cytokines Predict the Development of Insulin Resistance in a

Prospective Finnish Population Cohort. *J Clin Endocrinol Metab*, jc20162081.

SANTANGELO, P. J., ROGERS, K. A., ZURLA, C., BLANCHARD, E. L., GUMBER, S., STRAIT, K., CONNOR-STROUD, F., SCHUSTER, D. M., AMANCHA, P. K., HONG, J. J., BYRAREDDY, S. N., HOXIE, J. A., VIDAKOVIC, B., ANSARI, A. A., HUNTER, E. & VILLINGER, F. 2015. Whole-body immunoPET reveals active SIV dynamics in viremic and antiretroviral therapy-treated macaques. *Nat Methods,* 12**,** 427-32.

SCHAEFER, L., BABELOVA, A., KISS, E., HAUSSER, H. J., BALIOVA, M., KRZYZANKOVA, M., MARSCHE, G., YOUNG, M. F., MIHALIK, D., GÖTTE, M., MALLE, E., SCHAEFER, R. M. & GRÖNE, H. J. 2005. The matrix component biglycan is proinflammatory and signals through Toll-like receptors 4 and 2 in macrophages. *J Clin Invest,* 115**,** 2223-33.

SCHAEFER, L. & SCHAEFER, R. M. 2010. Proteoglycans: from structural compounds to signaling molecules. *Cell Tissue Res,* 339**,** 237-46.

SCHMIDT, C., PLATE, A., ANGELE, B., PFISTER, H. W., WICK, M., KOEDEL, U. & RUPPRECHT, T. A. 2011. A prospective study on the role of CXCL13 in Lyme neuroborreliosis. *Neurology,* 76**,** 1051-8.

SCHMIT, V. L., PATTON, T. G. & GILMORE, R. D. 2011. Analysis of Borrelia burgdorferi Surface Proteins as Determinants in Establishing Host Cell Interactions. *Front Microbiol,* 2**,** 141.

SCHULTE-SPECHTEL, U., FINGERLE, V., GOETTNER, G., ROGGE, S. & WILSKE, B. 2006. Molecular analysis of decorin-binding protein A (DbpA) reveals five major groups among European Borrelia burgdorferi sensu lato strains with impact for the development of serological assays and indicates lateral gene transfer of the dbpA gene. *Int J Med Microbiol,* 296 Suppl 40**,** 250-66.

SCHULZE, R. J. & ZÜCKERT, W. R. 2006. Borrelia burgdorferi lipoproteins are secreted to the outer surface by default. *Mol Microbiol,* 59**,** 1473-84.

SCHVARTZ, G., EPP, T., BURGESS, H. J., CHILTON, N. B. & LOHMANN, K. L. 2015. Comparison between available serologic tests for detecting antibodies against Anaplasma phagocytophilum and Borrelia burgdorferi in horses in Canada. *J Vet Diagn Invest,* 27**,** 540-6.

SENEL, M., RUPPRECHT, T. A., TUMANI, H., PFISTER, H. W., LUDOLPH, A. C. & BRETTSCHNEIDER, J. 2010. The chemokine CXCL13 in acute neuroborreliosis. *J Neurol Neurosurg Psychiatry,* 81**,** 929-33.

SEYMOUR, L. M., DEUTSCHER, A. T., JENKINS, C., KUIT, T. A., FALCONER, L., MINION, F. C., CROSSETT, B., PADULA, M., DIXON, N. E., DJORDJEVIC, S. P. & WALKER, M. J. 2010. A processed multidomain mycoplasma hyopneumoniae adhesin binds fibronectin, plasminogen, and swine respiratory cilia. *J Biol Chem,* 285**,** 33971-8.

SHAW, D. K., HYDE, J. A. & SKARE, J. T. 2012. The BB0646 protein demonstrates lipase and haemolytic activity associated with Borrelia burgdorferi, the aetiological agent of Lyme disease. *Mol Microbiol,* 83**,** 319-34.

SHECHTER, R., LONDON, A. & SCHWARTZ, M. 2013. Orchestrated leukocyte recruitment to immune-privileged sites: absolute barriers versus educational gates. *Nat Rev Immunol,* 13**,** 206-18.

SHI, Y., XU, Q., MCSHAN, K. & LIANG, F. T. 2008a. Both decorin-binding proteins A and B are critical for the overall virulence of Borrelia burgdorferi. *Infect Immun,* 76**,** 1239-46.

SHI, Y., XU, Q., SEEMANAPLLI, S. V., MCSHAN, K. & LIANG, F. T. 2008b. Common and unique contributions of decorin-binding proteins A and B to the overall virulence of Borrelia burgdorferi. *PLoS One,* 3**,** e3340.

SIGAL, L. H. 1997. Lyme disease: a review of aspects of its immunology and immunopathogenesis. *Annu Rev Immunol,* 15**,** 63-92.

SIITONEN, R., PIETIKÄINEN, A., LILJENBÄCK, H., KÄKELÄ, M., SÖDERSTRÖM, M., JALKANEN, S., HYTÖNEN, J. & ROIVAINEN, A. 2017. Targeting of vascular adhesion protein-1 by positron emission tomography visualizes sites of inflammation in Borrelia burgdorferi-infected mice. *Arthritis Res Ther,* 19**,** 254.

SILLANPÄÄ, H., SKOGMAN, B. H., SARVAS, H., SEPPÄLÄ, I. J. & LAHDENNE, P. 2013. Cerebrospinal fluid chemokine CXCL13 in the diagnosis of neuroborreliosis in children. *Scand J Infect Dis,* 45**,** 526-30.

SINGH, S. K. & GIRSCHICK, H. J. 2004. Lyme borreliosis: from infection to autoimmunity. *Clin Microbiol Infect,* 10**,** 598-614.

SKARE, J. T., SHAW, D. K., TRZECIAKOWSKI, J. P. & HYDE, J. A. 2016. In Vivo Imaging Demonstrates That Borrelia burgdorferi ospC Is Uniquely Expressed Temporally and Spatially throughout Experimental Infection. *PLoS One,* 11**,** e0162501.

SKOGMAN, B. H., LAGER, M., HENNINGSSON, A. J. & TJERNBERG, I. 2017. The recomBead Borrelia antibody index, CXCL13 and total IgM index for laboratory diagnosis of Lyme neuroborreliosis in children. *Eur J Clin Microbiol Infect Dis,* 36**,** 2221-2229.

SMITH, J. R., BRAZIEL, R. M., PAOLETTI, S., LIPP, M., UGUCCIONI, M. & ROSENBAUM, J. T. 2003. Expression of B-cell-attracting chemokine 1 (CXCL13) by malignant lymphocytes and vascular endothelium in primary central nervous system lymphoma. *Blood,* 101**,** 815-21.

SNOW, A. D., KINSELLA, M. G., PARKS, E., SEKIGUCHI, R. T., MILLER, J. D., KIMATA, K. & WIGHT, T. N. 1995. Differential binding of

vascular cell-derived proteoglycans (perlecan, biglycan, decorin, and versican) to the beta-amyloid protein of Alzheimer's disease. *Arch Biochem Biophys,* 320**,** 84-95.

SORMUNEN, J. J., PENTTINEN, R., KLEMOLA, T., HÄNNINEN, J., VUORINEN, I., LAAKSONEN, M., SÄÄKSJÄRVI, I. E., RUOHOMÄKI, K. & VESTERINEN, E. J. 2016. Tick-borne bacterial pathogens in southwestern Finland. *Parasit Vectors,* 9**,** 168.

SOYER, M. & DUMÉNIL, G. 2011. Introducing shear stress in the study of bacterial adhesion. *J Vis Exp***,** e3241.

SPADONI, I., FORNASA, G. & RESCIGNO, M. 2017. Organ-specific protection mediated by cooperation between vascular and epithelial barriers. *Nat Rev Immunol,* 17**,** 761-773.

ST JOHN, A. & PRICE, C. P. 2014. Existing and Emerging Technologies for Point-of-Care Testing. *Clin Biochem Rev,* 35**,** 155-67.

STANEK, G., FINGERLE, V., HUNFELD, K. P., JAULHAC, B., KAISER, R., KRAUSE, A., KRISTOFERITSCH, W., O'CONNELL, S., ORNSTEIN, K., STRLE, F. & GRAY, J. 2011. Lyme borreliosis: clinical case definitions for diagnosis and management in Europe. *Clin Microbiol Infect,* 17**,** 69-79.

STANEK, G. & STRLE, F. 2018. Lyme borreliosis-from tick bite to diagnosis and treatment. *FEMS Microbiol Rev,* 42**,** 233-258.

STEERE, A. C. 2001. Lyme disease. *N Engl J Med,* 345**,** 115-25.

STEERE, A. C., BRODERICK, T. F. & MALAWISTA, S. E. 1978. Erythema chronicum migrans and Lyme arthritis: epidemiologic evidence for a tick vector. *Am J Epidemiol,* 108**,** 312-21.

STEERE, A. C., MALAWISTA, S. E., BARTENHAGEN, N. H., SPIELER, P. N., NEWMAN, J. H., RAHN, D. W., HUTCHINSON, G. J., GREEN, J., SNYDMAN, D. R. & TAYLOR, E. 1984. The clinical spectrum and treatment of Lyme disease. *Yale J Biol Med,* 57**,** 453-61.

STEERE, A. C., MALAWISTA, S. E., HARDIN, J. A., RUDDY, S., ASKENASE, W. & ANDIMAN, W. A. 1977a. Erythema chronicum migrans and Lyme arthritis. The enlarging clinical spectrum. *Ann Intern Med,* 86**,** 685-98.

STEERE, A. C., MALAWISTA, S. E., SNYDMAN, D. R., SHOPE, R. E., ANDIMAN, W. A., ROSS, M. R. & STEELE, F. M. 1977b. Lyme arthritis: an epidemic of oligoarticular arthritis in children and adults in three connecticut communities. *Arthritis Rheum,* 20**,** 7-17.

STEERE, A. C., STRLE, F., WORMSER, G. P., HU, L. T., BRANDA, J. A., HOVIUS, J. W., LI, X. & MEAD, P. S. 2016. Lyme borreliosis. *Nat Rev Dis Primers,* 2**,** 16090.

STERNBACH, G. & DIBBLE, C. L. 1996. Willy Burgdorfer: Lyme disease. *J Emerg Med,* 14**,** 631-4.

STEVENSON, B., FINGERLE, V., WORMSER, G. P. & MARGOS, G. 2018. Public health and patient safety concerns merit retention of Lyme borreliosis-associated spirochetes within the genus Borrelia, and rejection of the genus novum Borreliella. *Ticks Tick Borne Dis*.

STEVENSON, B., VON LACKUM, K., RILEY, S. P., COOLEY, A. E., WOODMAN, M. E. & BYKOWSKI, T. 2006. Evolving models of Lyme disease spirochete gene regulation. *Wien Klin Wochenschr,* 118**,** 643-52.

STICHEL, C. C., KAPPLER, J., JUNGHANS, U., KOOPS, A., KRESSE, H. & MÜLLER, H. W. 1995. Differential expression of the small chondroitin/dermatan sulfate proteoglycans decorin and biglycan after injury of the adult rat brain. *Brain Res,* 704**,** 263-74.

STINCO, G., RUSCIO, M., BERGAMO, S., TROTTER, D. & PATRONE, P. 2014. Clinical features of 705 Borrelia burgdorferi seropositive patients in an endemic area of northern Italy. *ScientificWorldJournal,* 2014**,** 414505.

STONE, B. L. & BRISSETTE, C. A. 2017. Host Immune Evasion by Lyme and Relapsing Fever Borreliae: Findings to Lead Future Studies for Borrelia miyamotoi. *Front Immunol,* 8**,** 12.

STROTHER, K. O., BROADWATER, A. & DE SILVA, A. 2005. Plasmid requirements for infection of ticks by Borrelia burgdorferi. *Vector Borne Zoonotic Dis,* 5**,** 237-45.

SZCZEPANSKI, A., FURIE, M. B., BENACH, J. L., LANE, B. P. & FLEIT, H. B. 1990. Interaction between Borrelia burgdorferi and endothelium in vitro. *J Clin Invest,* 85**,** 1637-47.

TAKATA, F., DOHGU, S., YAMAUCHI, A., MATSUMOTO, J., MACHIDA, T., FUJISHITA, K., SHIBATA, K., SHINOZAKI, Y., SATO, K., KATAOKA, Y. & KOIZUMI, S. 2013. In vitro blood-brain barrier models using brain capillary endothelial cells isolated from neonatal and adult rats retain age-related barrier properties. *PLoS One,* 8**,** e55166.

TAKAYAMA, K., ROTHENBERG, R. J. & BARBOUR, A. G. 1987. Absence of lipopolysaccharide in the Lyme disease spirochete, Borrelia burgdorferi. *Infect Immun,* 55**,** 2311-3.

TAKEMIYA, K., NING, X., SEO, W., WANG, X., MOHAMMAD, R., JOSEPH, G., TITTERINGTON, J. S., KRAFT, C. S., NYE, J. A., MURTHY, N., GOODMAN, M. M. & TAYLOR, W. R. 2018. Novel PET and Near Infrared Imaging Probes for the Specific Detection of Bacterial Infections Associated With Cardiac Devices. *JACC Cardiovasc Imaging*.

THOMAS, D. D. & COMSTOCK, L. E. 1989. Interaction of Lyme disease spirochetes with cultured eucaryotic cells. *Infect Immun,* 57**,** 1324-6.

THOMAS, W. E., NILSSON, L. M., FORERO, M., SOKURENKO, E. V. & VOGEL, V. 2004. Shear-

dependent 'stick-and-roll' adhesion of type 1 fimbriated Escherichia coli. *Mol Microbiol,* 53**,** 1545-57.

THOMAS, W. E., TRINTCHINA, E., FORERO, M., VOGEL, V. & SOKURENKO, E. V. 2002. Bacterial adhesion to target cells enhanced by shear force. *Cell,* 109**,** 913-23.

TJERNBERG, I., HENNINGSSON, A. J., ELIASSON, I., FORSBERG, P. & ERNERUDH, J. 2011. Diagnostic performance of cerebrospinal fluid chemokine CXCL13 and antibodies to the C6-peptide in Lyme neuroborreliosis. *J Infect,* 62**,** 149-58.

TROWBRIDGE, J. M. & GALLO, R. L. 2002. Dermatan sulfate: new functions from an old glycosaminoglycan. *Glycobiology,* 12**,** 117R-25R.

TÖTEMEYER, S., FOSTER, N., KAISER, P., MASKELL, D. J. & BRYANT, C. E. 2003. Toll-like receptor expression in C3H/HeN and C3H/HeJ mice during Salmonella enterica serovar Typhimurium infection. *Infect Immun,* 71**,** 6653-7.

USHIYAMA, A., KATAOKA, H. & IIJIMA, T. 2016. Glycocalyx and its involvement in clinical pathophysiologies. *J Intensive Care,* 4**,** 59.

VAIDYANATHAN, S., PATEL, C. N., SCARSBROOK, A. F. & CHOWDHURY, F. U. 2015. FDG PET/CT in infection and inflammation--current and emerging clinical applications. *Clin Radiol,* 70**,** 787-800.

VALIYAVEETTIL, M., ACHUR, R. N., MUTHUSAMY, A. & GOWDA, D. C. 2004. Characterization of chondroitin sulfate and dermatan sulfate proteoglycans of extracellular matrices of human umbilical cord blood vessels and Wharton's jelly. *Glycoconj J,* 21**,** 361-75.

VAN BEEK, J., SAJANTI, E., HELVE, O., OLLGREN, J., VIRTANEN, M. J., RISSANEN, H., LYYTIKÄINEN, O., HYTÖNEN, J. & SANE, J. 2018. Population-based Borrelia burgdorferi sensu lato seroprevalence and associated risk factors in Finland. *Ticks Tick Borne Dis,* 9**,** 275-280.

VAN BURGEL, N. D., BAKELS, F., KROES, A. C. & VAN DAM, A. P. 2011. Discriminating Lyme neuroborreliosis from other neuroinflammatory diseases by levels of CXCL13 in cerebrospinal fluid. *J Clin Microbiol,* 49**,** 2027-30.

VAN DAM, A. P., KUIPER, H., VOS, K., WIDJOJOKUSUMO, A., DE JONGH, B. M., SPANJAARD, L., RAMSELAAR, A. C., KRAMER, M. D. & DANKERT, J. 1993. Different genospecies of Borrelia burgdorferi are associated with distinct clinical manifestations of Lyme borreliosis. *Clin Infect Dis,* 17**,** 708-17.

VAN DEN WIJNGAARD, C. C., HOFHUIS, A., SIMÕES, M., ROOD, E., VAN PELT, W., ZELLER, H. & VAN BORTEL, W. 2017. Surveillance perspective on Lyme borreliosis across the European Union and European Economic Area. *Euro Surveill,* 22.

VAN DUIJVENDIJK, G., COIPAN, C., WAGEMAKERS, A., FONVILLE, M., ERSÖZ, J., OEI, A., FÖLDVÁRI, G., HOVIUS, J., TAKKEN, W. & SPRONG, H. 2016. Larvae of Ixodes ricinus transmit Borrelia afzelii and B. miyamotoi to vertebrate hosts. *Parasit Vectors,* 9**,** 97.

WAGNER, J. N., WEIS, S., KUBASTA, C., PANHOLZER, J. & VON OERTZEN, T. J. 2017. CXCL13 as a diagnostic marker of neuroborreliosis and other neuroinflammatory disorders in an unselected group of patients. *J Neurol*.

WANG, Q., WÜRTZ, P., AURO, K., MORIN-PAPUNEN, L., KANGAS, A. J., SOININEN, P., TIAINEN, M., TYNKKYNEN, T., JOENSUU, A., HAVULINNA, A. S., AALTO, K., SALMI, M., BLANKENBERG, S., ZELLER, T., VIIKARI, J., KÄHÖNEN, M., LEHTIMÄKI, T., SALOMAA, V., JALKANEN, S., JÄRVELIN, M. R., PEROLA, M., RAITAKARI, O. T., LAWLOR, D. A., KETTUNEN, J. & ALA-KORPELA, M. 2016. Effects of hormonal contraception on systemic metabolism: cross-sectional and longitudinal evidence. *Int J Epidemiol*.

WANG, X. 2012. Solution structure of decorin-binding protein A from Borrelia burgdorferi. *Biochemistry,* 51**,** 8353-62.

WEENING, E. H., PARVEEN, N., TRZECIAKOWSKI, J. P., LEONG, J. M., HÖÖK, M. & SKARE, J. T. 2008. Borrelia burgdorferi lacking DbpBA exhibits an early survival defect during experimental infection. *Infect Immun,* 76**,** 5694-705.

WEINSTEIN, E. A., LIU, L., ORDONEZ, A. A., WANG, H., HOOKER, J. M., TONGE, P. J. & JAIN, S. K. 2012. Noninvasive determination of 2-[18F]-fluoroisonicotinic acid hydrazide pharmacokinetics by positron emission tomography in Mycobacterium tuberculosis-infected mice. *Antimicrob Agents Chemother,* 56**,** 6284-90.

WEINSTEIN, E. A., ORDONEZ, A. A., DEMARCO, V. P., MURAWSKI, A. M., POKKALI, S., MACDONALD, E. M., KLUNK, M., MEASE, R. C., POMPER, M. G. & JAIN, S. K. 2014. Imaging Enterobacteriaceae infection in vivo with 18F-fluorodeoxysorbitol positron emission tomography. *Sci Transl Med,* 6**,** 259ra146.

WEIS, J. J. 2002. Host-pathogen interactions and the pathogenesis of murine Lyme disease. *Curr Opin Rheumatol,* 14**,** 399-403.

WILHELMSSON, P. & LINDGREN, P. E. 2016. Detection of a novel Lyme borreliosis pathogen. *Lancet Infect Dis,* 16**,** 511-512.

WOOTEN, R. M. & WEIS, J. J. 2001. Host-pathogen interactions promoting inflammatory Lyme arthritis: use of mouse models for dissection of disease processes. *Curr Opin Microbiol,* 4**,** 274-9.

WORMSER, G. P., MCKENNA, D., CARLIN, J., NADELMAN, R. B., CAVALIERE, L. F., HOLMGREN, D., BYRNE, D. W. & NOWAKOWSKI, J. 2005. Brief communication: hematogenous dissemination in early Lyme disease. *Ann Intern Med,* 142**,** 751-5.

WU, J., WEENING, E. H., FASKE, J. B., HÖÖK, M. & SKARE, J. T. 2011. Invasion of eukaryotic cells by Borrelia burgdorferi requires β(1) integrins and Src kinase activity. *Infect Immun,* 79**,** 1338-48.

WU, X. B., CAO, D. L., ZHANG, X., JIANG, B. C., ZHAO, L. X., QIAN, B. & GAO, Y. J. 2016. CXCL13/CXCR5 enhances sodium channel Nav1.8 current density via p38 MAP kinase in primary sensory neurons following inflammatory pain. *Sci Rep,* 6**,** 34836.

WUTTE, N., BERGHOLD, A., LÖFFLER, S., ZENZ, W., DAGHOFER, E., KRAINBERGER, I., KLEINERT, G. & ABERER, E. 2011. CXCL13 chemokine in pediatric and adult neuroborreliosis. *Acta Neurol Scand,* 124**,** 321-8.

XU, Q., SEEMANAPLLI, S. V., MCSHAN, K. & LIANG, F. T. 2007. Increasing the interaction of Borrelia burgdorferi with decorin significantly reduces the 50 percent infectious dose and severely impairs dissemination. *Infect Immun,* 75**,** 4272-81.

YANG, D., CHEN, Q., HOOVER, D. M., STALEY, P., TUCKER, K. D., LUBKOWSKI, J. & OPPENHEIM, J. J. 2003. Many chemokines including CCL20/MIP-3alpha display antimicrobial activity. *J Leukoc Biol,* 74**,** 448-55.

YANG, J., HAN, X., LIU, A., BAO, F., PENG, Y., TAO, L., MA, M., BAI, R. & DAI, X. 2017. Chemokine CXC Ligand 13 in Cerebrospinal Fluid Can Be Used as an Early Diagnostic Biomarker for Lyme Neuroborreliosis: A Meta-Analysis. *J Interferon Cytokine Res,* 37**,** 433-439.

YANG, Z., TANG, L., ZHOU, Z. & ZHONG, G. 2016. Neutralizing antichlamydial activity of complement by chlamydia-secreted protease CPAF. *Microbes Infect,* 18**,** 669-674.

YEGUTKIN, G. G., HYTÖNEN, J., SAMBURSKI, S. S., YRJÄNÄINEN, H., JALKANEN, S. & VILJANEN, M. K. 2010. Disordered lymphoid purine metabolism contributes to the pathogenesis of persistent Borrelia garinii infection in mice. *J Immunol,* 184**,** 5112-20.

YRJÄNÄINEN, H., HYTÖNEN, J., HARTIALA, P., OKSI, J. & VILJANEN, M. K. 2010. Persistence of borrelial DNA in the joints of Borrelia burgdorferi-infected mice after ceftriaxone treatment. *APMIS,* 118**,** 665-73.

ZHANG, J. R., HARDHAM, J. M., BARBOUR, A. G. & NORRIS, S. J. 1997. Antigenic variation in Lyme disease borreliae by promiscuous recombination of VMP-like sequence cassettes. *Cell,* 89**,** 275-85.

ZÜCKERT, W. R., LLOYD, J. E., STEWART, P. E., ROSA, P. A. & BARBOUR, A. G. 2004. Cross-species surface display of functional spirochetal lipoproteins by recombinant Borrelia burgdorferi. *Infect Immun,* 72**,** 1463-9.

Annales Universitatis Turkuensis

Turun yliopisto
University of Turku

ISBN 978-951-29-7500-6 (PRINT)
ISBN 978-951-29-7501-3 (PDF)
ISSN 0355-9483 (Print) ISSN 2343-3213 (Online)

Grano Oy, Turku , Finland 2018